

TECHNISCHE UNIVERSITÄT MÜNCHEN

Lehrstuhl für Ernährungsphysiologie

Amino acid homeostasis in *Caenorhabditis elegans* lacking the intestinal peptide transporter PEPT-1 and identification of PEPT-1 modulator proteins

Jacqueline Benner

Vollständiger Abdruck der von der Fakultät Wissenschaftszentrum Weihenstephan für Ernährung, Landnutzung und Umwelt der Technischen Universität München zur Erlangung des akademischen Grades eines

Doktors der Naturwissenschaften

genehmigten Dissertation.

Vorsitzender: Univ.-Prof. Dr. D. Haller
Prüfer der Dissertation: 1. Univ.-Prof. Dr. H. Daniel
2. Univ.-Prof. Dr. M. Schemann

Die Dissertation wurde am 07.03.2011 bei der Technischen Universität München eingereicht und durch die Fakultät Wissenschaftszentrum Weihenstephan für Ernährung, Landnutzung und Umwelt am 18.07.2011 angenommen.

*„Hypothesen sind Netze;
nur der wird fangen, der auswirft.“*

Novalis

TABLE OF CONTENT

SUMMARY	10
ZUSAMMENFASSUNG	12
1. INTRODUCTION	14
1.1. Model organism <i>Caenorhabditis elegans</i>	14
1.2. Amino acid transporters	17
1.3. Peptide transporters	22
1.4. Amino acid sensing via TOR pathway	24
1.5. Aim of the work	28
2. RESULTS	29
2.1. Amino acid homeostasis in <i>C. elegans</i>	29
2.1.1. Investigations into the role of HAT subunit homologues in <i>pept-1(lg601) C. elegans</i>	30
2.1.1.1. HAT heavy subunit homologues	30
2.1.1.2. HAT light subunit homologues	36
2.1.2. Investigations on the PAT homologues in <i>pept-1(lg601) C. elegans</i>	38
2.1.3. Further characterisation of the role of <i>aat-6</i> and Y4C6B.2 in <i>pept-1(lg601) C. elegans</i>	40
2.1.3.1. Functionality of <i>aat-6</i> and Y4C6B.2 RNAi in <i>pept-1(lg601) C. elegans</i>	40
2.1.3.2. Influence of <i>aat-6</i> and Y4C6B.2 RNAi on growth development and reproduction	41
2.1.3.3. Effects of amino acid supplementation on <i>aat-6</i> and Y4C6B.2 depleted <i>pept-1(lg601) C. elegans</i>	43

2.1.3.4. PEPT-1, ATGP-1 and ATGP-2 protein expression in an <i>aat-6</i> (RNAi) background.....	46
2.2. Identification of PEPT-1 regulating genes/proteins.....	47
2.2.1. Selection of genes/proteins affecting <i>C. elegans</i> PEPT-1 function	47
2.2.2. Phenotypic analysis of worms after gene silencing of the preselected PEPT-1 regulator genes	54
2.2.2.1. Postembryonic body size development and reproduction of worms treated with RNAi for the PEPT-1 modulator proteins..	54
2.2.2.2. <i>pept-1</i> promoter activity and mRNA expression after treating worms with RNAi for the PEPT-1 modulator genes.....	56
2.2.2.3. PEPT-1 protein expression is selectively altered by gene silencing of the modulators	58
2.2.2.4. Regulator gene knockdown modulates resistance to oxidative stress	60
2.2.3. Further characterisation of the PEPT-1 regulators.....	66
2.2.3.1. PEPT-1 is only one of the proteins affected by the ER cargo transport protein C54H2.5	66
2.2.3.2. The peptidases encoded by ZC416.6 and R11H6.1 appear to control PEPT-1 transport capacity	67
2.2.3.3. TOR appears to affect PEPT-1 protein levels and function.....	70
3. DISCUSSION	72
3.1. Amino acid homeostasis in <i>C. elegans</i>	72
3.1.1. Role of the HSHAT proteins ATGP-1 and ATGP-2 in <i>C. elegans</i>	72
3.1.2. The LSHAT subunit <i>aat-6</i> is necessary for amino acid homeostasis in <i>pept-1(lg601)</i> <i>C. elegans</i>	75
3.1.3. The PAT homologue Y4C6B.2 represents a second amino acid transporter essential for amino acid homeostasis in <i>pept-1(lg601)</i> <i>C. elegans</i>	77

3.2. Identification of proteins that can alter PEPT-1 function in	
<i>C. elegans</i>	79
3.2.1. Silencing F26E4.12 induces an increased PEPT-1 transporter function	80
3.2.2. The ER cargo transport protein C54H2.5 not only alters PEPT-1 expression and function	83
3.2.3. Gene silencing of both aminopeptidases ZC416.6 and R11H6.1 cause altered PEPT-1 expression and protein levels	85
3.2.4. A novel predicted interaction between TORC2 and PEPT-1 may play an important role in transporter expression and function	87
4. CONCLUSION	91
5. METHODS	93
5.1. General <i>C. elegans</i> methods	93
5.1.1. Cultivation of <i>C. elegans</i>	93
5.1.2. Preparation of synchronised <i>C. elegans</i> populations.....	93
5.1.3. Protein extraction and Bradford assay.....	93
5.1.4. RNA interference	93
5.2. Molecular biological techniques	94
5.2.1. Single-worm nested PCR	94
5.2.2. Crossing of <i>rsks-1(ok1255)</i> with wild type	94
5.2.3. Cloning of bacteria for RNA interference of <i>aat-4</i> and <i>aat-9</i>	94
5.2.4. mRNA-expression levels of <i>C. elegans</i>	98
5.3. Assays for developmental and progeny studies	98
5.3.1. Body length and developmental studies	98
5.3.2. Number of progeny	99
5.3.3. Amino acid supplementation studies	99

5.3.4. Resistance to oxidative stress induced by paraquat	99
5.4. Uptake experiments and staining assays.....	99
5.4.1. Fluorescent dipeptide β -Ala-Lys-AMCA uptake assay (Screen) ..	99
5.4.2. Labelling <i>C. elegans</i> with a fluorescent free fatty acid probe	101
5.4.3. Sudan Black B fat staining	101
5.4.4. Measurement of mitochondrial ROS levels	101
5.5. Proteobiochemical methods.....	102
5.5.1. Membrane protein extraction <i>Xenopus laevis</i> oocytes	102
5.5.2. Membrane protein extraction and protein detection	102
5.6. Others	103
5.6.1. promoter <i>pept-1::gfp</i> expression analysis	103
5.6.2. Measurement of glutathione levels	103
5.7. Statistical analysis	105
6. MATERIALS.....	106
6.1. <i>C. elegans</i> strains and <i>E. coli</i> bacteria	106
6.2. Chemicals, reagents and kits	107
6.3. Buffers and media	109
6.4. Plasmids, oligonucleotides and antibodies	113
6.5. Instruments	114
7. REFERENCES	115
8. APPENDIX	133

8.1. Index of figures	133
8.2. Index of tables	135
8.3. Abbreviations	136
8.4. Supplementary data	138
8.4.1. Absolute fluorescence values of the controls of the β -Ala-Lys-AMCA screen	138
8.4.2. Calculation of the relative β -Ala-Lys-AMCA uptake of <i>C. elegans</i> with individual RNAi gene silencing compared to control.....	145
8.4.3. Entire relative results of the β -Ala-Lys-AMCA uptake screen	147
8.5. Danksagung.....	151
8.6. List of scientific publications.....	152
8.7. Curriculum Vitae	153
8.8. Erklärung	154

SUMMARY

The intestinal peptide transporter PEPT-1 is responsible for the absorption of amino acids in di- and tripeptide bound form. Transporter-deficient *pept-1(lg601)* *C. elegans* are characterised by increased fatty acid absorption, obesity, impaired growth, retarded postembryonic development, reduced reproduction, increased oxidative stress resistance, and a decreased intracellular concentration of amino acids. As the lack of PEPT-1 might be partly compensated by an increased expression of amino acid transport systems in the intestine, the first part of this thesis assessed the role of amino acid transporters of the heterodimeric (HAT) and proton-coupled (PAT) families on overall amino acid homeostasis in worms. The mRNA-profiling revealed that expression of several HAT subunit homologues was significantly increased and the mRNA level of the PAT homologue (Y4C6B.2) was even 18-fold higher in *pept-1(lg601)* *C. elegans* than in wild type animals. RNA interference (RNAi) applied for those genes indicated that the HAT light subunit AAT-6 and the PAT homologue Y4C6B.2 are of crucial importance for amino acid homeostasis in *pept-1(lg601)* worms, as their loss in a *pept-1* knockout background significantly reduced adult body size and caused sterility. Tissue expression, intracellular distribution and the substrate specificity of AAT-6 and Y4C6B.2 transporters were assessed as well to better define the putative roles of these proteins in PEPT-1 deficient *C. elegans*.

The second part of the thesis was directed to identification of proteins that could act as modulators of PEPT-1 function in *C. elegans*. In a functional RNA interference screen with 162 genes known to be expressed in the intestine, RNAi knockdown of three genes (ZC416.6, R11H6.1 and C54H2.5) with predicted mammalian homologous proteins impaired the uptake of the fluorescent dipeptide substrate β -Ala-Lys-AMCA. In addition silencing of these genes simultaneously increased fat accumulation as shown for the PEPT-1 deficient strain before. In contrast, knockdown of F26E4.12 - a putative glutathione-peroxidase 4 - induced an increased PEPT-1 transport function. Further characterisation of the selected genes revealed that C54H2.5 which most likely acts as an ER-cargo protein not only affected PEPT-1 protein expression but also other membrane proteins. Most strikingly two intracellular peptidases (ZC416.6 and R11H6.1) appeared to act specifically as modulators of PEPT-1. Based on the obtained data a model was

developed by which a decreased intracellular free amino acid concentration may be sensed by TOR (target of rapamycin) complex 1 and 2 (TORC1 and TORC2) which could initiate the degradation of the PEPT-1 protein and/or reduce its expression. By contrast, knockdown of F26E4.12 might increase translocation of PEPT-1 into the membrane via TORC2 as indicated by an increased dipeptide uptake.

ZUSAMMENFASSUNG

Der intestinale Peptidtransporter PEPT-1 in *C. elegans* ist für die Aufnahme großer Mengen an Aminosäuren in Form von Di- und Tripeptiden verantwortlich. Das Fehlen des Transporters in *pept-1(lg601)* Würmern führt zur erhöhten Aufnahme von Fettsäuren, der Akkumulation von Fett vor allem in den Darmepithelzellen, einer verlangsamten Entwicklung, einer reduzierten Körperlänge, einer verminderten Reproduktionsrate, einer erhöhten Resistenz gegenüber oxidativem Stress und einer niedrigeren Konzentration an freien Aminosäuren im Körper. Der erste Teil der vorliegenden Arbeit beschreibt Studien, die das Ziel hatten mögliche Kompensationsmechanismen zu identifizieren, die mit einem Verlust der Resorptionsleistung für Aminosäuren aufgrund eines PEPT-1 Mangels in *C. elegans* einhergehen. Hierfür wurden die Untereinheiten von heterodimeren Aminosäuretransportern der HAT-Familie und *C. elegans* Homologe von protonen-gekoppelten Aminosäuretransportern der PAT-Familie untersucht, deren mRNA Expression in *pept-1(lg601)* Würmern stark erhöht ist. Sowohl AAT-6 (leichte HAT Untereinheit) wie auch Y4C6B.2 (PAT-Homolog) scheinen für die Aminosäurehomöostase in *pept-1(lg601)* Würmern essentiell zu sein. Ein Fehlen dieser Transporter führte zu einer eindeutig verringerten Körpergröße und Sterilität.

Der zweite Teil der Arbeit basiert auf der Annahme, dass PEPT-1 durch andere zelluläre Proteine in seiner Aktivität reguliert werden könnte. Im Falle des Natrium-Protonen-Austauschers NHX-2 wurde dies bereits belegt. Er ist funktionell an PEPT-1 gekoppelt und vermittelt den Export von Protonen zurück in das Darmlumen. Die Suche nach Modulatoren für PEPT-1 erfolgte mittels eines RNA Interferenz (RNAi) Screens für 162 in Darmzellen exprimierter Gene. Dabei wurden drei Gene (ZC416.6, R11H6.1 und C54H2.5) identifiziert, deren verminderte Expression zu einer verringerten Dipeptidaufnahme und gleichzeitig zu einer erhöhten Fettakkumulation führten. Nur im Falle von F26E4.12 kam es zu einer Erhöhung der β -Ala-Lys-AMCA Aufnahme. Weiterführende Studien belegten, dass C54H2.5 nicht ausschließlich die Funktion von PEPT-1, sondern auch von weiteren integralen Membranproteinen beeinflusst. F26E4.12, ZC416.6 und R11H6.1 scheinen dagegen spezifisch auf die Expression und Funktion von

PEPT-1 zu wirken. Basierend auf den erzielten Befunden wurde ein Modell postuliert, welches die Interaktion von TOR (target of rapamycin) Komplex 1 und 2 (TORC1 und TORC2) mit der Expression und Funktion von PEPT-1 in einen Zusammenhang stellt. Hierbei steht ein „sensing“ der intrazellulären freien Aminosäuren im Mittelpunkt. Die verminderte Expression der Peptidasen ZC416.6 und R11H6.1 und die daraus resultierende Verringerung der Konzentration an freien Aminosäuren könnte in der Folge durch TORC1 und 2 wahrgenommen und einerseits in PEPT-1 Degradation übersetzt werden und andererseits dessen Expression mindern. Eine erhöhte Aufnahme von Dipeptiden, wie nach RNAi-Behandlung mit F26E4.12 beobachtet, könnte zu einer Aktivierung von TORC2 und einer Erhöhung der Translokation von PEPT-1 in die apikale Membran der Darmzellen führen.

1. INTRODUCTION

1.1. Model organism *Caenorhabditis elegans*

Caenorhabditis elegans (*C. elegans*) is a free living nematode of about 1 mm in length which lives in temperate soil environment. It was introduced as a model organism by Sydney Brenner (1), obtaining the Noble Price for his research on *C. elegans* in 2002. In 1998, the entire genome of *C. elegans* became available with approximately 19,000 genes identified (2). *C. elegans* has been used as a model organism especially for studies on development and cell biology and has since then advanced to one of the most important scientific tools. The simple multicellular organism is cultivated easily, has varied tissues (i.e. muscles, nerves, intestinal cells), and a short generation time. The entire cell lineage of each cell during embryogenesis and post-embryonic development is known (3). Hermaphrodites (Figure 1A) can maintain homozygous mutations and males (Figure 1B) can be used for genetic crossing.

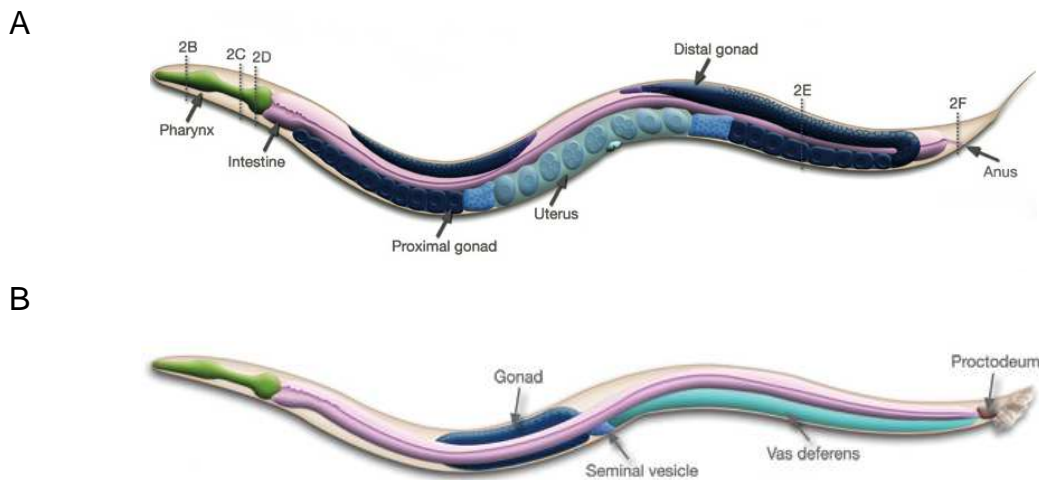


Figure 1: *Caenorhabditis elegans* hermaphrodite and male

(A) Schematic picture of the major anatomical features of a *C. elegans* hermaphrodite. (B) Diagram of the major anatomical differences in *C. elegans* males. Left = anterior part, right = posterior part (modified from Wormatlas).

The animals are transparent which allows the use of fluorescent reporter-gene-constructs encoding for example the green fluorescent protein (GFP) to study gene expression patterns. Gene knockdown of a specific gene by using RNA interference (RNAi) is simple in *C. elegans* just by feeding *E. coli* bacteria which

produce dsRNA of the gene of interest (4). 99.9% of a population of worms are self-fertilizing hermaphrodites (XX) possessing 959 somatic cells. Deriving from non-disjunction of X-chromosomes 0.1% of a population are males (X0) with 1031 somatic cells (4). Self-fertilized wild type hermaphrodites produce around 300 eggs, whereas male-fertilized hermaphrodites are able to lay more than 1000 eggs. The life cycle of *C. elegans* after embryogenesis consists of four larval stages, L1 to L4 (Figure 2). When *C. elegans* is grown on *E. coli* OP50 at 20°C the postembryonic development takes 3.5 days.

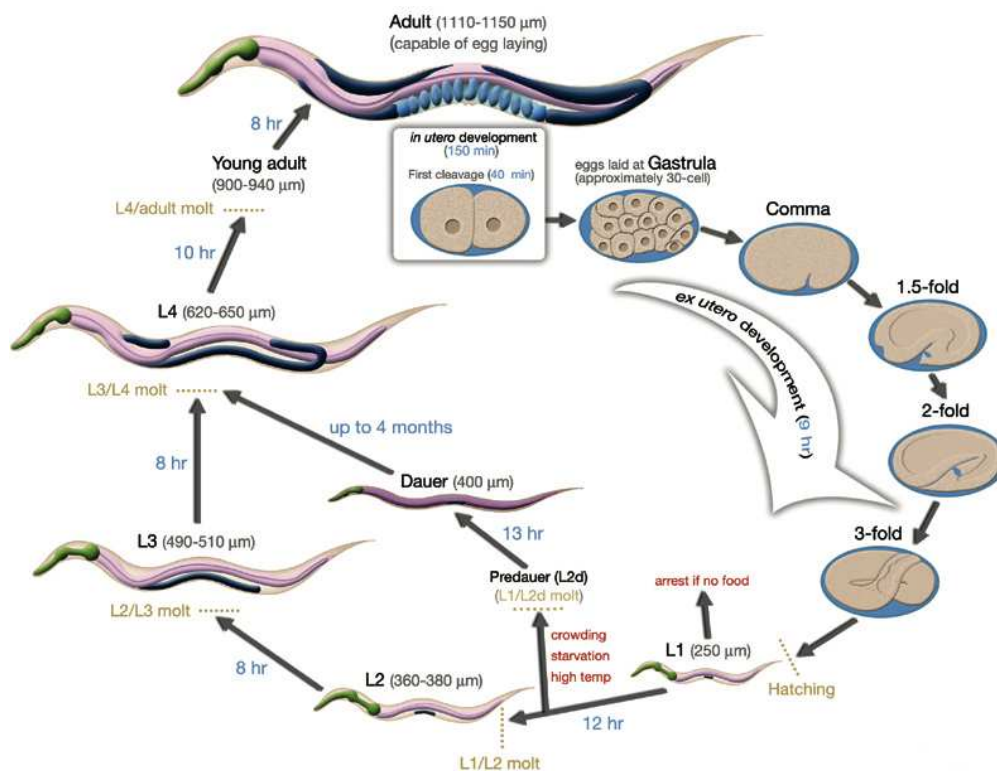


Figure 2: Life cycle of a *C. elegans* hermaphrodite

An adult hermaphrodite is shown at the top of the cycle. With sufficient food supply and at a temperature of about 20°C, L1 larvae hatch out of the eggshell and develop through L2 to L4 stages until they reach adulthood. Each larval stage is initiated with a moult. If there is a lack of food, crowding or high temperature L1 larvae will enter an alternative life state and become first predauer and then dauer larvae until conditions get better. Blue numbers along the arrows indicate the time spent at each state (WormAtlas).

The average life span of wild type *C. elegans* is two to three weeks. When there are harsh environmental conditions like limited food supply, high population density or high temperatures, L1 larvae can switch to dauer larval state (Figure 2). In this state they show structural, metabolic, and behavioural adaptations that

increase life span between four to eight times. Once food becomes available dauer larvae continue development into adulthood (5).

As for all other organisms, food intake is essential for life and reproduction of *C. elegans*. Therefore, the intestine is a central organ comprising roughly one third of the total somatic cell mass. It is mainly responsible for food digestion and absorption, but the intestine is also a storage organ for diverse macromolecules and fat (6). *Escherichia coli* (*E. coli*) bacteria serve as food source for *C. elegans* and it was shown that the average residence time for a bacterium within the intestine is less than two minutes (7). Digestive and assimilative capacity of the worm intestine is huge even though it only consists of 20 cells. These cells build nine rings referred to as “ints” (8). Int1 (the anterior ring) has four cells and int2 to int9 are composed of two cells which together enclose the intestinal lumen.

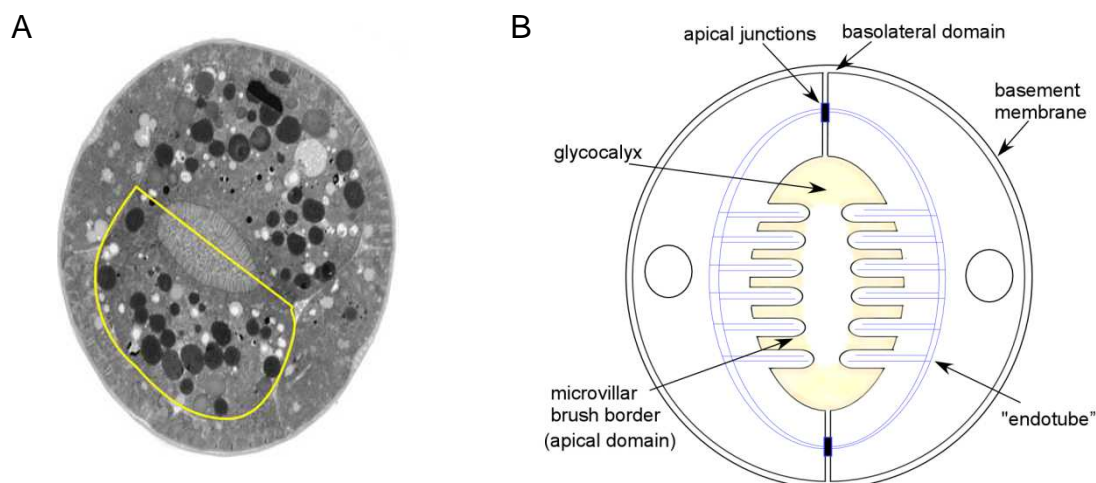


Figure 3: Cross-section of *C. elegans* intestine

(A) The transmission electron micrograph is of a cross-section of a newly hatched L1 larva, where one intestinal cell is marked yellow. (B) Schematic picture of two intestinal cells which build the intestinal lumen (modified from (6)).

The most prominent feature of the intestinal apical domain like in other species is the microvillar brush border into which a large number of nutrient transporters are embedded including SID-1 (responsible for uptake of dsRNA) (9), NAC-2 (sodium-coupled citrate transporter) (10), NHX-2 (sodium-proton-exchanger) (11) and PEPT-1 (di- and tripeptide transporter) (12). The intestinal transporters are responsible for the uptake of nutrients like carbohydrates, amino acids/peptides and fatty acids. The microvilli are surrounded by a layer called “glycocalyx” or “peritrophic matrix”, a relatively unstructured collection of highly modified

glycoproteins (13). This matrix has several functions. It protects the microvillar surface, serves as a filter and provides a scaffold for presenting digestive enzymes. *C. elegans* enterocytes are connected by apical junctions and structural strength of the cells is provided by the endotube. The basolateral domain of the intestine as well as the pharynx is covered by a basement membrane (6).

1.2. Amino acid transporters

About 300 g of amino acids and peptides are absorbed every day in humans, of which only the equivalent of 10 g appears as faecal nitrogen (14). A major site of amino acid and peptide absorption from the food is the proximal jejunum. Reabsorption of amino acids (95-99%) from the primary urine is mediated in the proximal tubule of the kidney nephron. In the body amino acids are delivered to all tissues, where they have several different functions. Amino acids are necessary for protein biosynthesis, acting as precursors for a wide variety of bioactive molecules and are used as energy substrates (15). Several different amino acid transport systems have been identified. Based on functional studies in kidney and intestine of mammals and by analysis of the amino acid profiles in the urine of individuals with different aminoacidurias, five categories of transport activities were proposed (16): (a) The “neutral system” or “methionine preferring system” transports all neutral amino acids (system B⁰, ASC, system L, system T and system A). (b) The “basic system” is responsible for the uptake of cationic amino acids together with cystine (system b^{0,+}, system y^{+L}, CAT-1 and system x_C⁻). (c) The “acidic system” mediates the absorption of glutamate and aspartate (system X_{AG}⁻ and AGT1). (d) The “iminoglycine system” is necessary for proline, hydroxyproline and glycine transport (PAT1, PAT2, system IMINO and XT2), and (e) is the “β-amino acid system” (TauT and BGT1). The class of heteromeric amino acid transporters (HATs) are represented in three of these five transport classes.

Heteromeric amino acid transporters (HATs)

HATs are composed of a catalytic multi-transmembrane spanning subunit (light chain, LSHATs) and a type II N-glycoprotein subunit (heavy chain, HSHATs) linked by a disulfide bridge (17). Two known HSHATs from the SLC3 family are

rBAT and 4F2hc (Table 1). Nine light subunits (SLC7 family members from SLC7A5 to SLC7A13) have been identified. Six of them form heterodimers with 4F2hc (LAT1, LAT2, y^+ LAT1, y^+ LAT2 and xCT) while only one is the partner for rBAT ($b^{0,+}$ AT). Two LSHATs (AGT1, asc2) seem to interact with yet unknown heavy subunits (18). Heteromeric amino acid transport systems are mainly expressed in intestine and kidney.

Table 1: Heteromeric amino acid transporters

Heteromeric amino acid transporters (HATs) are composed of a heavy (HSHAT) and a light (LSHAT) chain subunit and build functional transport systems for the uptake of amino acids. Amino acids are given in one-letter codes; O (ornithine), AA⁰ (neutral amino acids). Tissue distribution is coded as follows: K (kidney), I (intestine), AM (apical membrane), BM (basolateral membrane), Ub (ubiquitous) (modified from (15)).

HSHAT	LSHAT	Gene	System	AA substrates	Tissue	References
4F2hc		SLC3A2				
	y^+ LAT1	SLC7A7	y^+ L	K, R, Q, H, M, L	K, I (BM)	(19)
	y^+ LAT2	SLC7A6	y^+ L	K, R, Q, H, M, L, A, C	K, I (BM)	(20)
	LAT1	SLC7A5	L	H, M, L, I, V, F, Y, W		(21)
	LAT2	SLC7A8	L	AA ⁰ , except P	K, I (BM)	(22)
	asc1	SLC7A10	asc	G, A, S, C, T	K	(23)
	xCT	SLC7A11	x_c^-	E, cystine	Ub	(24)
rBAT		SLC3A1				
	$b^{0,+}$ AT	SLC7A11	$b^{0,+}$	R, K, O, cystine	K, I (AM)	(25)
	?					
	AGT1	SLC7A13		Asp, Glu	K	(26)
	asc2	SLC7A12	asc			(27)

Human rBAT (~90 kDa) and 4F2hc (~80 kDa) are type II membrane *N*-glycoproteins with a single transmembrane domain, a short intracellular NH₂ terminus and a large extracellular COOH terminus significantly homologous to insect and bacterial α -glucosidases (28). rBAT is mainly expressed at the apical side of epithelial cells of kidney, proximal tubule and in the brush border membrane of the small intestine (Figure 4). 4F2hc is ubiquitously expressed, with a basolateral location in epithelial cells (29). LSHATs with a mass of ~50 kDa are

not *N*-glycosylated and are highly hydrophobic with twelve putative transmembrane domains and with the NH_2 and COOH termini located inside the cell. The light and the corresponding heavy subunit are linked by a disulfide bridge. The relevant cysteine residues are located in the putative extracellular loop EL3-4 of LSHATs, a few amino acid residues distal of the transmembrane domain of HSHATs. There is solid evidence of the formation of heterodimers from a variety of heterologous expression systems. LSHAT members need coexpression with the corresponding HSHAT to reach the plasma membrane. LSHATs confer specific amino acid transport activity to the heteromeric complex. For example, rBAT is essential for the cell surface expression of $\text{b}^{0,+}\text{AT}$, but it is not required for reconstituted $\text{b}^{0,+}\text{AT}$ transport activity (30).

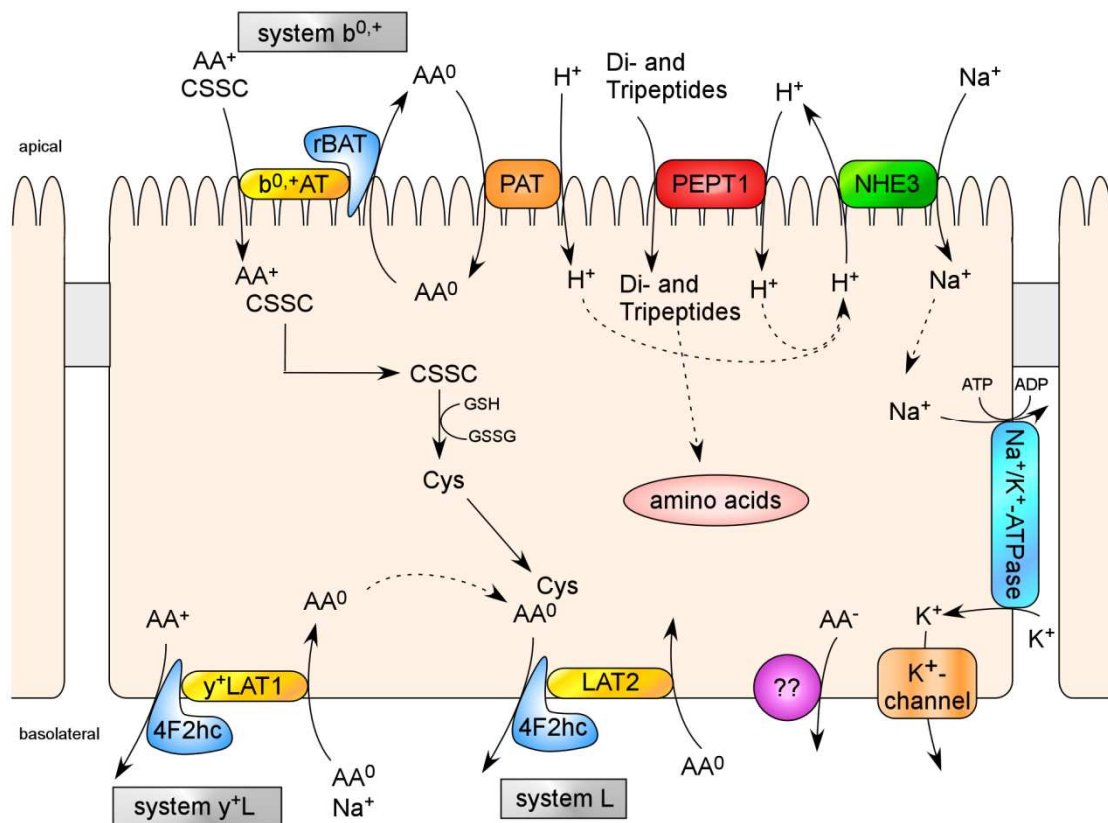


Figure 4: Mammalian intestinal heteromeric and proton-coupled amino acid and peptide transporters

Schematic drawing of a mammalian intestinal cell with heteromeric amino acid transporters (blue heavy subunit, yellow light subunit), an unknown transporter for acidic amino acids (pink), proton-coupled amino acid transporter PAT (orange), peptide transporter PEPT-1 (red), sodium-proton-exchanger NHE3 (green) and $\text{Na}^+/\text{K}^+\text{-ATPase}$ (turquoise), K^+ -channel (brown). Acidic amino acids = AA^- , neutral amino acids = AA^0 , dibasic amino acids = AA^+ , CSSC = cystine, Cys = cysteine, GSH = glutathione (red.) and GSSG = glutathione (oxd.).

The physiological relevance of HATs is increasingly recognized. Mutations in $b^{0,+}AT$ -rBAT and y^+LAT1 -4F2hc cause cystinuria and lysinuric protein intolerance (31).

Cystinuria (OMIM 220100) is caused by a defective transport of cystine and dibasic amino acids across the apical membranes of proximal renal tubular and jejunal epithelial cells. It is an autosomal-recessive disorder with a prevalence of 1 in 7,000 births (32). It is characterised by the occurrence of excessive amounts of arginine, lysine, ornithine and cystine in the urine (33). There are three classified types of cystinuria: type I, non-type I (type II) and type III. Mutational and linkage studies demonstrated that mutations in the HAT heavy subunit rBAT (SLC3A1) cause type I cystinuria (34) (35). Over 60 distinct mutations in rBAT have been described over the last years (reviewed by (36)). Heterozygous patients with type I cystinuria have no aminoaciduria whereas heterozygous patients with type II cystinuria excrete cystine and lysine in their urine. Type II cystinuria is caused by mutations in $b^{0,+}AT$ (SLC7A9) (37) where the intestinal uptake of cationic amino acids is defective and cystine transport is reduced. In type III cystinuria, the amino acid transport defect is incomplete for cationic amino acids and cystine (38).

Lysinuric protein intolerance (LPI, OMIM 222700) is a rare autosomal-recessive disease caused by the defective transport of dibasic amino acids at the basolateral membrane of epithelial cells in the renal tubules and the small intestine (39). Besides defective transport of dibasic amino acids, the disease is characterised by low dibasic amino acid plasma concentration, protein intolerance, orotic aciduria and probably dysfunction of the urea cycle. Excretion of arginine, lysine and ornithine in the urine was postulated (33). 25 mutations within the y^+LAT1 gene (SLC7A7) have been characterised which all cause LPI (reviewed in (32)). In contrast to cystinuria the defect of dibasic amino acid uptake in LPI cannot be compensated by peptides containing these amino acids (40).

There are nine *C. elegans* genes which encode homologues of HAT light chain subunits, namely *aat-1* to *aat-9* (amino acid transporter catalytic chain). The homologues AAT-1 to AAT-3 are more closely related to mammalian transporters (39-45% identity) than AAT-4 to AAT-9 (28-31% identity). Only AAT-1, AAT-2 and

AAT-3 exhibit the conserved cysteine residue which is necessary for the disulfide bridge between the light and the heavy subunit. The other six *C. elegans* LSHATs may not need to associate with a heavy subunit for functional expression and membrane targeting (41). There are also two *C. elegans* genes which express homologues of mammalian HAT type II glycoprotein subunits, *atgp-1* and *atgp-2* (amino acid transporter glycoprotein subunits). The two corresponding proteins have an identity to h4F2hc and hrBAT of approximately 30% and possess the conserved cysteine close to the predicted transmembrane domain.

Veljkovic et al. (41) have shown that only coexpression of either AAT-1 or AAT-3 together with the heavy subunit ATGP-2 in *Xenopus* oocytes caused a functional, Na⁺-independent transport system for small neutral amino acids. Transport characteristics of AAT-1/ATGP-2 and AAT-3/ATGP-2 are similar to the mammalian transport systems L and asc. Coexpression of either AAT-1 or AAT-3 with ATGP-1 showed no surface expression and thus no functional transport of amino acids in *Xenopus* oocytes. However, AAT-9 is able to reach the *Xenopus* oocyte cell membrane and perform transport of aromatic amino acids exclusively without interacting with an exogenous heavy chain subunit (42). Therefore, it resembles the mammalian transporter TAT1 which is expressed in humans mostly in kidney, skeletal muscle, placenta and heart (43).

Proton-coupled amino acid transporters (PATs)

Proton-coupled amino acid transporters (PATs, SLC36A) mediate the uptake of small neutral amino acids (β -alanine, glycine, L-proline, γ -aminobutyric acid (GABA), α -(methylamino)-isobutyric acid) (44) and pharmacologically relevant compounds (D-cycloserin, L-azetidine-2-carboxylic acid) (45). They are found at the apical membrane of small intestinal cells of mammals (Figure 4), but are also expressed in colon, kidney, and brain. PAT1 (SLC36A1) was originally identified as the lysosomal amino acid transporter (LYAAT1) in rat brain (46). It is responsible for the transport of amino acids from luminal protein digestion or lysosomal proteolysis. PAT1 additionally can mediate the electroneutral cotransport of a proton with a short-chain fatty acid (47). The transport of substrates is driven by an inwardly directed H⁺ gradient with a stoichiometry of one proton together with one amino acid or fatty acid resulting in an acidification

of the cytosol during substrate uptake. All substrates are transported with a low affinity (48).

A second but high affinity member of the proton-assisted amino acid transporters is PAT2 (SLC36A2). It has significant functional and sequence similarity to PAT1 (49) and is also responsible for the uptake of alanine, glycine, proline, and short-chain fatty acids together with one proton (47). A difference in substrate specificity between PAT1 and PAT2 is the very low affinity of PAT2 for GABA, β -alanine and D-alanine. In contrast to PAT1, PAT2 has a high affinity to H^+ (1nM) and, therefore can act at higher pH. PAT2 is strongly expressed in heart, lung, and weakly in kidney and in muscle tissue.

Mutations in PAT1 and PAT2 are associated with iminoglycinuria (OMIM 242600) (50). It is a multigenetic autosomal recessive disorder with a prevalence of 1:15,000 (51). It is characterised by the excretion of proline, hydroxyproline and glycine in the urine and impaired intestinal transport is observed in some pedigrees (52). In *C. elegans* no knowledge exists about homologues of PAT1 and PAT2, but blast results suggest that there are some *C. elegans* homologues of the PAT-family namely T27A1.5, Y43F4B.7 and Y4C6B.2.

1.3. Peptide transporters

Dietary proteins are hydrolysed within the intestinal lumen into oligopeptides which in turn are cleaved into small di- and tripeptides and free amino acids by several membrane anchored peptidases at the intestinal brush border membrane (53). Amino acid transporters are responsible for the uptake of free amino acids, while in parallel bulk quantities of amino acids are taken up in form of di- and tripeptides via the intestinal peptide transporter PEPT1 (SLC15A1) which was first isolated from the small intestine of rabbit (54). Peptide transport across cell membranes is widely distributed throughout species like bacteria, yeasts, nematodes and mammals. Mammalian PEPT1 is located at the brush border membrane of the duodenum, jejunum and ileum (55). It is a symporter for small peptides and protons (stoichiometry 1:1) in a low-affinity, high-capacity pattern (Figure 4). PEPT1 has a very broad substrate specificity and accepts, with only few exceptions, all 400 dipeptides and 8,000 tripeptides resulting from digestion of dietary protein (56). Additionally, PEPT1 enables uptake of drugs and

pharmaceutical compounds like β -lactam antibiotics, angiotensin-converting enzyme (ACE) inhibitors, anti-cancer drugs and antiviral agents like acyclovir, ganciclovir and azidothymidine (57) (58). As PEPT1 is an electrogenic proton-coupled symporter, uptake of substrates leads to an acidification of the cytosol. The driving force for absorption is the inwardly directed H^+ -electrochemical gradient in combination with the inside negative membrane potential which allows accumulation above extracellular concentration (59). To maintain this gradient and to guarantee transport capacity of PEPT1, a sodium-proton-exchanger called NHE3 (SLC9A3) located on the apical membrane of intestinal cells (60), exchanges one proton against sodium. In turn three sodium ions are exchanged against two potassium ions via a sodium-potassium-ATPase (Na^+/K^+ -ATPase) on the basolateral side (Figure 4). Studies have suggested that the inhibition of NHE3 reduces transport capacity of PEPT-1 (61) and also of the proton-driven amino acid transporter PAT1 (62).

The renal isoform of di- and tripeptide transporter is called PEPT-2 (SLC15A2) and mainly found in kidney tubule segment S3 (63), but also in choroid plexus, glia cells, testis, prostate, ovary and uterus (64). It is the high-affinity, low-capacity variant, although it transports the same substrates like PEPT-1. The stoichiometry determined for PEPT-2 is 2 protons for neutral and 3 protons for anionic peptides (65). Both peptide transporters have 12 predicted transmembrane domains with amino and carboxy termini located inside the cytosol.

These mechanisms are also conserved in *C. elegans*, where three peptide transporter isoforms are known (66). They are called PEPT-1 (formerly OPT-2, PEP-2), PEPT-2 (formerly OPT-1, PEP-1) and PEPT-3 (formerly OPT-3). For characterisation of their substrate specificity, transport studies were obtained in *Xenopus laevis* oocytes. It was shown that di- and tripeptides, and to a minor extent also tetrapeptides are transported, but no free amino acids (66). The *C. elegans pept-1* gene encodes a protein with 36.9 % amino acid sequence identity to human PEPT-1 which also functionally represents the low-affinity, high-capacity isoform. It is solely expressed in the intestine and PEPT-1 is exclusively responsible for uptake of amino acids in form of di- and tripeptides. When the gene is deleted, absorption of a fluorescent labelled dipeptide (β -Ala-Lys-AMCA)

is completely abolished (12). The uptake via PEPT-1 is independent of sodium and chloride, but accompanied by H^+ uptake resulting in acidification of the cytoplasm. A major decrease of pH_{in} is prevented by the function of NHX-2 an ortholog to mammalian sodium-proton-exchanger NHE3 which is located on the apical side of intestinal cells (11). The knockout of *C. elegans pept-1* causes amino acid deficiency, decelerated larval development (1.8-fold delayed), increased reproductive life span (9 days instead 5 days), smaller body size (~75%), reduced brood size (approximately one third), enhanced stress resistance (12) and increased fat storage with enlarged fat droplets, when compared to wild type worms (67). A similar phenotype was observed for *C. elegans* treated with *nhx-2* RNAi. Therefore, as in mammals, PEPT-1 requires NHX-2 for proper function (11).

The second homologue to the mammalian peptide transporter is PEPT-2 which is expressed in a variety of cells including vulval, pharyngeal and anal muscles but it is not found in the intestine (11). It is the high-affinity and low-capacity transporter isoform. Although the substrate specificity is similar to that of PEPT-1 (66), loss of *pept-2* does not result in an obvious phenotype (68).

PEPT-3, the third H^+ -coupled *C. elegans* peptide transporter is mainly expressed in neurons, but also in the pharynx (Wightman et al., 2005). This isoform seems to function as a H^+ -channel rather than transporter and is important for H^+ -homeostasis in *C. elegans* (69). The knockdown of *pept-3* via RNAi causes a high incidence of males in the population (70).

1.4. Amino acid sensing via TOR pathway

Amino acid transporters and the peptide transporter are responsible for maintaining intracellular amino acid concentrations. But how these levels are recognised by the cell and how altered amino acid concentrations in the cell affect the expression and function of the membrane transporters is not known. One predicted key sensor for intracellular amino acids is the target of rapamycin (TOR) pathway (Figure 5). The TOR pathway is regulated by a variety of cellular signals, not only amino acids, but also hormones such as insulin, as well as glucose, the cellular energy status and stress conditions.

TOR complex 1 and 2

Mammalian TOR (called LET-363 in *C. elegans*) forms two major types of complexes, TORC1 (TOR complex 1) and TORC2 (TOR complex 2). TORC1 and TORC2 undergo reciprocal negatively regulation (71). Rapamycin-sensitive TORC1 controls several pathways that collectively determine the mass/size of the cell (72). TORC1 is a ternary complex containing TOR, raptor (regulatory associated protein of TOR) and GβL (G-protein beta-subunit-like protein). Raptor (called DAF-15 in *C. elegans*) provides the substrate binding function to TORC1 and thus loss of raptor phenocopies loss of TORC1 (73). Activated TORC1 mediates the phosphorylation of the ribosomal protein S6K (S6 kinase) (called RSKS-1 in *C. elegans*) and 4EBP (also known as PHAS1 (phosphorylated heat-stable and acid-stable protein)) which in turn promotes protein translation and protein turnover in favorable conditions (74).

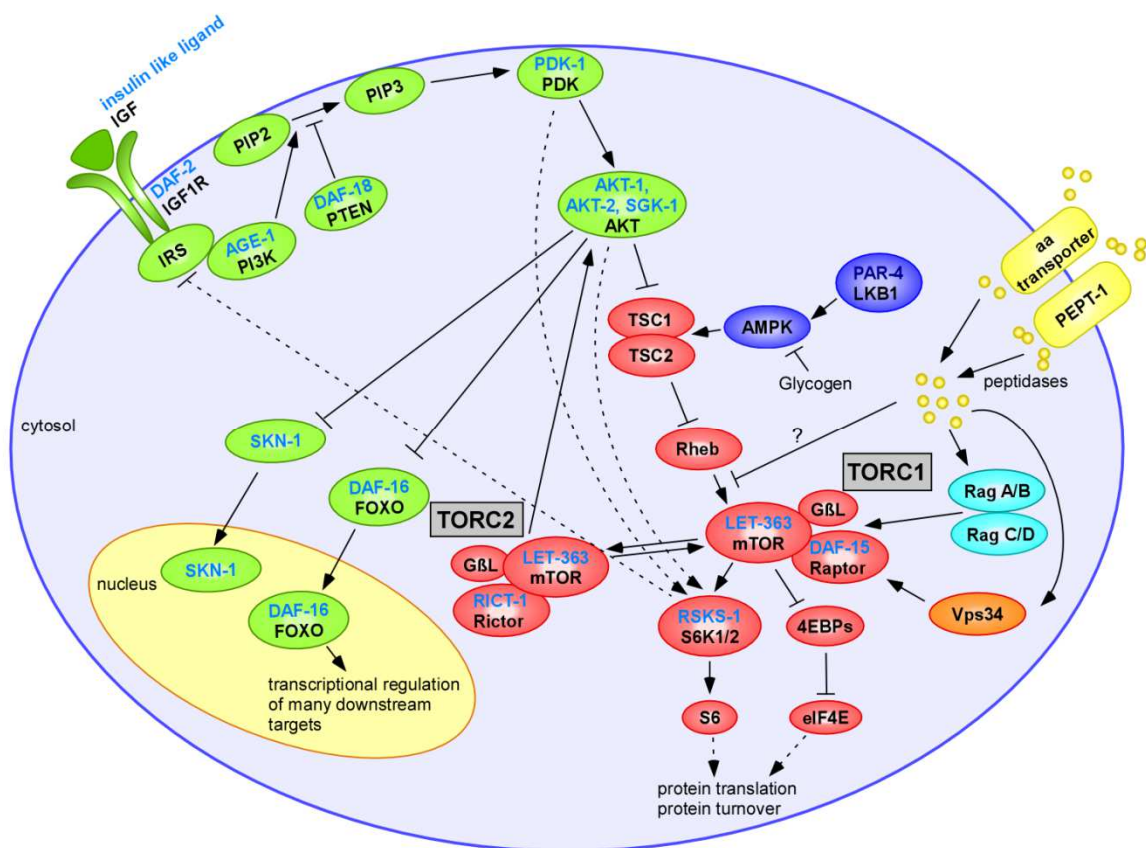


Figure 5: Interaction of different pathways with the TOR pathway

Interplay of different pathways (insulin-like signalling cascade (green), AMPK (blue)) on TOR pathway (red) and intracellular amino acid sensing via Rag proteins (light blue) and Vps34 (orange). The mammalian proteins are denoted in black, whereas known *C. elegans* homologues are denoted in blue.

Until now, no homologues to 4EBP were found in *C. elegans*. Rapamycin-insensitive TORC2 controls the actin cytoskeleton and thereby determines the shape of the cell. Its complex consists of TOR, GβL and rictor (RICT-1 called in *C. elegans*) and is proposed to directly control AKT phosphorylation and activation (75).

Cellular signals mediated via TOR

AKT (AKT-1, AKT-2, SGK-1 in *C. elegans*), a part of the insulin-like signalling cascade (ILS) affects indirectly also TOR through the actions of TSC1/TSC2 (tuberous sclerosis complex). In *C. elegans* no homologues to the TSC complex are known yet. In mammals the physical association of the proteins TSC1 (hamartin) and TSC2 (tuberin) produces a functional complex that inhibits mTOR through inactivation of a small GTPase known as RHEB (Ras homolog enriched in brain) (76).

AMPK (adenosine 5-monophosphate-activated protein kinase) can also modulate TOR. It functions as the key energy-sensing kinase by sensing the increase in the cellular AMP/ATP ratio which promotes AMPK phosphorylation and activation. Activated AMPK in turn phosphorylates TSC2, apparently promoting its activation (77). This in turn inhibits the action of TOR activity and, therefore, inhibits cell growth and proliferation. The Rag proteins (small guanosine triphosphatases, GTPases) A/B associate as heterodimers with Rag C/D and function as obligatory heterodimers. They bind raptor and mediate amino acid signaling to mTORC1 (78).

Thus, TOR kinase participates in critical events that integrate external signals with internal signals, coordinating cellular growth and proliferation. TOR receives signals that indicate whether transcription and translation machinery should be upregulated and efficiently transmits these signals to the appropriate pathways (79).

Amino acid sensing via TOR pathway

The TOR pathway promotes protein synthesis which in turn requires both amino acids, as precursors and metabolic energy (80). A lack of amino acids leads to dephosphorylation of 4EBP1 (81) and S6K1 is inhibited (82), suggesting that the effects of amino acids are mediated via TOR pathway (Figure 5). It was shown

that intracellular amino acids regulate TORC1 signalling (83), whereas withdrawal of leucine or arginine is each nearly as effective in downregulating TORC1 signalling as depletion of all amino acids (84). At the same time intracellular glutamine stimulates mTORC1 signalling by promoting the uptake of leucine into the cell by amino acid exchange of glutamine against leucine (85). Two amino acid regulation sites have been considered so far. The first one is Rheb, downstream of TSC1/2, that activates TORC1 through a direct interaction with mTOR (86) and withdrawal of amino acids diminishes the ability of Rheb to bind to mTOR, therefore decreasing mTORC1 activity (87). The second one comprises Rag proteins which do not stimulate the *in vitro* kinase activity of mTORC1, but they are suggested to modulate the intracellular localisation of mTORC1 in response to amino acids. In amino acid depleted cells mTOR was located in tiny punctua throughout the cytoplasm, whereas in cells stimulated with amino acids, mTOR localised to the perinuclear region of the cell and/or to large vesicular structures, the same intracellular compartment that contains its activator Rheb (78). But the ability of Rag proteins to stimulate mTORC1 requires Rheb, indicating that they may operate in parallel and not in series to regulate mTORC1 (88).

TOR activity influences amino acid transporter expression

The activity of TORC1 is to some extent dependent on the intracellular amino acid concentration, but it might be also influenced by so-called transceptors. It has been shown that activated TORC1 induces transcription and translation of LAT1 (89) (90) and system A transporters (91), and also endocytosis and degradation of 4F2hc as a subunit of heterodimeric amino acid transporters (92) (93). Transceptors were first investigated in *S. cerevisiae* (94) and studies in *Drosophila* suggest that PATs (proton-coupled amino acid transporters) regulate growth via TOR activation in a transport-independent amino acid sensing mechanism (95).

1.5. Aim of the work

The work is divided into two parts. The aim of the first part was the identification of amino acid transporters which are essential for amino acid homeostasis in *pept-1(lg601) C. elegans*. The main focus was on the class of heteromeric amino acid transporters and proton-coupled amino acid transporters, as it was recently shown that mRNA expression of those was increased in peptide transporter deficient worms.

The second part attempted to identify cellular modulator or interactor proteins of PEPT-1 in *C. elegans* which influence transcription, translation or function. One already known PEPT-1 modulator is the sodium-proton-exchanger NHX-2 which is necessary for maintaining the transmembrane proton gradient.

2. RESULTS

2.1. Amino acid homeostasis in *C. elegans*

Pept-1 deficient *C. elegans* display an overall reduced concentration of intracellular free amino acids as a consequence of the loss of the intestinal di- and tripeptide transporter (Figure 6). Interestingly, previous studies have shown that the mRNA expression levels of several heteromeric amino acid transporter (HAT) subunit homologues (*atgp-1*, *atgp-2*, *aat-2*, *aat-5* and *aat-6*) were increased in these worms when compared to wild type animals. This indicated a compensatory mechanism with increased transcription of various amino acid transporter systems.

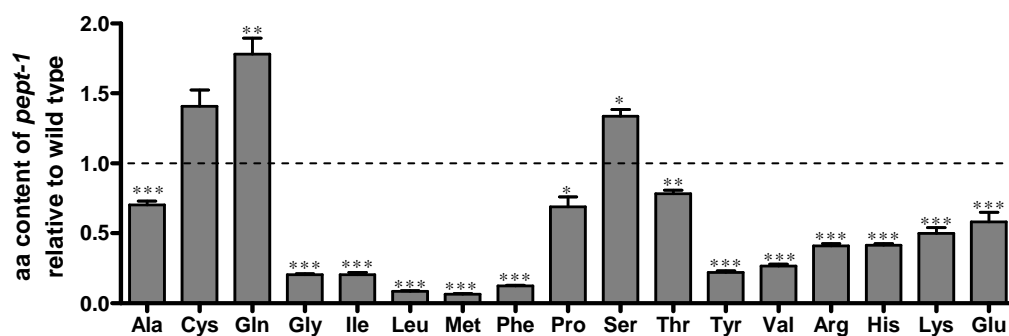


Figure 6: Relative amino acid content of *pept-1(lg601)* *C. elegans*

Amino acid (aa) composition of *pept-1(lg601)* relative to wild type *C. elegans*. Twelve independent measurements were performed. Statistical analysis was performed with a Student's *t*-Test and significance (* $p < 0.05$, ** $p < 0.01$, *** $p < 0.001$) of each amino acid of *pept-1* to its corresponding amino acid in wild type is denoted.

Transcriptome data also revealed that the mRNA expression of the proton-coupled amino acid transporter (PAT) homologue Y4C6B.2 was approximately 18-fold increased in *pept-1(lg601)* worms. Hence, two groups of amino acid transporters seem to undergo a compensatory regulation to increase amino acid absorption when the peptide transporter is lacking. According to this hypothesis HATs and PATs were selected to assess their role in overall amino acid absorption and homeostasis in peptide transporter deficient *C. elegans*.

2.1.1. Investigations into the role of HAT subunit homologues in *pept-1(lg601)*

C. elegans

Previous studies in *C. elegans* on HAT subunits determined that a co-expression of AAT-1/ATGP-2 and AAT-3/ATGP-2 was necessary to build functional transport systems in *Xenopus laevis* oocytes responsible for uptake of small neutral amino acids (41). To investigate, whether these subunits were also responsible for amino acid homeostasis in *pept-1(lg601)* worms the different *C. elegans* HAT subunits were examined.

2.1.1.1. HAT heavy subunit homologues

In mammals the HAT heavy subunits rBAT and 4F2hc are responsible for the translocation of the catalytic light subunits to the membrane where they build functional transport systems. When there is a lack of heavy subunits, the light subunits remain in the cytosol and are not able to reach the membrane and therefore, no amino acid transport can occur (96) (97). It was reported that mutations in rBAT and 4F2hc-y⁺LAT1 complex cause two diseases: cystinuria (35) and lysinuric protein intolerance (39). Due to the important role of these proteins in functional amino acid transport in mammals it was hypothesised that the *C. elegans* HAT heavy subunit homologues ATGP-1 and ATGP-2 may play an important role in increasing amino acid absorption to compensate for the loss of PEPT-1.

When there is a lack of nutrients the number of progeny as an indicator of fitness decreases (98) which was also observed for *pept-1(lg601)* *C. elegans* (12). If HAT heavy subunits are as important in *C. elegans* as in mammals, the knockout of ATGP-1 or ATGP-2 might result in a decreased number of progeny. Hence the brood size was determined for wild type (N2), *atgp-1(ok388)* and *atgp-2(ok352)* knockout *C. elegans*. As normal plasma amino acid levels were described in patients with cystinuria which was postulated to arise from compensatory uptake of amino acids in peptide bound form (99), additional RNAi knockdown of *atgp-1* and *atgp-2* was performed in *pept-1(lg601)* worms and the number of progeny was determined as well (Figure 7).

There was no significant alteration in the number of progeny neither in *atgp-1(ok388)* (170 ± 8) nor in *atgp-2(ok352)* (150 ± 5) knockout strain compared with wild type (172 ± 22) *C. elegans*. Additional RNAi silencing of *atgp-1* (29 ± 2) and *atgp-2* (30 ± 2) in *pept-1(lg601)* worms did also not affect the number of progeny.

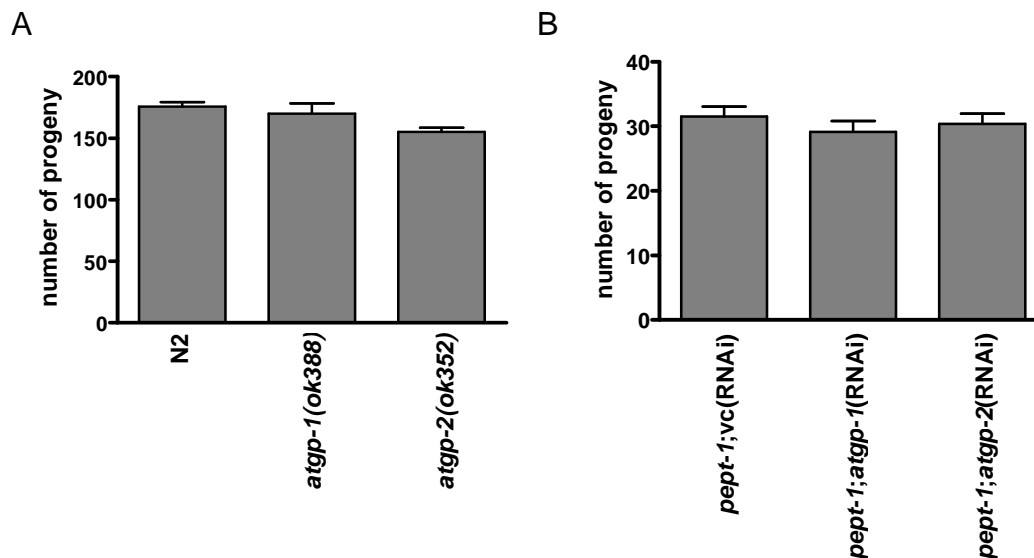


Figure 7: Brood size of HAT heavy subunit deficient *C. elegans*

(A) Number of progeny of wild type (N2), *atgp-1(ok388)* and *atgp-2(ok352)* worms and (B) with RNAi silencing of *atgp-1* and *atgp-2* in *pept-1(lg601)* worms compared with *pept-1;vc(RNAi)*. Each experiment was performed two times, whereby each time the number of progeny of 25 to 35 worms per group was counted.

In general, the reproduction rate of *pept-1(lg601)* worms grown on vector control RNAi bacteria was strongly reduced when compared to *pept-1* grown on *E. coli* OP50 (31 ± 2 progeny to approximately 100 progeny), an effect that was also reported by Brooks et al. (100).

As RNAi silencing of *atgp-1* and *atgp-2* in *pept-1(lg601)* *C. elegans* did not alter the number of progeny, a double RNAi knockdown of one HAT heavy subunit (ATGP-1 or ATGP-2) together with one HAT light subunit (AAT-1 or AAT-3) was performed in *pept-1(lg601)* worms (Figure 8).

Neither in *pept-1(lg601)* worms with the double RNAi knockdown of the functional transport systems AAT-1/ATGP-2 (22 ± 2) and AAT-3/ATGP-2 (26 ± 2), nor in *pept-1;aat-1/atgp-2*(RNAi) (27 ± 2) and in *pept-1;aat-3/atgp-1*(RNAi) (26 ± 2) worms an alteration in reproduction could be observed.

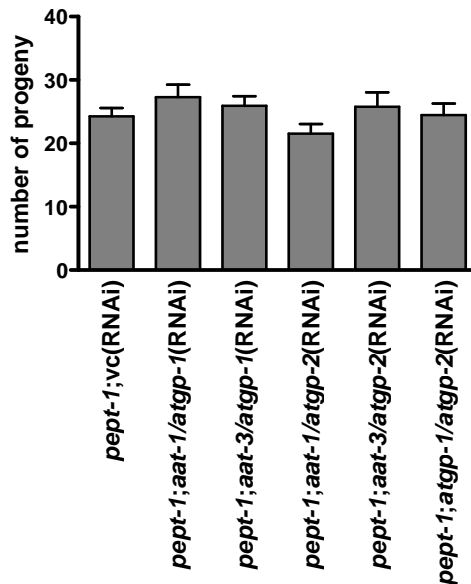


Figure 8: Brood size of *pept-1(lg601)* worms with RNAi double knockdown of HAT subunits

An RNAi double knockdown of the heavy subunit homologues *atgp-1* and *atgp-2* in combination with the light subunits *aat-1* and *aat-3* was performed in *pept-1(lg601)* worms and the number of progeny was counted. Also a double knockdown of both heavy subunit homologues was investigated. The experiment was performed two times, whereby each time the number of progeny of 25 to 29 worms per group was counted.

Also RNAi double knockdown of both heavy subunit homologues *atgp-1* and *atgp-2* (24 ± 2) failed to cause a significant reduction in reproduction.

To determine whether silencing of *atgp-1* and *atgp-2* had an effect on protein expression of PEPT-1, western blot analysis was performed (Figure 9). *C. elegans* PEPT-1 protein has an estimated molecular weight of 94.1 kDa. *Xenopus laevis* oocytes expressing *C. elegans* PEPT-1 were used as positive control and there the detected protein appeared at approximately 95 kDa (Figure 9, left lane).

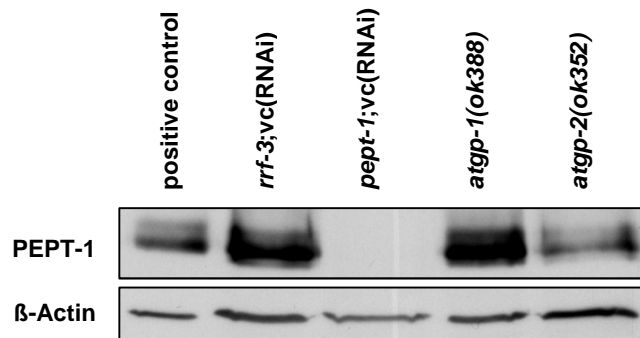


Figure 9: PEPT-1 protein expression in *C. elegans* with HSHAT knockout

PEPT-1 protein expression of membrane protein lysates of controls (*rrf-3*, *pept-1*) and *atgp-1(ok388)* and *atgp-2(ok352)* knockout worms was determined. 20 μ g protein lysates were loaded per lane. Oocytes expressing *C. elegans* PEPT-1 were used as a positive control and β -Actin was used as a loading control.

As expected, *pept-1;vc(RNAi)* worms lacked the PEPT-1 protein. Compared with *rrf-3(pk1426)* worms PEPT-1 expression in *atgp-1(ok388)* *C. elegans* was slightly increased, while it was decreased in *atgp-2(ok352)* worms. To investigate whether knockout of one HAT heavy subunit could be compensated by the other one, ATGP-1 and ATGP-2 protein expression was also examined (Figure 10).

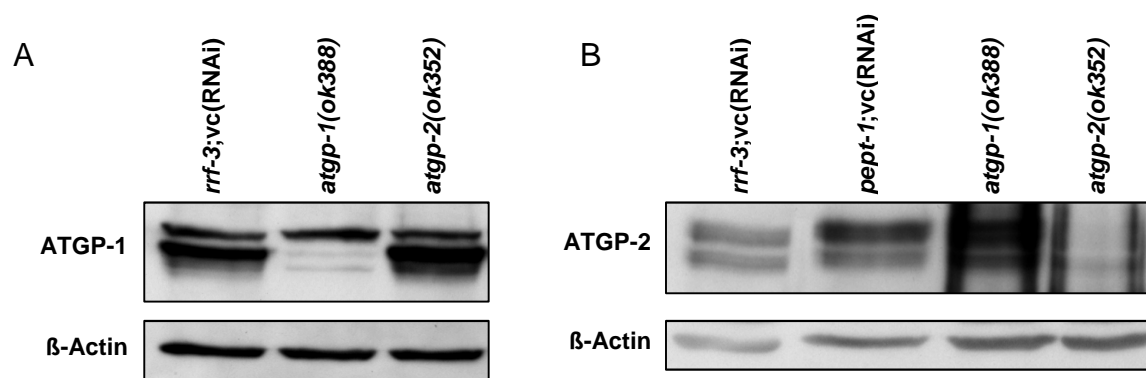


Figure 10: ATGP-1 and ATGP-2 protein expression in *C. elegans* with HSHAT knockout

(A) ATGP-1 and (B) ATGP-2 protein expression of membrane protein lysates of controls (*rrf-3*, *pept-1*) and *atgp-1(ok388)* and *atgp-2(ok352)* knockout worms was determined. 20 μ g protein lysates were loaded per lane. β -Actin was used as a loading control.

The calculated molecular weight of ATGP-1 is 69.3 kDa. When using an ATGP-1 specific antibody in worm membrane protein lysates two bands could be observed. The lower band is represented by the ATGP-1 protein, because in *atgp-1(ok388)* knockout worms this band was missing. In *atgp-2(ok352)* worms ATGP-1 protein level was increased (Figure 10A). ATGP-2 has an estimated

weight of 73.4 kDa and two bands appeared at 65 and 75 kDa respectively. Both bands were related to ATGP-2, because in *atgp-2(ok352)* worms both were missing. In *pept-1(lg601)* as well as in *atgp-1(ok388)* worms ATGP-2 protein expression was strongly elevated (Figure 10B). Hence it seems that the knockout of one HAT heavy subunit could be at least partly compensated by increased protein expression of the other one.

Single knockout and even additional RNAi knockdown of the heavy subunit homologues in *pept-1(lg601)* worms alone or in combination with a light subunit did not affect the number of progeny. This however does not exclude that the heavy subunit homologues ATGP-1 and ATGP-2 are as important for amino acid absorption and homeostasis in worms as in mammals with their loss-of-function leading to changes in overall amino acid status and composition. Hence, amino acid concentration was measured in *atgp-1(ok388)* and *atgp-2(ok352)* knockout *C. elegans* (Figure 11).

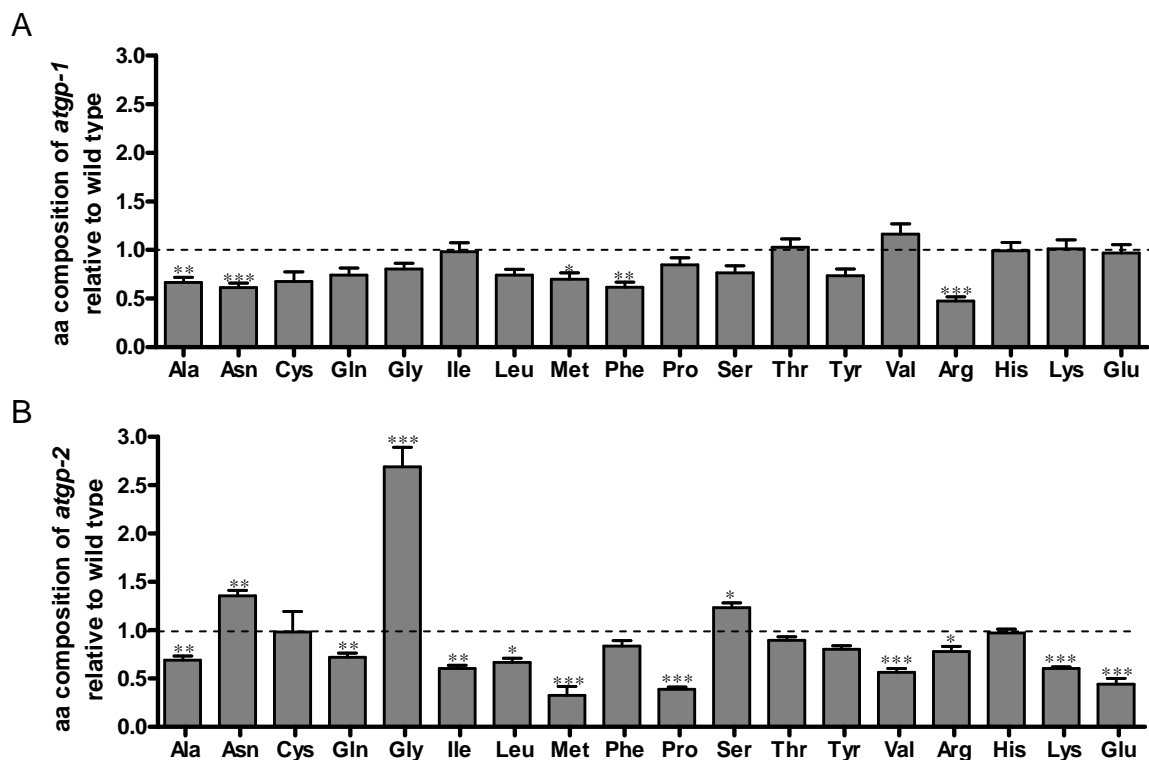


Figure 11: Amino acid content of *atgp-1* and *atgp-2* *C. elegans* relative to wild type
 Amino acid (aa) composition of (A) *atgp-1(ok388)* and (B) *atgp-2(ok352)* *C. elegans* relative to wild type. Five independent measurements were performed. Statistical analysis was performed with a Student's *t*-Test and significance (* $p < 0.05$, ** $p < 0.01$, *** $p < 0.001$) of each amino acid of *atgp-1/atgp-2* worms to its corresponding amino acid in wild type worms is denoted.

In *atgp-1(ok388)* knockout *C. elegans* only slight changes in amino acid composition compared with wild type could be observed (Figure 11A), whereas worms with a knockout of the heavy subunit homologue *atgp-2(ok352)* showed distinct differences (Figure 11B). Concentrations of 10 out of 18 analysed proteinogenic amino acids including glutamine, proline and methionine were significantly decreased compared to wild type worms, while three amino acids and in particular glycine levels were significantly increased. Hence, ATGP-2 deficiency seems to have a stronger effect than the lack of ATGP-1 on overall amino acid composition in *C. elegans*.

Glutathione is composed of three amino acids: glutamine, cysteine and glycine. As the amino acid concentration of glutamine and glycine was significantly altered in *atgp-2(ok352)* worms and the predicted mammalian homologue rBAT is responsible for transport of cystine which is rapidly reduced to cysteine, the limiting substrate for the synthesis of intracellular glutathione (101), tGSH and GSSG levels were measured in *atgp-2(ok352)* knockout *C. elegans* (Figure 12).

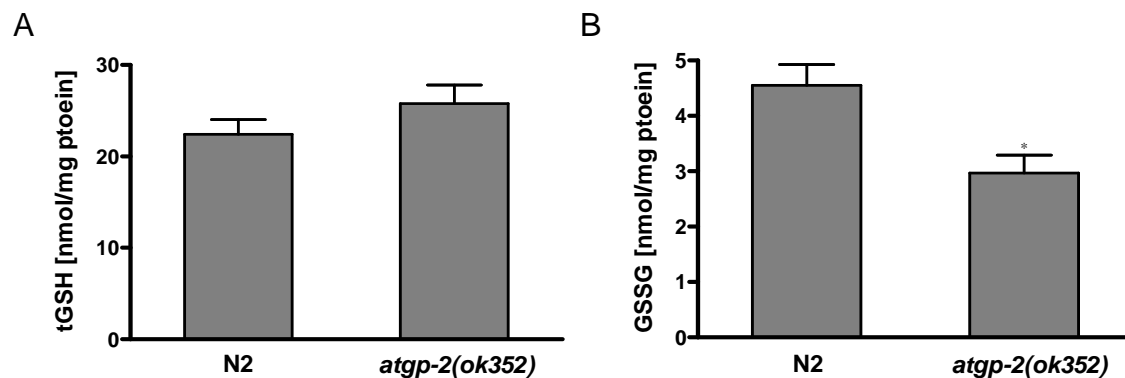


Figure 12: Total GSH and GSSG content of wild type and *atgp-2(ok352)* *C. elegans*
 Measurement of (A) total GSH (tGSH) and (B) GSSG levels of wild type (N2) and *atgp-2(ok352)* *C. elegans*. The experiment was performed at least four times, each time with repeated determination. Statistical analysis was performed by a Student's *t*-Test. Significance (* $p < 0.05$) compared with N2 is denoted.

No alteration in the concentration of total GSH (Figure 12A) was determined for *atgp-2(ok352)* *C. elegans*, while GSSG levels (Figure 12B) were significantly ($p < 0.05$) reduced to 2.9 ± 0.3 nmol GSSG/mg protein compared with wild type (4.5 ± 0.4 nmol GSSG/mg protein).

2.1.1.2. HAT light subunit homologues

Besides the two heavy subunit homologues ATGP-1 and ATGP-2 there are also nine homologues to mammalian HAT light subunits (AAT-1 to AAT-9) known in *C. elegans*. Because two RNAi bacteria (for *aat-4* and *aat-9*) were missing in the RNAi library of J. Ahringer, they have been cloned and tested (Figure 13) and afterwards the effect of RNAi knockdown of all HAT light subunit homologues on the number of progeny of *pept-1(lg601)* *C. elegans* was performed (Figure 14).

Measurements of mRNA expression of *aat-4* in *pept-1;aat-4(RNAi)* and *aat-9* in *pept-1;aat-9(RNAi)* worms was performed to discover the functionality of the corresponding RNAi bacteria (Figure 13).

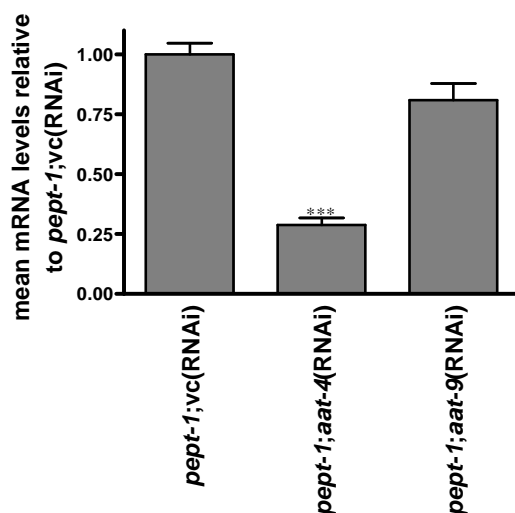


Figure 13: Functionality of *aat-4* and *aat-9* RNAi

Mean normalised mRNA expression of *aat-4* and *aat-9* of *pept-1* *C. elegans* treated with corresponding RNAi relative to *pept-1;vc(RNAi)*. The experiment was performed two times with two technical replicates. Statistical analysis was performed by a Student's *t*-Test. Significance (***) $p < 0.001$ to *pept-1;vc(RNAi)* is denoted.

Gene silencing in worms treated with *aat-4* RNAi decrease the mRNA level approximately 75 %, while the expression of *aat-9* mRNA in *C. elegans* grown on *aat-9* RNAi bacteria was reduced by only 20 %. The main expression of AAT-9 occurs in head neurons and only some expression is found in pharynx muscle cells (42). A combination of a delayed and less robust response of RNAi in the nervous system (102) might explain the poor decrease of mRNA levels observed (Figure 13).

To investigate the role of the light subunits AAT-1 to AAT-9 in animals lacking PEPT-1 the corresponding genes were silenced via RNAi and the number of progeny was counted (Figure 14).

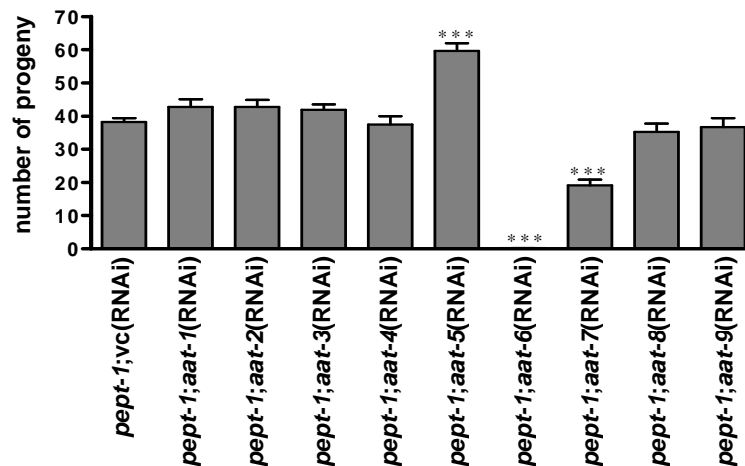


Figure 14: Brood size of *pept-1(lg601)* *C. elegans* with RNAi of LSHAT subunits

The number of progeny of *pept-1* *C. elegans* with single knockdown of all HAT light subunit homologues (*aat-1* to *aat-9*) was counted. The experiment was performed two times, whereby each time the number of progeny of 23 to 30 worms per group was counted. Statistical analysis was performed by a Student's *t*-Test. Significance (***) $p < 0.001$ to *pept-1;vc(RNAi)* is denoted.

The number of progeny of *pept-1(lg601)* worms with single RNAi silencing of HAT light subunit genes was in most cases (*aat-1*, *aat-2*, *aat-3*, *aat-4*, *aat-8* and *aat-9*) not altered (Figure 14), while RNAi knockdown of *aat-5* significantly increased (60 ± 3) the progeny compared with control animals (38 ± 1).

By contrast, knockdown of *aat-6* and *aat-7* caused a significantly reduced brood size or even sterility (0 and 19 ± 2). To determine whether these alterations in brood size of *pept-1(lg601)* worms treated with *aat-5*, *aat-6* and *aat-7* RNAi were dependent on the lack of di- and tripeptides they were additionally knocked down in *rrf-3(pk1426)* worms (Figure 15).

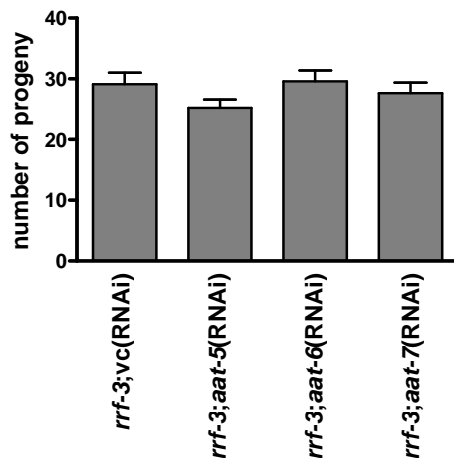


Figure 15: Brood size of *rrf-3(pk1426)* *C. elegans* treated with RNAi of *aat-5*, *aat-6* and *aat-7* LSHAT subunits

Number of progeny was counted in *rrf-3(pk1426)* *C. elegans* with RNAi knockdown of *aat-5*, *aat-6* and *aat-7*. The experiment was performed two times whereby each time the number of progeny of 30 to 36 worms per group was counted.

Since the number of progeny in *rrf-3(pk1426)* worms grown on *aat-5*, *aat-6* and *aat-7* RNAi bacteria was not affected (Figure 15), but in *pept-1(lg601)* it can be speculated that the peptide transporter may compensate effects on brood size by providing sufficient amino acid uptake in form of di- and tripeptides when the two amino acid transporters have impaired function.

2.1.2. Investigations on the PAT homologues in *pept-1(lg601)* *C. elegans*

In mammals members of the SLC36 family (proton-coupled amino acid transporters, PATs) are responsible for the export of lysosomal proteolysis products into the cytosol as well as for the absorption of amino acids in the intestine (103). Based on BLAST data there are three predicted homologues of mammalian PAT proteins present in *C. elegans*, T27A1.5, Y43F4B.7 and Y4C6B.2. Transcriptome data revealed an approximately two-fold (T27A1.5) respectively 18-fold (Y4C6B.2) increase in the mRNA level in *pept-1(lg601)* worms when compared to wild type animals. Hence, this class of amino acid transporters might also be involved in the amino acid homeostasis of peptide transporter deficient worms. The number of progeny of *pept-1(lg601)* worms treated with RNAi of the three PAT homologues (T27A1.5, Y43F4B.7 and

Y4C6B.2) was counted to assess the role of these transporters in processes related to reproduction (Figure 16).

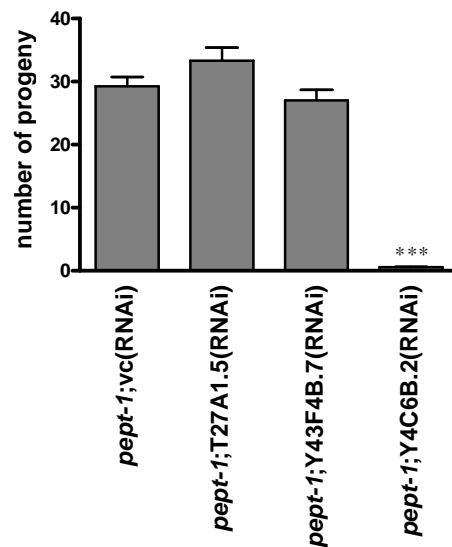


Figure 16: Brood size of *pept-1(lg601)* *C. elegans* treated with RNAi of PAT homologues

The number of progeny was counted in *pept-1(lg601)* *C. elegans* grown on T27A1.5, Y43F4B.7 and Y4C6B.2 RNAi bacteria. The experiment was performed two times whereby each time the number of progeny of 27 to 30 worms per group was counted. Statistical analysis was performed by a Student's *t*-Test. Significance (***) $p < 0.001$ to *pept-1*;vc(RNAi) is denoted.

Treatment of *pept-1(lg601)* with RNAi of T27A1.5 (33 ± 2 progeny) and Y43F4B.7 (27 ± 2) caused no alterations in the number of progeny compared to control animals (29 ± 2) while knockdown of Y4C6B.2 in *pept-1(lg601)* worms resulted in an almost sterile phenotype. To determine whether this effect was dependent on a *pept-1* knockout background, Y4C6B.2 was silenced in *rff-3(pk1426)* *C. elegans* (Figure 17).

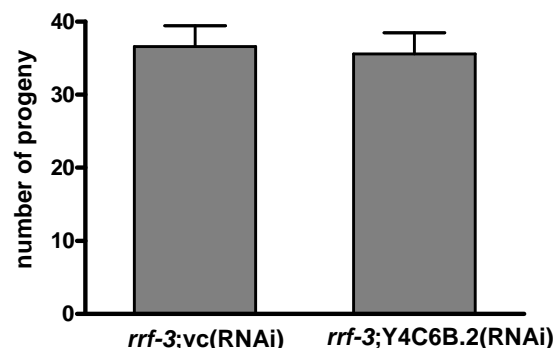


Figure 17: Brood size of *rff-3(pk1426)* *C. elegans* treated with Y4C6B.2 RNAi

The number of progeny of *rff-3(pk1426)* worms grown on vector control and Y4C6B.2 RNAi was determined. The experiment was performed two times whereby each time 22 to 27 worms per group were counted.

Knockdown of Y4C6B.2 in wild type background caused no significant reduction in the number of progeny compared with control worms (Figure 17). It was proven that the sterile phenotype in *pept-1;Y4C6B.2(RNAi)* worms was dependent on the lack of the di- and tripeptide transporter.

2.1.3. Further characterisation of the role of *aat-6* and Y4C6B.2 in *pept-1(lg601) C. elegans*

RNAi knockdown of *aat-6* and Y4C6B.2 evoked the strongest phenotype of all tested HAT subunits and PAT homologues in *pept-1(lg601)* worms. They were the most relevant candidates responsible for amino acid homeostasis in *pept-1(lg601) C. elegans*. Therefore the phenotypic characteristics of *pept-1;aat-6(RNAi)* and *pept-1;Y4C6B.2(RNAi)* worms were further investigated.

2.1.3.1. Functionality of *aat-6* and Y4C6B.2 RNAi in *pept-1(lg601) C. elegans*

To prove that the investigated sterile phenotypes in *pept-1(lg601)* treated with *aat-6* and Y4C6B.2 RNAi were due to degradation of the corresponding mRNAs, real-time RT-PCR was performed (Figure 18).

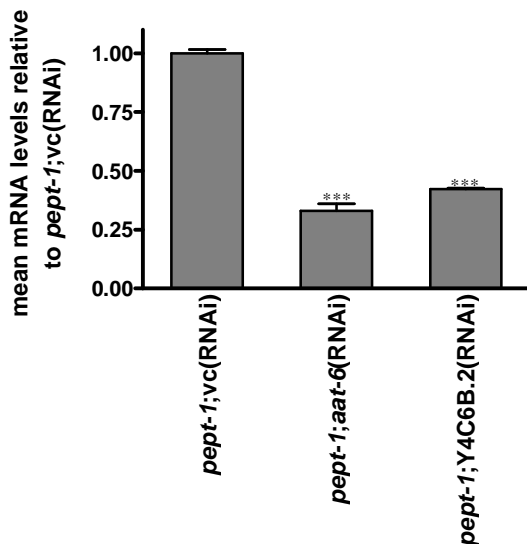


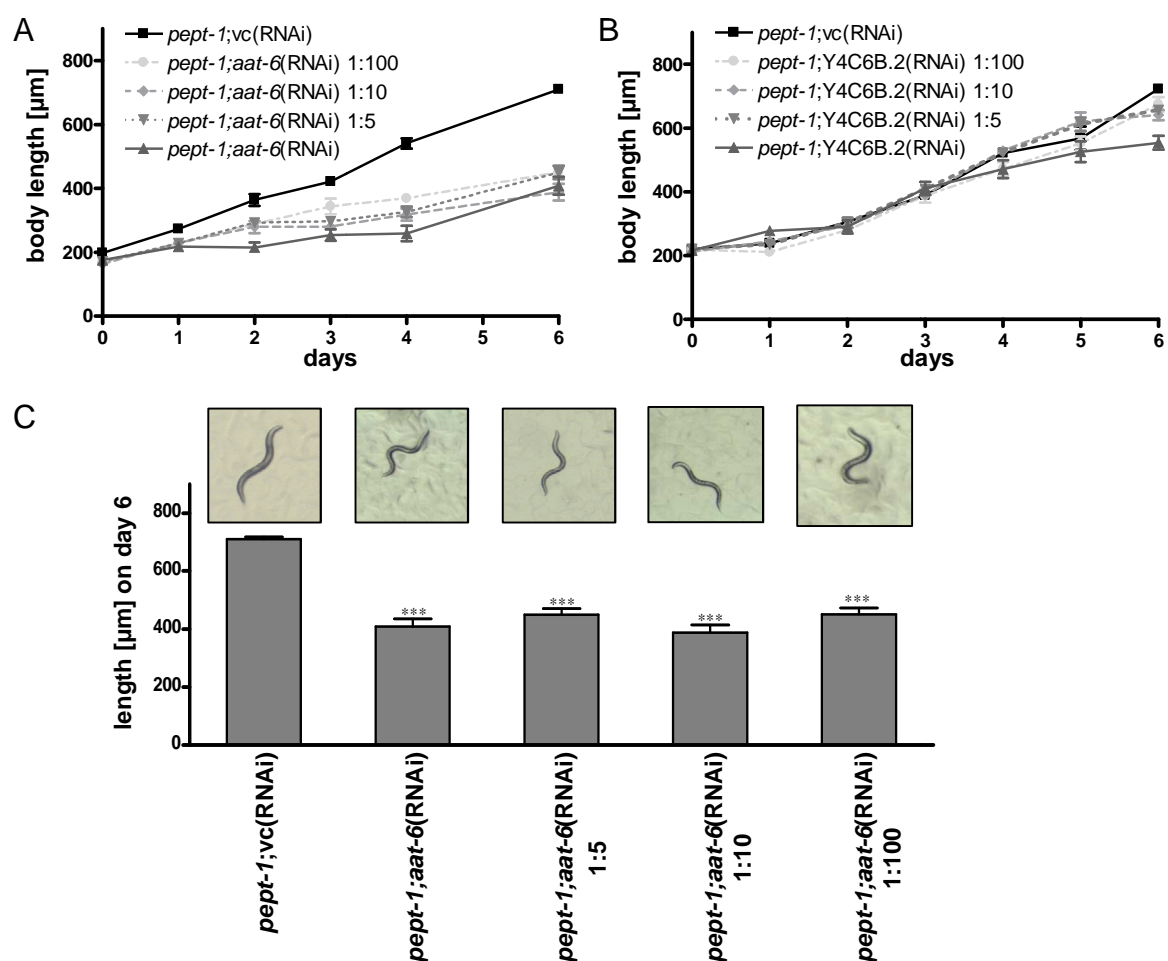
Figure 18: Functionality of *aat-6* and Y4C6B.2 RNAi

Mean normalised mRNA levels relative to *pept-1;vc(RNAi)* of *aat-6* in *pept-1;aat-6(RNAi)* worms and Y4C6B.2 in *pept-1;Y4C6B.2 RNAi* worms. The experiment was performed two times with two technical replicates. Statistical analysis was performed by a Student's *t*-Test. Significance (***) $p < 0.001$ to *pept-1;vc(RNAi)* is denoted.

RNAi knockdown of *aat-6* caused a reduction in mRNA level by almost 70 %, whereas mRNA of Y4C6B.2 in *pept-1;Y4C6B.2(RNAi)* worms was diminished to 42 % when compared with *pept-1(lg601)* treated with vector control. Hence the observed phenotypes in *pept-1(lg601)* *C. elegans* were actually caused by gene silencing of *aat-6* and Y4C6B.2.

2.1.3.2. Influence of *aat-6* and Y4C6B.2 RNAi on growth development and reproduction

A growth developmental assay was performed to examine the effect of *aat-6* and Y4C6B.2 gene silencing in *pept-1(lg601)* worms on postembryonic development and body size besides the observed sterile phenotype. RNAi bacteria of *aat-6* and Y4C6B.2 were diluted with vector control bacteria in a ratio 1:5, 1:10 and 1:100 to determine how strong the effect was (Figure 19).



D

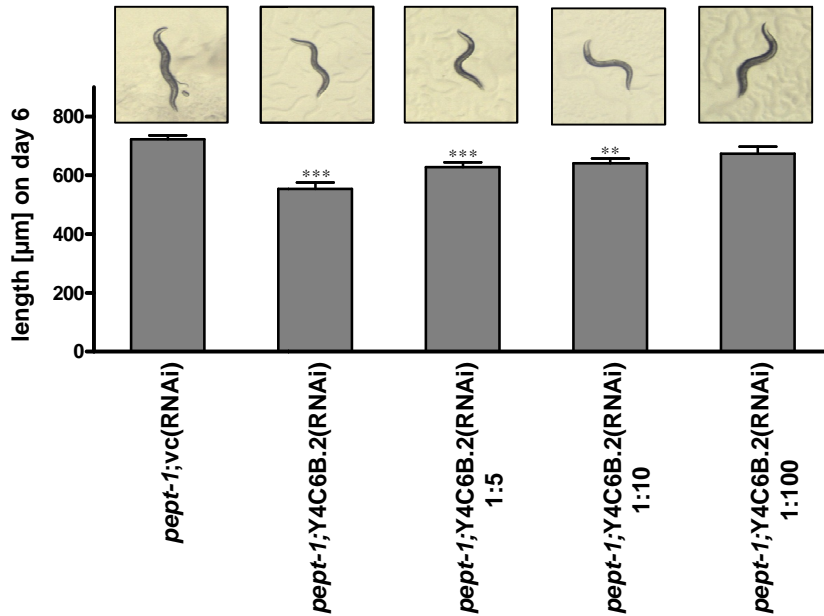


Figure 19: Development of *pept-1(lg601)* worms on diluted *aat-6* and Y4C6B.2 RNAi bacteria

Larval development of *C. elegans* treated with diluted (A) *aat-6* and (B) Y4C6B.2 RNAi bacteria. Eight worms per group were photographed daily (24 h period) and body length was measured. (C) Images of final body length and mean length of *pept-1(lg601)* worms grown on *aat-6* RNAi and (D) Y4C6B.2 RNAi. A 40x magnification was used. Statistical analysis was performed by a Student's *t*-Test. Significance (** $p < 0.01$, *** $p < 0.001$) to *pept-1;vc(RNAi)* is denoted.

Examination of the postembryonic growth started with synchronised L1 larvae and lasted until day six, when *pept-1;vc(RNAi)* worms reached adulthood with a body length of $710 \pm 8 \mu\text{m}$. In *pept-1(lg601)* worms treated with various dilutions of *aat-6* RNAi the growth was impaired (between 388 and 455 μm final body length on day six) as shown in Figure 19A while growth development of *pept-1;Y4C6B.2(RNAi)* was comparable to control animals until day three (Figure 19B). On day six *pept-1(lg601)* worms grown on Y4C6B.2 RNAi bacteria (1:1 and 1:5 dilutions) had a significant decrease in final body size (554 respectively 627 μm), whereas 1:10 and especially 1:100 dilutions could partly diminish this phenotype. Hence both RNAi knockdowns (*aat-6* and Y4C6B.2) caused a retarded development and reduced adult body size, with much stronger effects of *aat-6* than Y4C6B.2 in *pept-1(lg601)* worms (Figure 19C and D). Furthermore, the effect of the increasing dilutions of *aat-6* and Y4C6B.2 RNAi bacteria on the number of progeny was quantified (Figure 20).

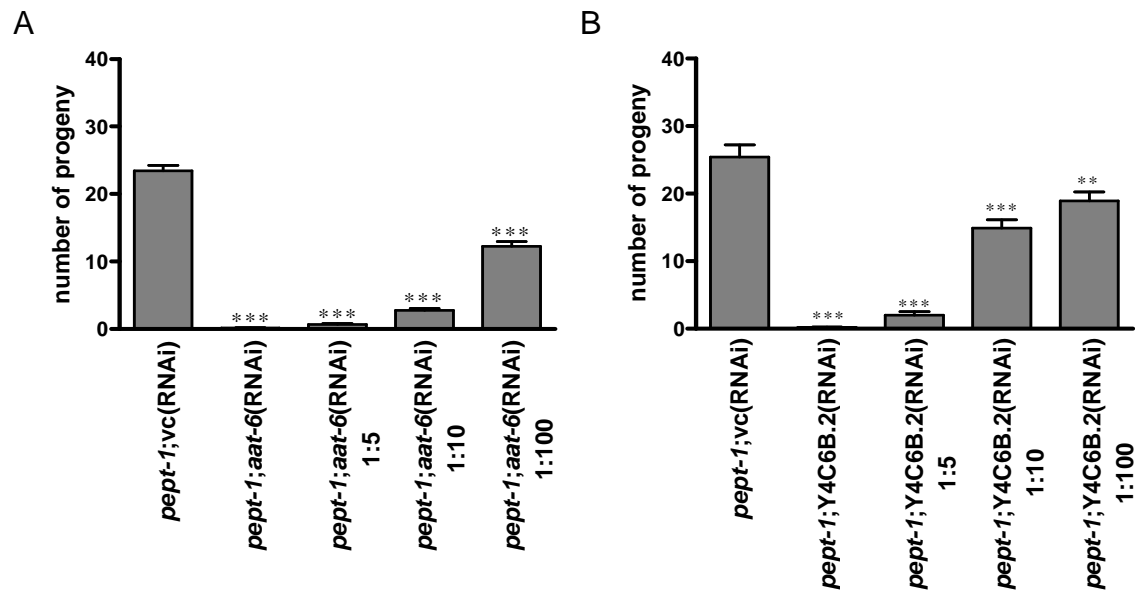


Figure 20: Brood size of *pept-1(lg601)* worms treated with diluted *aat-6* and Y4C6B.2 RNAi

Number of progeny of *pept-1(lg601)* *C. elegans* grown on different diluted (A) *aat-6* and (B) Y4C6B.2 RNAi bacteria was determined. The experiment was performed three times whereby each time the number of progeny of 26 to 33 worms per group was counted. Statistical analysis was performed by a Student's *t*-Test. Significance (** $p < 0.01$, *** $p < 0.001$) to *pept-1;vc(RNAi)* is denoted.

Impaired growth and development in *pept-1;aat-6(RNAi)* worms could not be rescued by dilution of *aat-6* RNAi bacteria, while the dilutions could partially counteract the sterile phenotype (Figure 20A). A 1:100 dilution enhanced the number of progeny up to 12 ± 1 , but it was significantly less than in control worms (24 ± 1). Dilutions of Y4C6B.2 RNAi bacteria in turn were also able to increase the number of progeny up to 19 ± 1 (dilution 1:100) as shown in Figure 20B. Thus, the sterile phenotype of *pept-1;aat-6(RNAi)* could be partially rescued by dilutions, whereas they did not affect reduced body size and retarded development. By contrast, in Y4C6B.2 RNAi treated *C. elegans* dilutions were able to partly counteract both phenotypic characteristics.

2.1.3.3. Effects of amino acid supplementation on *aat-6* and Y4C6B.2 depleted *pept-1(lg601)* *C. elegans*

Meissner and co-workers (12) had shown that free amino acid supplementation of *pept-1(lg601)* *C. elegans* could significantly increase the number of progeny and modestly reduce generation time. Therefore, the effect of amino acid

supplementation in *pept-1;aat-6(RNAi)* and *pept-1;Y4C6B.2(RNAi)* *C. elegans* on growth, development, adult body size and number of progeny was determined as well (Figure 21).

Amino acid supplementation had no influence on growth development and adult body size in control worms. RNAi knockdown of *aat-6* in *pept-1(lg601)* worms resulted in a retarded growth and development which could be compensated by amino acid supplementation until day five (Figure 21A). After that development stagnated and the final adult body length was comparable with *pept-1;aat-6(RNAi)* without additional free amino acids.

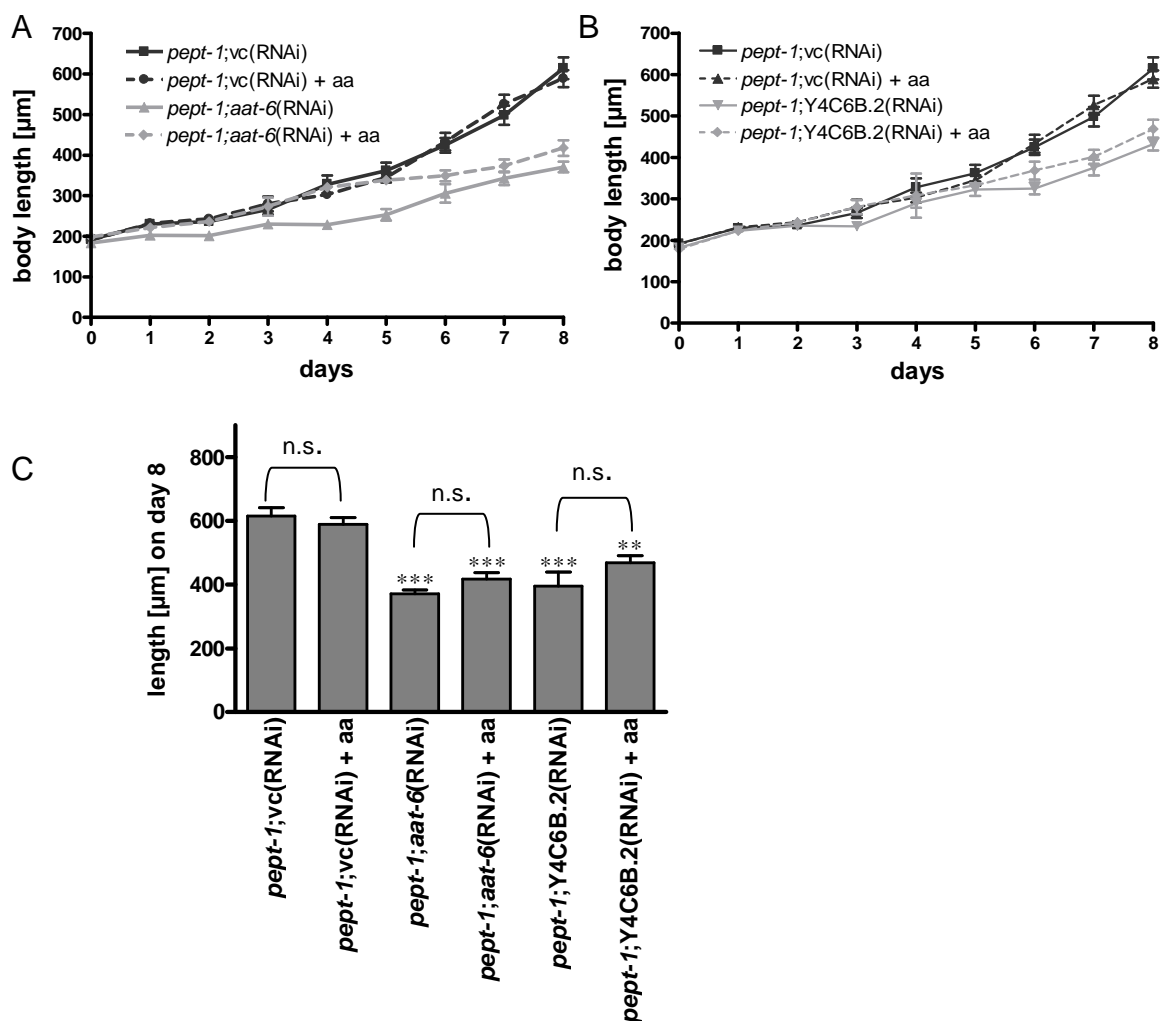


Figure 21: Influence of amino acid supplementation on development of *pept-1(lg601)* *C. elegans* treated with *aat-6* and *Y4C6B.2* RNAi

Larval development of *pept-1(lg601)* worms grown on vector control and (A) *aat-6* RNAi or (B) *Y4C6B.2* RNAi bacteria with and without amino acid (aa) supplementation. Eight worms per group were photographed daily (24 h period) and body length was measured. (C) Mean body length of *pept-1(lg601)* worms treated with vector control, *aat-6* and *Y4C6B.2* RNAi with and without aa supplementation on day eight. Statistical analysis was performed by a One-way-ANOVA with Turkey Post test. Significance (** $p < 0.01$, *** $p < 0.001$) to *pept-1;vc(RNAi)* is denoted, whereas n.s. = not significant.

Using *pept-1(lg601)* *C. elegans* treated with Y4C6B.2 the amino acid supplementation had almost no effect on growth and adult body size as shown in Figure 21B. These results were comparable with the effects of amino acid supplementation in *pept-1(lg601)* worms (12).

To examine whether the availability of additional free amino acids also affected the number of progeny, as demonstrated for *pept-1(lg601)* a brood size assay was performed (Figure 22). As previously described, the number of progeny of *pept-1(lg601)* worms when grown on the amino acid supplement was significantly increased (36 ± 2 versus 27 ± 2) (12). By contrast, neither in *pept-1;aat-6(RNAi)* nor in *pept-1;Y4C6B.2(RNAi)* *C. elegans* the sterile phenotype was affected by the availability of free amino acids (Figure 22).

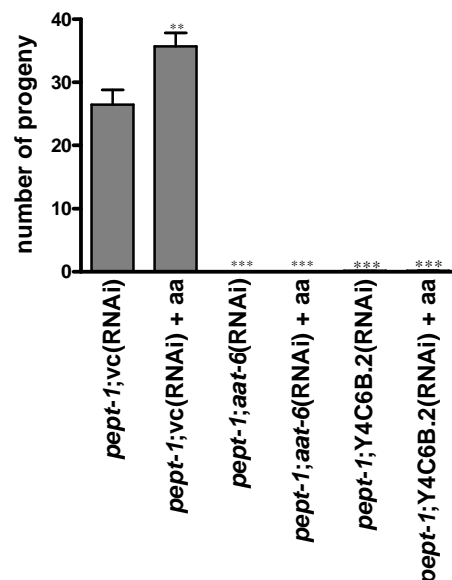


Figure 22: Influence of amino acid supplementation on the number of progeny

Number of progeny of *pept-1(lg601)* *C. elegans*, grown on vector control (vc), *aat-6* and Y4C6B.2 RNAi bacteria with and without amino acid (aa) supplementation was determined. The experiment was performed two times whereby each time the number of progeny of 30 to 33 worms per group was counted. Statistical analysis was performed by a Student's *t*-Test. Significance (***) $p < 0.001$ of each treatment to *pept-1;vc(RNAi)* control is denoted.

Both phenotypes (shortened body size and sterility) in *aat-6* and Y4C6B.2 RNAi treated *pept-1(lg601)* worms could not be rescued by amino acid supplementation.

2.1.3.4. PEPT-1, ATGP-1 and ATGP-2 protein expression in an *aat-6*(RNAi) background

To determine whether RNAi knockdown of *aat-6* and therefore diminished amino acid transport could be compensated by increased expression of the di- and tripeptide transporter PEPT-1 (in *rrf-3;aat-6*(RNAi) *C. elegans*) or the HAT heavy subunits (ATGP-1 or ATGP-2), western blot analysis of these proteins was performed (Figure 23 and 24).

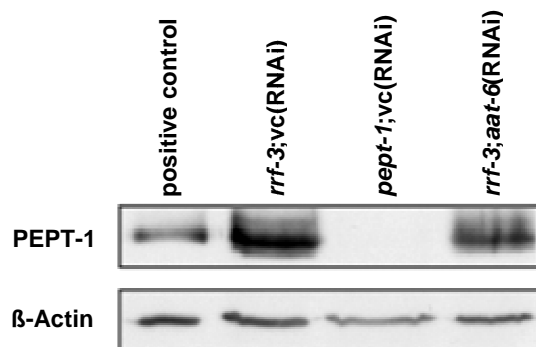


Figure 23: PEPT-1 protein level in an *aat-6*(RNAi) background

PEPT-1 protein expression of membrane protein lysates of controls (*rrf-3*, *pept-1*) and *rrf-3;aat-6*(RNAi) worms was determined. 20 µg protein lysates were loaded per lane. β-Actin was used as a loading control. Oocytes expressing *C. elegans* PEPT-1 were used as a positive control.

No PEPT-1 protein expression could be observed in *pept-1;vc*(RNAi) *C. elegans*. Compared with control, *rrf-3;aat-6*(RNAi) treated worms showed a reduction of PEPT-1 protein expression (Figure 23). In a next step it was investigated whether there might be some compensation mechanisms with HAT heavy subunits ATGP-1 and ATGP-2 (Figure 24).

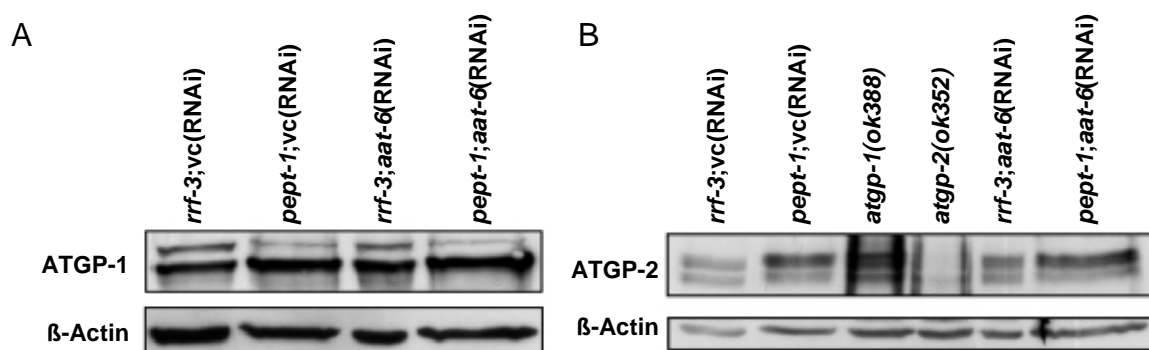


Figure 24: ATGP-1 and ATGP-2 protein levels in an *aat-6*(RNAi) background

(A) ATGP-1 and (B) ATGP-2 protein expression of membrane protein lysates of controls (*rrf-3*, *pept-1*, *atgp-1* and *atgp-2*) and *rrf-3;aat-6*(RNAi) and *pept-1;aat-6*(RNAi) worms was determined. 20 µg protein lysates were loaded per lane. β-Actin was used as a loading control.

The lower band shown in Figure 24A represents the protein ATGP-1. The signal for *pept-1(lg601)* worms grown on vector control and on *aat-6* RNAi was slightly stronger than in *rrf-3(pk1426)* control *C. elegans* (Figure 24A). Also a slightly increased ATGP-1 protein level could be observed in *pept-1;aat-6(RNAi)* worms. For ATGP-2, both bands were related to the protein, because in *atgp-2(ok352)* those were missing. The protein level of ATGP-2 was increased in all investigated *C. elegans* strains when compared with *rrf-3(pk1426)* control worms (Figure 24B). From these findings it may be concluded that when the peptide transporter and AAT-6 are missing that ATGP-2 seems to be more important than ATGP-1 regarding amino acid supply.

2.2. Identification of PEPT-1 regulating genes/proteins

Structure and functions of the intestinal peptide transporter have been extensively studied over the last twenty years (59), but very little is known about possible cellular modulator proteins or interaction partners. In the present study the model organism *C. elegans* was used, as a tool in a systematic screen for searching putative PEPT-1 interacting proteins.

2.2.1. Selection of genes/proteins affecting *C. elegans* PEPT-1 function

As *pept-1* is exclusively expressed in the intestine, the gene selection was based on the data of Pauli et al. (104), who identified 162 genes expressed in the intestine with a known anatomical expression pattern. For assessing PEPT-1 transport activity *in vivo* the accumulation of the dipeptide β -Ala-Lys-AMCA was used. β -Ala-Lys-AMCA is a fluorophore-conjugated dipeptide derivative which is slowly hydrolyzed and was shown to be a PEPT-1 substrate (105). In *pept-1(lg601)* *C. elegans* the transport of β -Ala-Lys-AMCA is completely abolished and it accumulates in the gut lumen (12). The screen was performed with *rrf-3(pk1426)* worms grown on RNAi with the preselected 162 genes and a fluorometric quantification of reporter substrate uptake. The genes for which a knockdown caused an alteration in β -Ala-Lys-AMCA uptake are listed in Table 2. The absolute control values, a detailed description of the calculation and the relative results with all 162 genes are provided in the appendix (8.4.2.).

Table 2: Significant results obtained in the β -Ala-Lys-AMCA uptake screen

34 out of 162 RNAi silencing experiments performed led to significantly ($p < 0.001$) altered levels in the uptake of the fluorescent labelled dipeptide β -Ala-Lys AMCA, whereas *pept-1;vc(RNAi)* was used as a negative control. *rrf-3;pept-1(RNAi)* worms with known impaired peptide absorption served as an additional control. Each experiment was performed at least two times with four technical replicates. Statistical analysis was performed by a Student's *t*-Test. Significance ($p < 0.001$) to *rrf-3;vc(RNAi)* is denoted.

Worm strain	Cosmid number (RNAi knockdown)	Gene	Relative β -Ala-Lys-AMCA uptake	Significance
controls				
<i>rrf-3(pk1426)</i>	pPD 129.36 vector control		0.98 \pm 0.03	
<i>pept-1(lg601)</i>	pPD 129.36 vector control		0.00 \pm 0.00	$p < 0.001$
<i>rrf-3(pk1426)</i>	K04E7.7	<i>pept-1</i>	0.13 \pm 0.04	$p < 0.001$
putative PEPT-1 modulators				
<i>rrf-3(pk1426)</i>	B0495.4	<i>nhx-2</i>	0.45 \pm 0.08	$p < 0.001$
<i>rrf-3(pk1426)</i>	B0041.5		0.37 \pm 0.08	$p < 0.001$
<i>rrf-3(pk1426)</i>	T08B2.10	<i>rps-17</i>	0.11 \pm 0.08	$p < 0.001$
<i>rrf-3(pk1426)</i>	K06A5.6		0.34 \pm 0.08	$p < 0.001$
<i>rrf-3(pk1426)</i>	F13G3.9	<i>mif-3</i>	0.41 \pm 0.03	$p < 0.001$
<i>rrf-3(pk1426)</i>	R11A5.4		0.34 \pm 0.06	$p < 0.001$
<i>rrf-3(pk1426)</i>	F26E4.12		2.95 \pm 0.43	$p < 0.001$
<i>rrf-3(pk1426)</i>	F54C9.7		0.47 \pm 0.06	$p < 0.001$
<i>rrf-3(pk1426)</i>	F37C12.9	<i>rps-14</i>	0.39 \pm 0.04	$p < 0.001$
<i>rrf-3(pk1426)</i>	F56C9.7		0.03 \pm 0.02	$p < 0.001$
<i>rrf-3(pk1426)</i>	R13A5.8	<i>rpl-9</i>	0.37 \pm 0.15	$p < 0.001$
<i>rrf-3(pk1426)</i>	K02D7.4	<i>dsc-4</i>	0.35 \pm 0.08	$p < 0.001$
<i>rrf-3(pk1426)</i>	Y66H1B.4	<i>spl-1</i>	0.54 \pm 0.09	$p < 0.001$
<i>rrf-3(pk1426)</i>	ZC416.6		0.58 \pm 0.04	$p < 0.001$
<i>rrf-3(pk1426)</i>	F49E8.5	<i>dif-1</i>	0.67 \pm 0.03	$p < 0.001$
<i>rrf-3(pk1426)</i>	F28D1.7	<i>rps-23</i>	0.45 \pm 0.10	$p < 0.001$
<i>rrf-3(pk1426)</i>	K08E7.1		0.23 \pm 0.07	$p < 0.001$
<i>rrf-3(pk1426)</i>	C49C3.5		0.30 \pm 0.05	$p < 0.001$
<i>rrf-3(pk1426)</i>	F11E6.5	<i>elo-2</i>	0.30 \pm 0.09	$p < 0.001$
<i>rrf-3(pk1426)</i>	C39F7.4	<i>rab-1</i>	0.19 \pm 0.03	$p < 0.001$
<i>rrf-3(pk1426)</i>	F39G3.1	<i>ugt-61</i>	0.37 \pm 0.04	$p < 0.001$
<i>rrf-3(pk1426)</i>	C02A12.4	<i>lys-7</i>	0.61 \pm 0.05	$p < 0.001$
<i>rrf-3(pk1426)</i>	Y22F5A.4	<i>lys-1</i>	0.10 \pm 0.03	$p < 0.001$
<i>rrf-3(pk1426)</i>	C13C4.5		0.37 \pm 0.11	$p < 0.001$
<i>rrf-3(pk1426)</i>	F58E10.4	<i>aip-1</i>	0.44 \pm 0.09	$p < 0.001$
<i>rrf-3(pk1426)</i>	T08G5.10	<i>mtl-2</i>	0.52 \pm 0.11	$p < 0.001$
<i>rrf-3(pk1426)</i>	C53A5.3	<i>hda-1</i>	0.18 \pm 0.04	$p < 0.001$
<i>rrf-3(pk1426)</i>	R11H6.1	<i>pes-9</i>	0.06 \pm 0.02	$p < 0.001$
<i>rrf-3(pk1426)</i>	F44G3.6	<i>skr-3</i>	0.19 \pm 0.02	$p < 0.001$
<i>rrf-3(pk1426)</i>	C03B1.12	<i>lmp-1</i>	0.59 \pm 0.02	$p < 0.001$
<i>rrf-3(pk1426)</i>	C54H2.5	<i>sft-4</i>	0.41 \pm 0.03	$p < 0.001$
<i>rrf-3(pk1426)</i>	F22F1.1	<i>hil-3</i>	0.35 \pm 0.04	$p < 0.001$
<i>rrf-3(pk1426)</i>	C33D3.1	<i>elt-2</i>	0.43 \pm 0.03	$p < 0.001$
<i>rrf-3(pk1426)</i>	F48C11.3	<i>nlp-3</i>	0.20 \pm 0.03	$p < 0.001$

The uptake of the fluorescent dipeptide β -Ala-Lys-AMCA in RNAi-treated *rrf-3(pk1426)* worms in comparison to *rrf-3;vc(RNAi)* and *pept-1;vc(RNAi)* was quantified. RNAi knockdown of *pept-1* (0.13 ± 0.04 fold) was used as another control. Silencing of 33 out of 162 genes caused significantly ($p < 0.001$) decreased uptake of the fluorescent dipeptide, whereas only one gene when silenced (F26E4.12) revealed an increased PEPT-1 transport function. Knockdown of the gene F27D4.1 caused lethality and was therefore excluded for secondary screens. The results of the screen were independently confirmed by image analysis via confocal microscopy with β -Ala-Lys-AMCA staining in *rrf-3(pk1426)* worms treated with RNAi of each one of the 34 potential candidate genes (Figure 25).

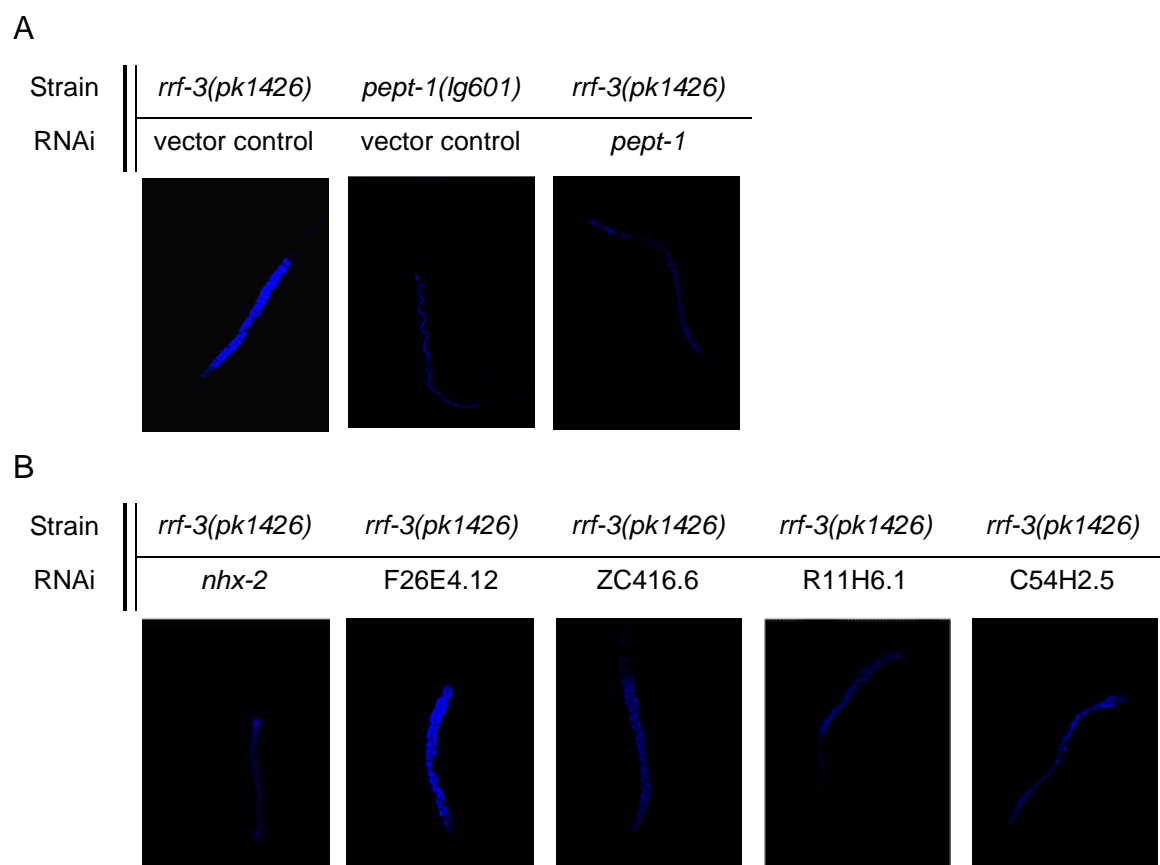


Figure 25: β -Ala-Lys-AMCA staining in worms after RNAi silencing of selected genes

(A) Images of β -Ala-Lys-AMCA uptake of controls. (B) Selection of pictures that confirmed the screen results, whereas RNAi of F26E4.12 originated an increased dipeptide uptake. Silencing of the other genes reduced the β -Ala-Lys-AMCA uptake as observed in the screen. The anterior end of the worms is located to the top. All images are fluorescent overlays of ten z-slices in a magnification of 20-fold and represent typical results.

There was a strong fluorescent signal of β -Ala-Lys-AMCA in intestinal cells of *rrf-3(pk1426)* control worms. By contrast in *pept-1;vc(RNAi)* and *rrf-3;pept-1(RNAi)* *C. elegans* the signal could only be detected in the gut lumen and not in intestinal cells, due to the lack of the di- and tripeptide transporter (Figure 25A). Knockdown of 11 genes significantly reduced the fluorescent signal in *C. elegans*, while RNAi of F26E4.12 increased the uptake and these results were confirmed by images (examples shown in Figure 25B). As a proof-of-concept *nhx-2* was identified amongst this group of relevant candidate genes within the screen. NHX-2 was demonstrated previously to be essential for PEPT-1 function (11) (106). 22 genes where the images did not confirm the screening results were excluded from the following experiments.

Table 3: List of genes that when silenced altered β -Ala-Lys-AMCA absorption

Cosmid number	Gene	NCBI COGs
B0495.4	<i>nhx-2</i>	Sodium-proton-exchanger
B0041.5		Predicted membrane protein
F13G3.9	<i>mif-3</i>	Macrophage migration inhibitory factor
F26E4.12		Glutathione peroxidase
F54C9.7		Nematode specific protein
F56C9.7		Uncharacterised protein
ZC416.6		Bifunctional leukotriene A4 hydrolase/ aminopeptidase LTA4H
F11E6.5	<i>elo-2</i>	Long chain fatty acid elongase
C02A12.4	<i>lys-7</i>	N-acetylmuraminidase/lysozyme
C13C4.5		Sugar transporter/spinster transmembrane protein
R11H6.1	<i>pes-9</i>	Metalloexopeptidases
C54H2.5	<i>sft-4</i>	Putative cargo transport protein ERV29

Based on these results 12 genes were preselected (Table 3), whereas only F26E4.12(RNAi) revealed an increased PEPT-1 transport activity and therefore was of special interest. By contrast, RNAi knockdown of the other 11 putative modulators caused a *pept-1*-like phenotype with a reduced dipeptide uptake. These genes were taken onto the next level of investigation. This included testing against other phenotypic features of *pept-1(lg601)* deficient *C. elegans* such as enlarged fat droplets and increased fatty acid absorption (67). A next series of

experiments assessed changes in fat accumulation by measuring fat droplet diameter in worms after Sudan Black B staining (Figure 26). Highest fat content and consequently largest fat droplets were measured in *pept-1;vc(RNAi)* worms with a mean size of $3.4 \mu\text{m} \pm 0.1 \mu\text{m}$.

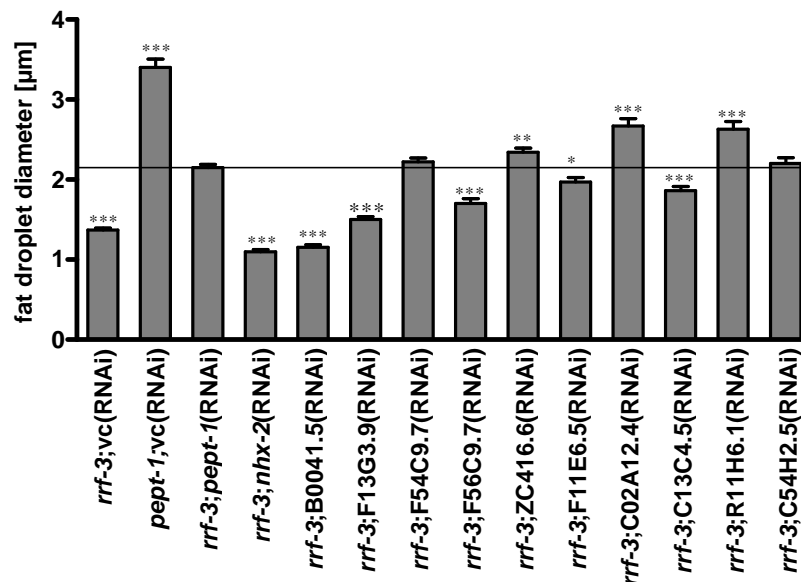


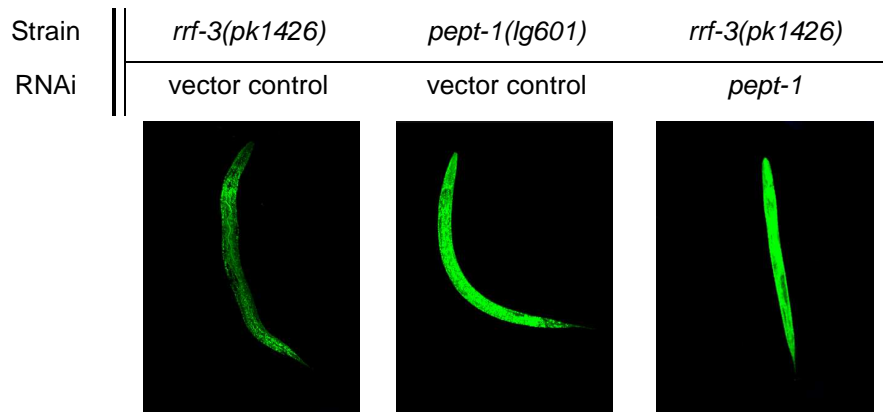
Figure 26: Sudan Black B staining after RNAi silencing of putative regulator genes
Fat droplet diameter of RNAi-treated worms with putative PEPT-1 modulator genes was measured after Sudan Black B staining. The experiment was performed two times and for each RNAi knockdown 140 to 200 fat droplets were analysed. Statistical analysis was performed by a Student's *t*-Test. Significance (* $p < 0.05$, ** $p < 0.01$ and *** $p < 0.001$) compared to *rrf-3;pept-1(RNAi)* is denoted.

Diameter of *rrf-3;pept-1(RNAi)* fat droplets were $2.1 \mu\text{m} \pm 0.03 \mu\text{m}$, while *rrf-3;vc(RNAi)* worms had considerably smaller fat droplets ($1.4 \mu\text{m} \pm 0.02 \mu\text{m}$). Fat accumulation and fat droplet diameters in worms treated with RNAi of the 11 selected genes was compared with that of *rrf-3;pept-1(RNAi)* worms. RNAi of five genes caused either nearly the same (F54C9.7 or C54H2.5) or even higher (ZC416.6, C02A12.4 and R11H6.1) fat droplet diameters than those in worms treated with *pept-1(RNAi)*. Knockdown of six genes (*nhx-2*, B0041.5, F13G3.9, F56C9.7, F11E6.5 and C13C4.5) did not increase fat accumulation or fat droplet diameter significantly.

In addition to fat accumulation, fatty acid absorption was semi-quantitatively assessed as well by using a C12 fatty acid, labelled with a fluorescent dye called BODIPY (Figure 27). As previously described (67) the uptake of the fatty acid

BODIPY-C12 was significantly increased in *pept-1;vc(RNAi)* and in *rrf-3;pept-1(RNAi)* when compared to control worms (Figure 27A).

A



B

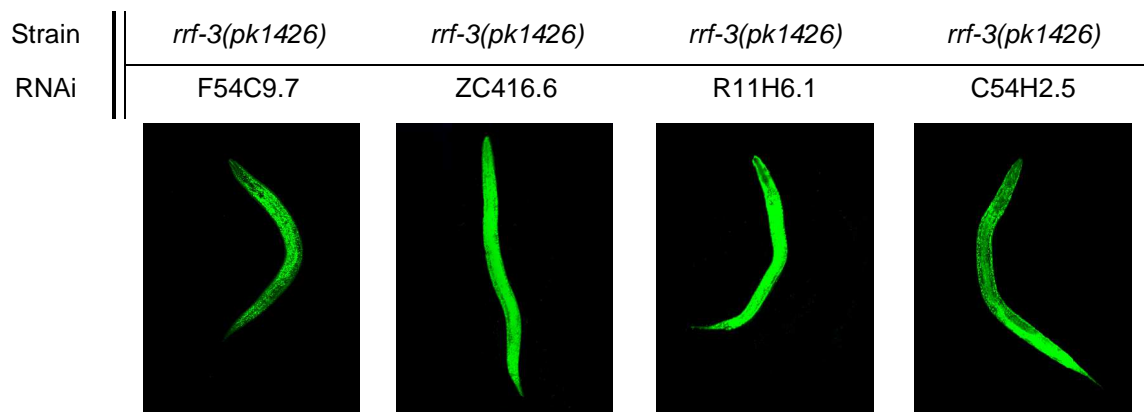


Figure 27: BODIPY-C12 uptake after RNAi silencing of putative PEPT-1 regulator genes

(A) Images of BODIPY-C12 uptake into control worms. (B) Pictures of *rrf-3(pk1426)* worms with RNAi knockdown of putative PEPT-1 modulators which showed a comparable phenotype to *pept-1;vc(RNAi)* and *rrf-3;pept-1(RNAi)*. The experiment was performed two times. The anterior end of the worm is located to the top. All images are fluorescent overlays of ten z-slices in a magnification of 20-fold and represent typical results.

Knockdown of seven predicted PEPT-1 modulators did not increase BODIPY-C12 uptake (*nhx-2*, B0041.5, F13G3.9, F56C9.7, F11E6.5, C02A12.4 and C13C4.5), while knockdown of four genes (F54C9.7, ZC416.6, R11H6.1, C54H2.5) showed corresponding phenotypic changes as in *pept-1(lg601)* worms (Figure 27B).

Hence, the stepwise selection finally revealed the four candidate genes ZC416.6, R11H6.1, C54H2.5 and F54C9.7 that caused almost identical phenotypes as a

PEPT-1 deficiency and one gene (F26E4.12) that when silenced increased PEPT-1 transport activity. F54C9.7 was not taken into further analysis as it encodes obviously a protein that is nematode-specific. The other four genes were further characterised in view of their effects on PEPT-1 activity.

F26E4.12

The gene F26E4.12 is coding for a homologue of a mammalian phospholipid hydroperoxide glutathione peroxidase (PHGPx, GPx4). PHGPx exclusively catalyses the reduction of phospholipid hydroperoxides by means of reduced glutathione (GSH) as an electron donor (107). PHGPx isoforms occur in the nucleus, cytosol, and mitochondria respectively (108).

ZC416.6

The gene ZC416.6 in *C. elegans* is coding for an ortholog of bifunctional leukotriene A4 hydrolase/aminopeptidase LTA4H which is homologous to the mammalian isoform 1 of LTA4H. Mammalian LTA4H has two main functions. It catalyzes the final step in biosynthesis of leukotriene B₄ (LTB₄) (109) and it operates as an aminopeptidase (110). Since *C. elegans* do not synthesise leukotrienes (111), the aminopeptidase activity is most likely the main function of ZC416.6 in worms.

R11H6.1

The gene R11H6.1 (*pes-9*) encodes a zinc-dependent exopeptidase homologous to human cytosolic non-specific dipeptidase 2 (CNDP2, CN2) which is a cytosolic enzyme with a broad range of substrates (112). Another orthologous enzyme Dug1p was recently identified in *Saccharomyces cerevisiae* and functions as a dipeptidase as well (113).

C54H2.5

C54H2.5 (*sft-4*) codes for a putative cargo transport protein. It is homologous to mammalian *surf4* which codes for a polytopic integral membrane protein located in the endoplasmic reticulum (ER) (114). The best known and investigated homologue of C54H2.5 is Erv29 (ER vesicle) in *S. cerevisiae*. Erv29p is an integral membrane protein which is required for the delivery of specific secretory, correctly folded proteins from the ER to the Golgi and likely acts during vesicle

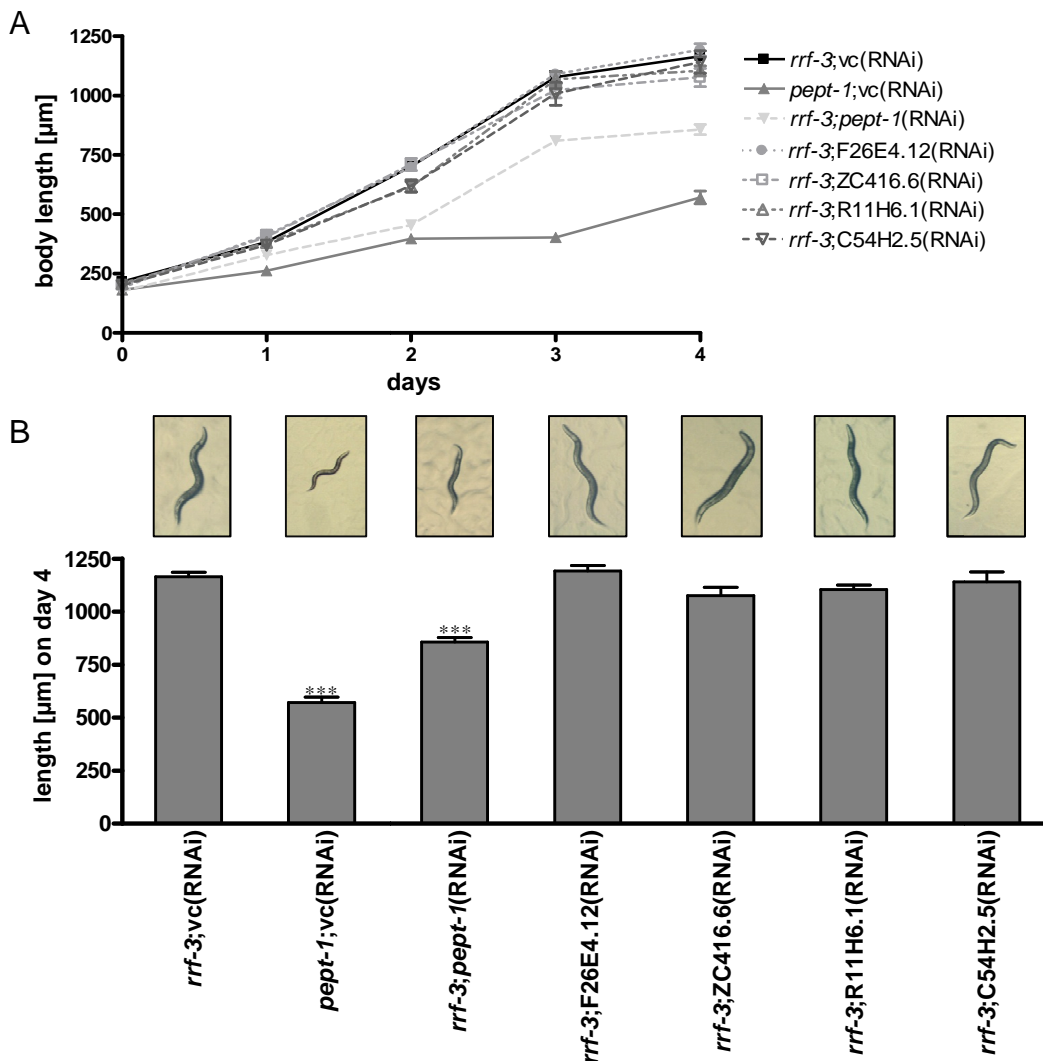
exit from ER (115). It is also involved in degradation of soluble misfolded proteins (116).

2.2.2. Phenotypic analysis of worms after gene silencing of the preselected PEPT-1 regulator genes

A further phenotypic characterisation of worms in which the four PEPT-1 regulating genes were silenced via RNAi, was performed to determine whether they deliver alterations as seen in peptide transporter deficient *C. elegans*.

2.2.2.1. Postembryonic body size development and reproduction of worms treated with RNAi for the PEPT-1 modulator proteins

In previous studies it was shown that animals lacking PEPT-1 have retarded growth development and reproduction (12). With silencing of the four genes these phenotypic changes were characterised as well (Figure 28).



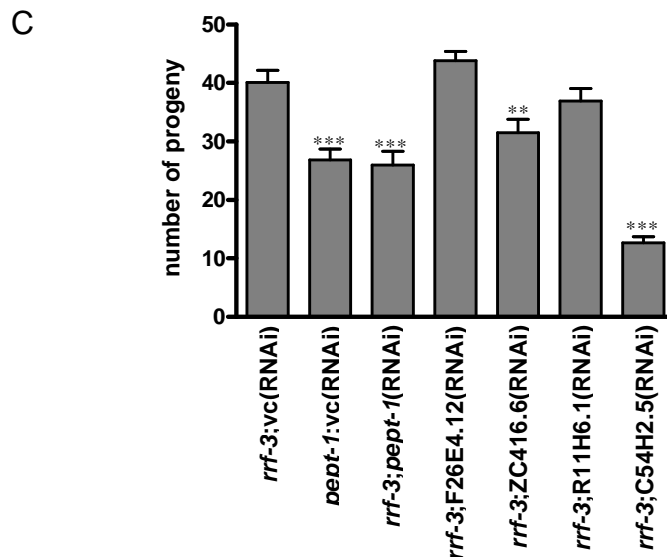


Figure 28: Development and brood size of worms treated with RNAi of preselected PEPT-1 modulators

(A) Larval development of *C. elegans* treated with RNAi of the PEPT-1 modulator genes and controls. Daily (every 24 hours) eight worms per group were photographed and body length was measured. (B) Final body length and mean length of RNAi treated worms and controls at the fourth day after hatching. (C) Number of progeny of control worms and *rrf-3(pk1426)* worms with knockdown of preselected modulators. For each RNAi construct the progeny of 28 to 35 worms was counted. Statistical analysis was performed by a Student's *t*-Test. Significance (** $p < 0.01$, *** $p < 0.001$) to *rrf-3;vc(RNAi)* is denoted.

Examination of the postembryonic growth started with synchronised L1 larvae and lasted until day four (Figure 28A), when *rrf-3;vc(RNAi)* worms reached adulthood with a body length of $1164 \pm 20 \mu\text{m}$ (Figure 28B). Retarded postembryonic growth of *pept-1;vc(RNAi)* animals caused a reduction of about 50 % in body length at day four. RNAi knockdown of *pept-1* resulted in decelerated growth, whereas knockdown of F26E4.12, ZC416.6, R11H6.1 and C54H2.5 in *rrf-3(pk1426)* *C. elegans* did not alter adult body size.

In general, the reproduction rate of *rrf-3(pk1426)* worms on vector control RNAi bacteria was strongly reduced when compared to *rrf-3(pk1426)* grown on *E. coli* OP50 bacteria (40 ± 2 versus 250 ± 10 hatched larvae), an effect that was also reported by Brooks et al. (100). When examining the number of progeny the knockdown of ZC416.6 and C54H2.5 significantly reduced reproduction to a degree that was similar to *pept-1;vc(RNAi)* and *rrf-3;pept-1(RNAi)* *C. elegans* (Figure 28C).

During previous brood size experiments it was shown that RNAi knockdown of C54H2.5 caused an extended egg laying period which should be investigated further (Figure 29), because the same effect was reported for *pept-1(lg601)* *C. elegans* as well (12).

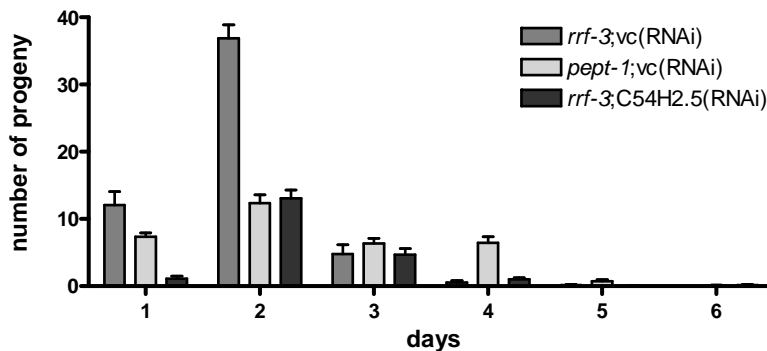


Figure 29: Extended reproduction period in C54H2.5(RNAi) treated *C. elegans*

During the reproduction period control worms (*rrf-3* and *pept-1*) as well as *rrf-3(pk1426)* treated with RNAi for C54H2.5 were transferred to fresh RNAi plates daily and the number of progeny produced by 24 worms per group was counted.

The maximum egg production rate in *rrf-3;vc(RNAi)* worms with 37 ± 2 eggs was observed on day two and the entire reproduction period lasted four days, while *rrf-3(pk1426)* worms grown on C54H2.5 RNAi as well as *pept-1(lg601)* possessed an extended egg laying period of six days (Figure 29).

2.2.2.2. *pept-1* promoter activity and mRNA expression after treating worms with RNAi for the PEPT-1 modulator genes

Effects of silencing of the four modulator genes on *pept-1* promoter activity was assessed by using *prompept-1::GFP* worms (BR2875) which show a strong GFP signal in intestinal cells and thereby showing *pept-1* promoter activity (Figure 30). Quantification of PEPT-1 mRNA levels in these worm strains was determined by realtime RT-PCR (Figure 31).

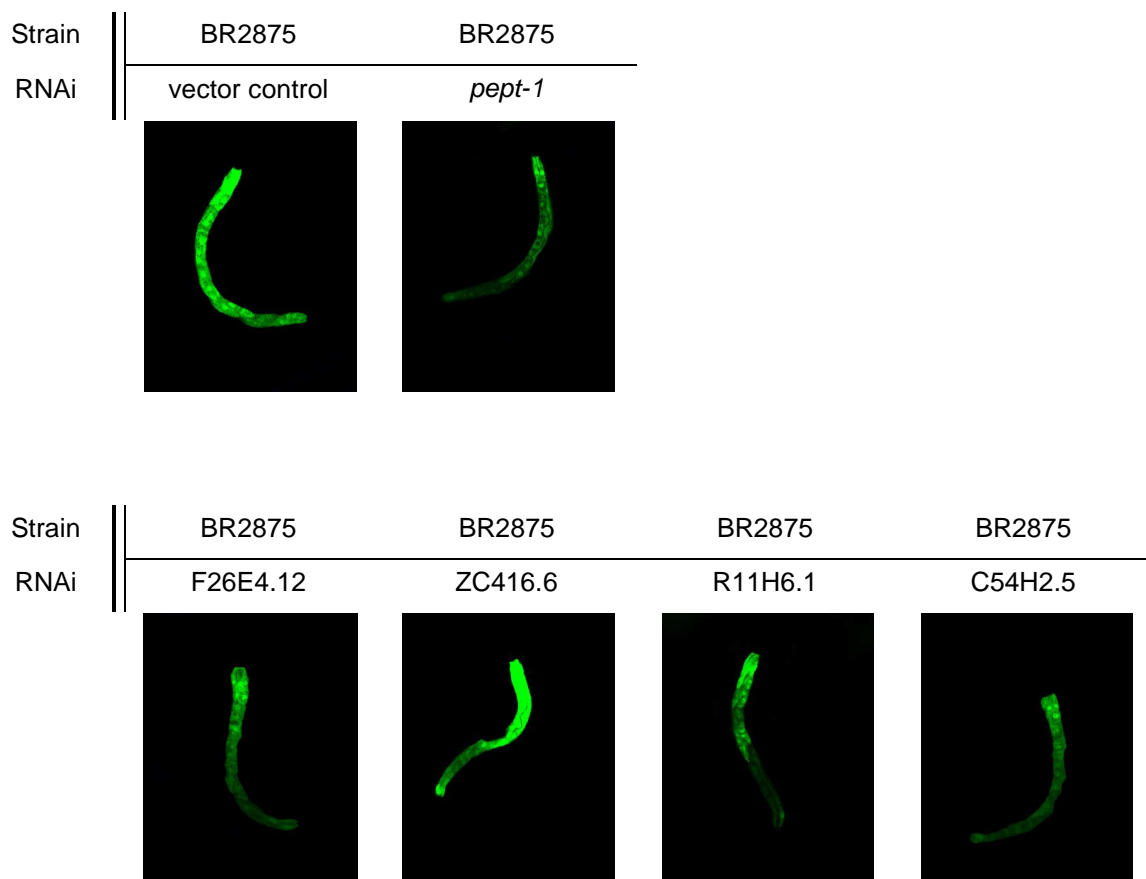


Figure 30: *pept-1* promoter activity of worms treated with RNAi of preselected PEPT-1 modulators

The fluorescent images show *prompept-1::GFP* (BR2875) *C. elegans* treated with RNAi of controls (*vc* = vector control, *pept-1*) and RNAi of the modulators. All images are fluorescent overlays of 10 z-slices in a magnification of 40-fold and represent typical results. The anterior end of the worms is located to the top. Each experiment was performed 2 times with 10 technical replicates.

Whereas silencing of *pept-1* via RNAi caused a reduced intestinal expression of the GFP reporter, gene silencing in case of F26E4.12, R11H6.1 and C54H2.5 resulted in only a slight reduction of *pept-1* promoter activity. By contrast, RNAi of ZC416.6 slightly increased it (Figure 30). To validate the data concerning promoter activity of *pept-1*, real-time RT-PCR of *pept-1* mRNA expression levels in *C. elegans* with RNAi of these four modulator genes was performed (Figure 31).

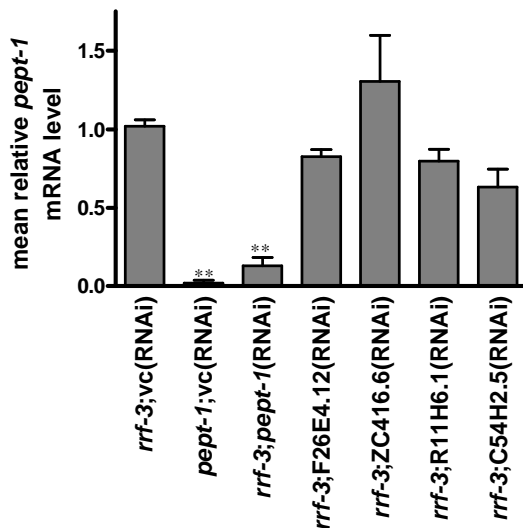


Figure 31: *pept-1* mRNA expression of worms treated with RNAi of preselected PEPT-1 modulators

Mean relative *pept-1* mRNA expression in control worms and *C. elegans* with RNAi knockdown of F26E4.12, ZC416.6, R11H6.1 and C54H2.5 was measured. The experiment was performed two times with two technical replicates. Statistical analysis was performed by a Student's *t*-Test. Significance (** $p < 0.01$) to *rrf-3;vc*(RNAi) is denoted.

Since *pept-1(lg601)* *C. elegans* have a 1.7 kb gene deletion (12) no specific mRNA was detectable (Figure 31). Treatment with *pept-1* dsRNA in *rrf-3(pk1426)* *C. elegans* decreased *pept-1* mRNA levels approximately to 15 % of that in control worms. RNAi knockdown of F26E4.12, R11H6.1 and C54H2.5 caused a small reduction of *pept-1* mRNA levels, whereas treatment with ZC416.6 slightly increased it. Although these changes all did not reach significance, they appear in line with the observed changes in *pept-1* promoter activity.

2.2.2.3. PEPT-1 protein expression is selectively altered by gene silencing of the modulators

Western blot analysis with a specific anti-CePEPT-1 antibody was performed to determine the effect of RNAi silencing of the four genes on PEPT-1 protein levels (Figure 32).

The *C. elegans* PEPT-1 protein has an estimated molecular weight of 94.1 kDa. *Xenopus laevis* oocytes expressing *C. elegans* PEPT-1 served as positive control and there the detected protein appeared at approximately 95 kDa. *C. elegans* protein extracts were fractionated into cytosolic and membrane protein lysates by

differential centrifugation. The membrane fraction included the membrane-bound proteins as well as proteins located in transport vesicles. In the cytosolic fraction nearly no PEPT-1 protein could be detected (Figure 32A).

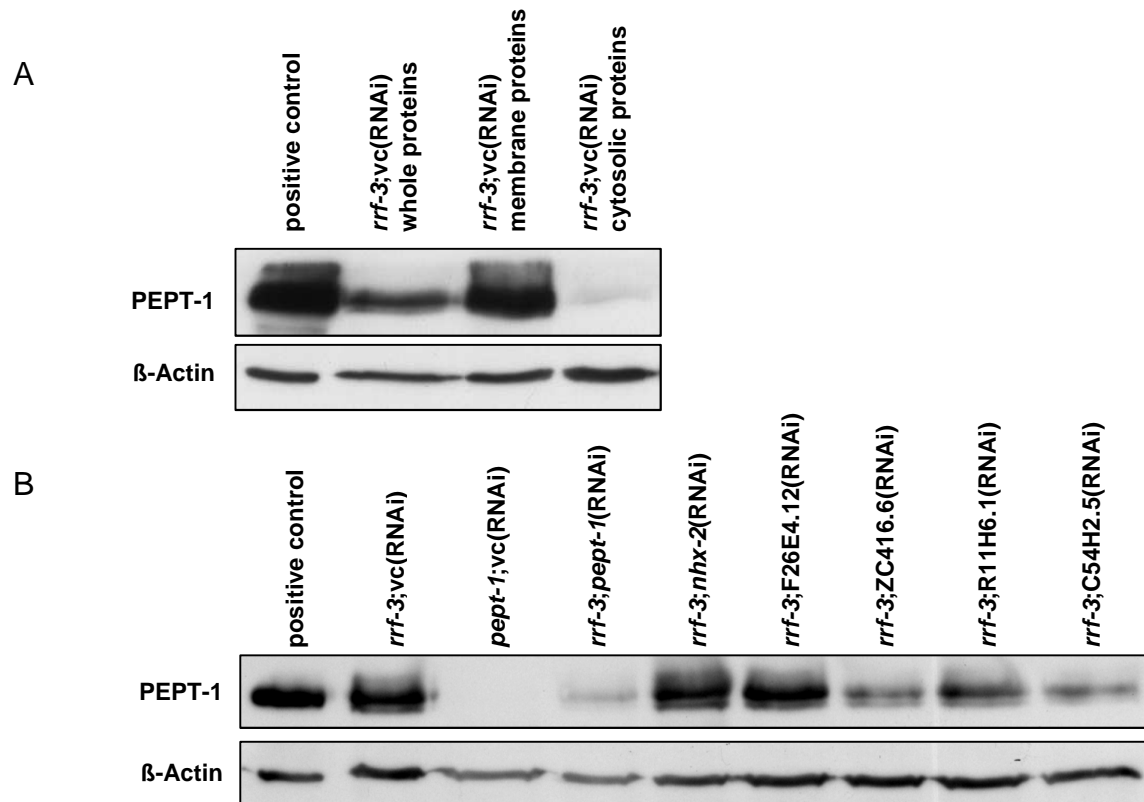


Figure 32: PEPT-1 expression is altered by gene silencing of the modulators

(A) PEPT-1 protein expression of whole protein lysates, membrane and cytosolic fractions of *rrf-3;vc(RNAi)* worms. (B) PEPT-1 protein expression of membrane proteins of *rrf-3(pk1426)* *C. elegans* treated with RNAi of controls (vc = vector control, *pept-1*) and PEPT-1 modulators. 20 μ g protein lysates were loaded per lane. Oocytes expressing *C. elegans* PEPT-1 were used as a positive control. In both cases β -Actin was used as a loading control.

As expected, in *pept-1;vc(RNAi)* worms no PEPT-1 protein was detected, whereas a low protein expression level could be observed in *rrf-3;pept-1(RNAi)* *C. elegans* samples. Gene silencing of *nhx-2* and F26E4.12 did not alter PEPT-1 protein levels while RNAi treatment for ZC416.6, R11H6.1 and C54H2.5 resulted in decreased PEPT-1 levels (Figure 32B). Although these findings are apparently contradictory to those of the mRNA, it is known that changes in mRNA expression do not necessarily correlate with alterations in protein level (117).

To assess, whether silencing the modulator genes exclusively altered PEPT-1 expression, protein levels of a second membrane protein, ATGP-1 (amino acid transporter glycoprotein subunit 1) were determined (Figure 33).

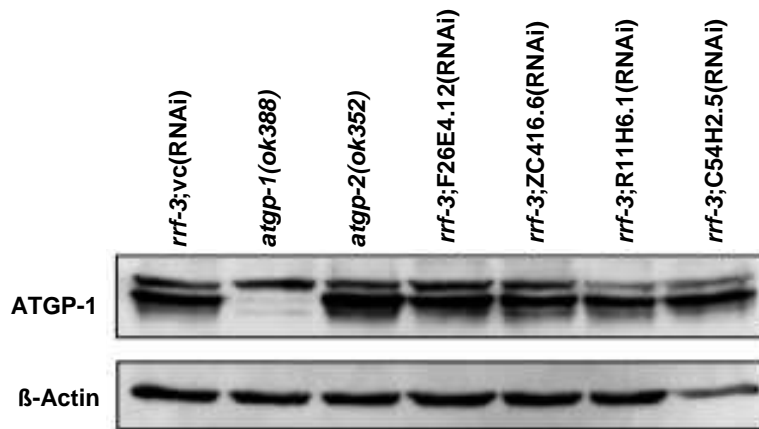


Figure 33: ATGP-1 protein expression of worms treated with RNAi of preselected PEPT-1 modulators

ATGP-1 protein expression of membrane protein lysates of *atgp-1(ok388)*, *atgp-2(ok352)* and *rrf-3(pk1426)* *C. elegans* treated with RNAi of control (vc = vector control) and PEPT-1 modulators. 30 µg membrane protein lysates were loaded per lane. β-Actin was used as a loading control.

The calculated molecular weight of ATGP-1 is 69.3 kDa. In worm membrane protein lysates the ATGP-1 protein appeared with a stronger and a weaker band with higher mass. The lower band has the proper molecular weight and was shown to represent ATGP-1 as in *atgp-1(ok388)* worms the protein was lacking (Figure 33). In *atgp-2(ok352)* worms the signal was stronger than in control *C. elegans*, while in *rrf-3(pk1426)* worms with silencing of the four PEPT-1 modulator genes no alterations in ATGP-1 expression were observed. Hence it is reasonable to assume that the decline in PEPT-1 protein levels is specific and causally linked to the knockdown of the four regulators.

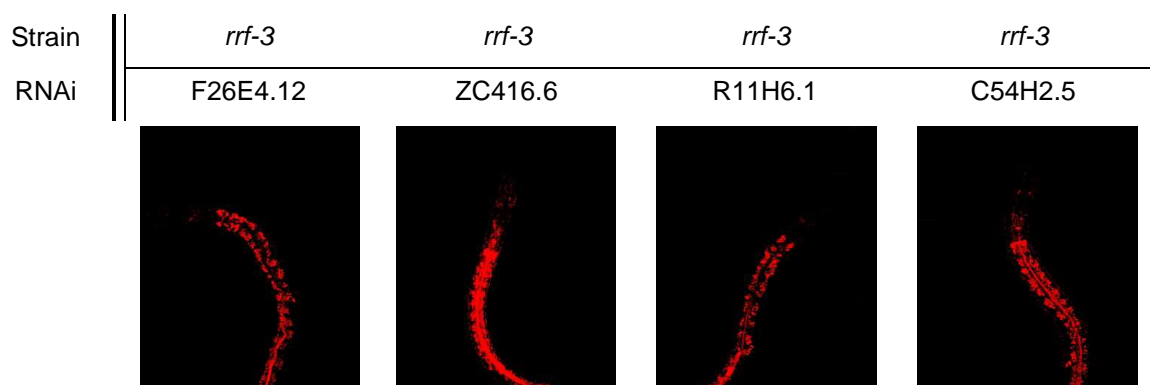
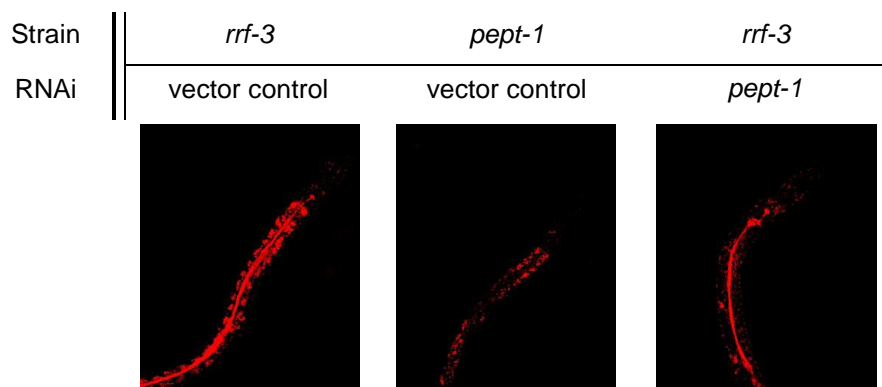
2.2.2.4. Regulator gene knockdown modulates resistance to oxidative stress

Reactive oxygen species (ROS) cover superoxide, hydroxyl, peroxy and alkoxy radicals as well as hypochlorous acid, ozone, singlet oxygen and hydroxide peroxide (118). Intracellular ROS are mainly produced during respiration in mitochondria, but they are also generated by enzymatic reactions (e.g. NADPH oxidases, NOX), inflammation processes, heat or UV exposure and in xenobiotic

metabolism via cytochrome P450. High ROS levels in cells can induce damage of DNA, proteins and lipids by peroxidation as well as induction of apoptosis and contribute to ageing (reviewed by (119)). However ROS are also necessary for pathogen killing and host defence (120).

To assess ROS status in worms the dye CM-H₂XRos (Mito Tracker Red) was used (Figure 34). CM-H₂XRos enters active respiring cells, accumulates in mitochondria and is exclusively oxidised by hydrogen peroxides (121). The oxidised species creates a fluorescent conjugate with thiol groups of mitochondrial proteins and peptides which can be detected using confocal microscopy.

A



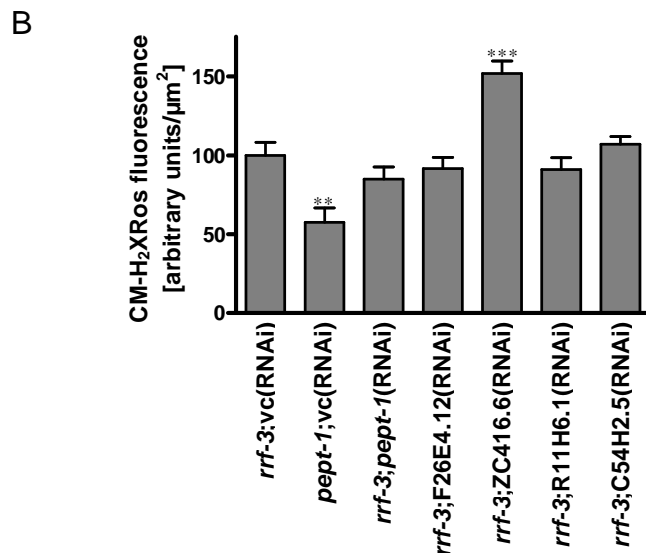


Figure 34: Mitochondrial ROS load of worms treated with RNAi of preselected PEPT-1 modulators

(A) Representative images from *rrf-3(pk1426)* and *pept-1(lg601)* *C. elegans* treated with RNAi of controls (vc = vector control, *pept-1*) and preselected PEPT-1 modulators after staining with CM-H₂XROS. All images are fluorescent overlays of 10 z-slices in a magnification of 40-fold. (B) Fluorescence intensities were determined for the area posterior of the pharynx using the Leica Confocal software 5.2. The experiment was performed two times and each time at least 10 worms per group were analysed. Statistical analysis was performed by a Student's *t*-Test. Significance (** $p < 0.01$, *** $p < 0.001$) to *rrf-3;vc*(RNAi) is denoted.

In the intestine of *pept-1(lg601)* worms, mitochondrial ROS levels were significantly ($p < 0.01$) reduced about 50 % compared to *rrf-3(pk1426)* *C. elegans*, whereas RNAi knockdown of ZC416.6 caused a significant increase ($p < 0.001$). Silencing of the other genes remained without an effect on ROS status in intestinal cells (Figure 34).

ROS status is controlled by production and exogenous and endogenous scavenging systems. These antioxidative processes are divided into non-enzymatic and enzymatic systems. The non-enzymatic part is mediated by α -tocopherol, ascorbic acid, carotenoids (α and β carotene), retinol, retinol binding protein (RBP), uric acid and glutathione (GSH and GSSG). The enzymatic scavenging system is composed of thioredoxin reductase, glucose-6-phosphate dehydrogenase, catalase, superoxide dismutase (SOD), glutathione peroxidase (GPx) and glutathione reductase (reviewed in (122)). The reaction of superoxide anion radical and water to hydrogen peroxide is catalysed by superoxide dismutases (SODs) (Figure 35). The H₂O₂ produced, is decomposed into water

and oxygen by catalase or into two water molecules by glutathione peroxidase (GPx). Simultaneously two GSH molecules (reduced glutathione) are oxidised by glutathione peroxidase to GSSG (oxidised glutathione, glutathione disulfide) which can be reduced to GSH by glutathione reductase which uses NADPH+H⁺ and FAD as cofactors (Figure 35).

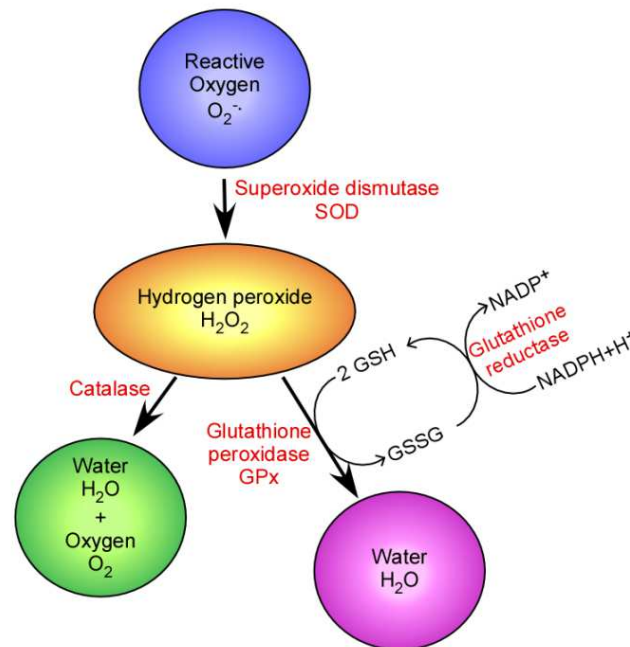


Figure 35: Enzymatic scavenging mechanisms of reactive oxygen species

The reaction of reactive oxygen and water to hydrogen peroxide is catalysed by superoxide dismutases (SODs). Hydrogen peroxide in turn is decomposed into water (and oxygen) by glutathione peroxidases or catalases.

The intracellular GSH/GSSG ratio of around 10:1 is maintained by the release of GSSG from cells, by glutathione reductase or by *de novo* synthesis of GSH via the γ -glutamyl-cycle (123). Since a high GSH concentration in PEPT-1 deficient worms is a hallmark of the phenotype, GSH and GSSG levels were measured in *C. elegans* treated with RNAi for silencing the four PEPT-1 modulators (Figure 36).

In *rrf-3(pk1426)* control worms 87.8 % of glutathione was present in the form of GSH, whereas only 12.2 % were detected as GSSG resulting in a normal GSH/GSSG ratio (123). GSH concentration (Figure 36A) was significantly increased ($p < 0.001$) in *pept-1(lg601)* worms (44.5 ± 1.3 nmol/mg protein) and in turn GSSG levels (Figure 36B) were significantly ($p < 0.001$) reduced (0.8 ± 0.05 nmol GSSG/mg protein). Thereby, the ratio between GSH and GSSG was shifted towards 98 % represented by GSH (Figure 36C). In *rrf-3;pept-1(RNAi)*

C. elegans both, total GSH levels and even more so GSSG levels were significantly increased ($p < 0.05$ and $p < 0.001$) when compared with control worms and the ratio was shifted towards more GSSG.

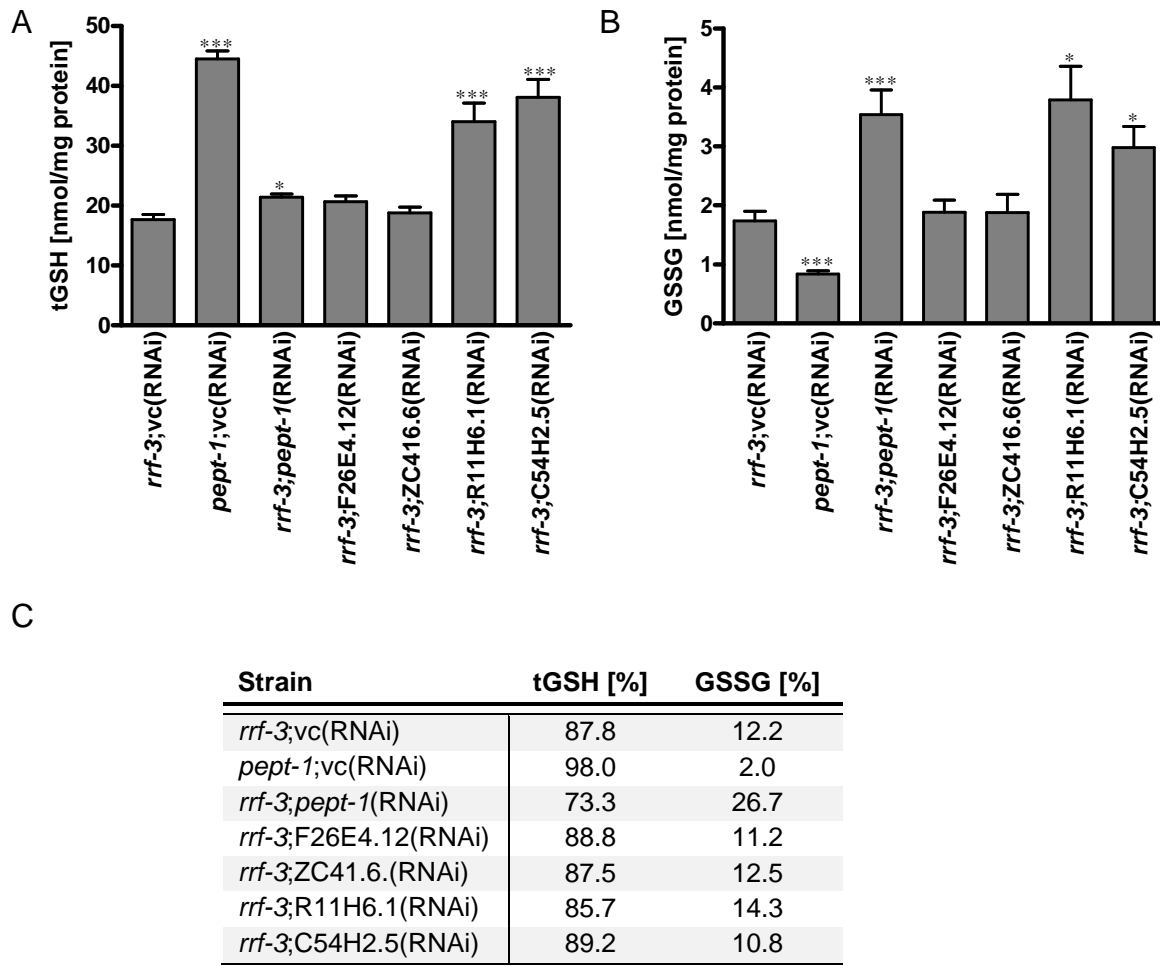


Figure 36: Glutathione homeostasis of worms treated with RNAi of preselected PEPT-1 modulators

(A) Total GSH and (B) GSSG levels of *pept-1(lg601)* and *rrf-3(pk1426)* *C. elegans* treated with RNAi of controls (vc = vector control, *pept-1*) and of four putative PEPT-1 modulators. (C) Ratio between GSH and GSSG content. The experiment was performed at least four times, each time in duplicates. Statistical analysis was performed by a Student's *t*-Test. Significance (* $p < 0.05$, *** $p < 0.001$) compared with *rrf-3;vc(RNAi)* is denoted.

In *C. elegans* with RNAi knockdown of R11H6.1 and C54H2.5 GSH and GSSG concentrations were both significantly elevated ($p < 0.001$), whereas the GSH/GSSG ratio remained unaffected. In contrast, RNAi knockdown of F26E4.12 and ZC416.6 did neither significantly alter GSH and GSSG levels nor its ratio in comparison to *rrf-3;vc(RNAi)*.

As the increased antioxidative capacity via GSH might directly translate in a better protection against ROS, the worms were stressed with the ROS inducer paraquat (Figure 37). Paraquat is reduced upon entry into the cell and induces oxidative stress by generating superoxide anion radicals from oxygen (124). It was previously shown that paraquat resistance is increased in *pept-1(lg601)* *C. elegans* (67).

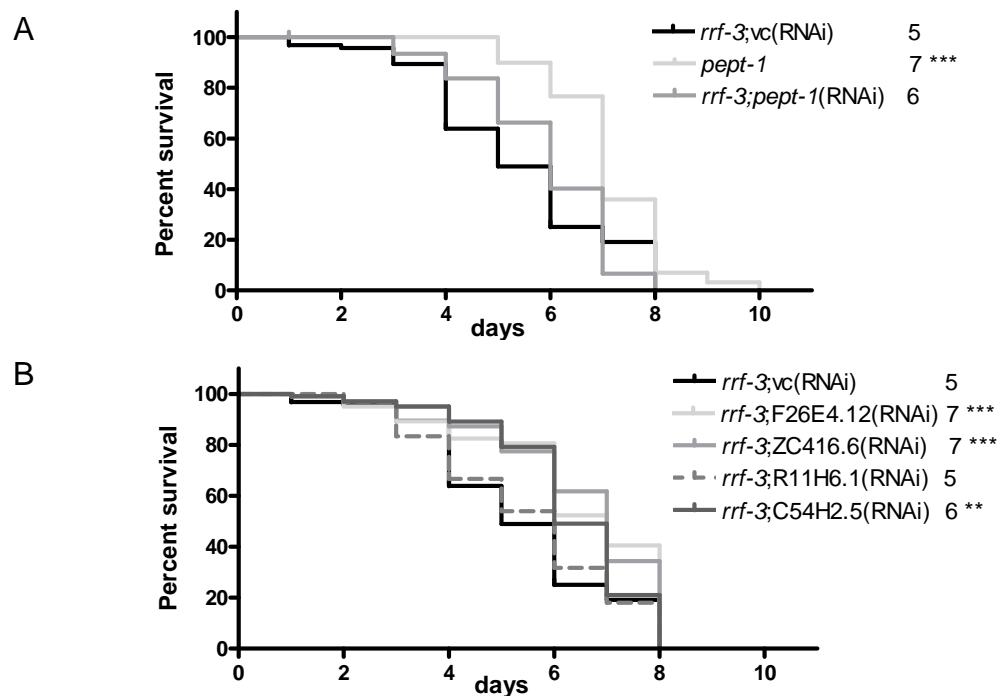


Figure 37: Stress resistance of worms treated with RNAi of preselected PEPT-1 modulators

(A) Survival curves of controls. (B) Survival curves of *rrf-3(pk1426)* worms treated with RNAi of preselected PEPT-1 modulators compared with *rrf-3(pk1426)* grown on vector control. For each RNAi construct the survival rate of 30 to 33 worms was measured three times. Numbers behind the strains indicate the median survival in days. Kaplan-Meier survival curves were statistically analysed with a Logrank-Test. Significance (** $p < 0.01$, *** $p < 0.001$) to *rrf-3;vc(RNAi)* survival curve is denoted.

When *rrf-3(pk1426)* control worms were grown on agar plates containing paraquat a maximum survival length of eight days and a median survival of five days was recorded. Both, *pept-1(lg601)* and *rrf-3;pept-1(RNAi)* *C. elegans* had a significantly ($p < 0.001$) increased stress resistance with a median survival rate of seven and six days, respectively (Figure 37A). Interestingly, RNAi knockdown of F26E4.12, ZC416.6 and C54H2.5 also led to an increased stress resistance, while knockdown of R11H6.1 revealed no changes (Figure 37B). Increased stress resistance observed for the F26E4.12, ZC416.6 and C54H2.5 RNAi

treated worms therefore matches the phenotype of a lack of PEPT-1. This provides another line of evidence that these genes may be important for a proper PEPT-1 function.

2.2.3. Further characterisation of the PEPT-1 regulators

To further address the question on how the different genes/proteins could regulate PEPT-1 function in *C. elegans* a series of additional studies was conducted.

2.2.3.1. PEPT-1 is only one of the proteins affected by the ER cargo transport protein C54H2.5

In *Erv29 Δ yeast cells (*Erv29* is homologous to C54H2.5) it has been demonstrated that the traffic of a subset of correctly folded proteins was interrupted while that of others remained unaffected (115). To examine whether the reduced expression level of PEPT-1 in a C54H2.5(RNAi) background was specific, it was assessed whether the membrane proteins ATGP-2 (amino acid transporter glycoprotein 2) and PGP-2 (member of the ABC transporter family) also show impaired expression or trafficking with the findings provided in Figure 38.*

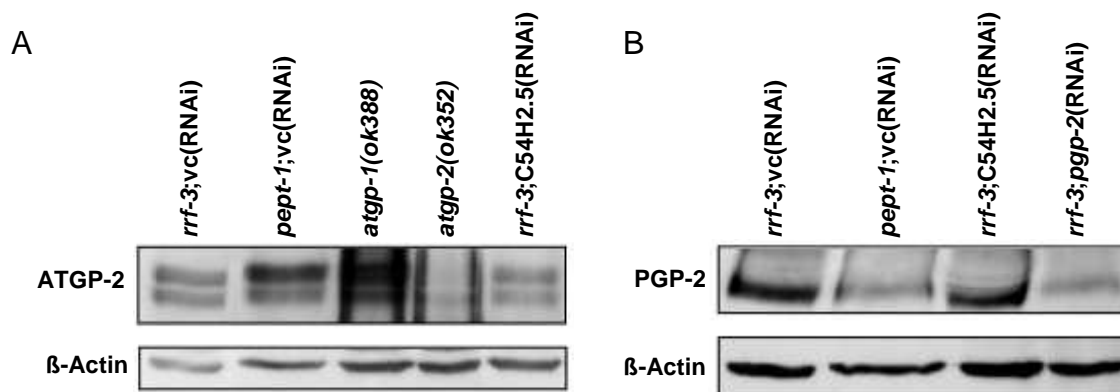


Figure 38: ATGP-2 and PGP-2 protein levels in a C54H2.5(RNAi) background

(A) ATGP-2 protein expression in membrane protein lysates of controls (vc = vector control RNAi, *pept-1*, *atgp-1* and *atgp-2*) and *rrf-3(pk1426)* *C. elegans* with RNAi silencing of C54H2.5. 20 μ g membrane protein lysates were loaded per lane. (B) PGP-2 protein expression of membrane protein lysates of *pept-1(lg601)* *C. elegans* and *rrf-3(pk1426)* treated with control RNAi (vc = vector control, *pgp-2*) and RNAi of C54H2.5. 30 μ g membrane protein lysates were loaded per lane. In both cases β -Actin was used as a loading control.

The amino acid transporter subunit ATGP-2 was shown to be located at the cell surface, when expressed in *Xenopus* oocytes (41). Its mass was estimated with 73.4 kDa and two bands were detected with the antibody with average masses of 65 and 75 kDa. The protein PGP-2 appears to function in gut granule biogenesis and is localised to the gut granule membrane with an estimated weight of 141 kDa. The antibody recognized the PGP-2 protein with a mass of 158 kDa. For ATGP-2 both detected bands were absent in *atgp-2(ok352)* worms, whereas ATGP-2 protein expression appeared to be increased in *atgp-1(ok388)* worms (Figure 38A). RNAi knockdown of C54H2.5 caused a slight reduction in expression of ATGP-2, while it did not alter PGP-2 expression. For PGP-2, *rff-3(pk1426)* worms with *pgp-2* RNAi knockdown served as an additional control with a distinct reduction in PGP-2 protein expression observed (Figure 38B). These results indicate that C54H2.5, like Erv29 in *S. cerevisiae* could be involved in the transport of a subset of proteins including PEPT-1 and ATGP-2 from ER to Golgi while ATGP-1 and PGP-2 remained unaffected by silencing C54H2.5.

2.2.3.2. The peptidases encoded by ZC416.6 and R11H6.1 appear to control PEPT-1 transport capacity

The genes ZC416.6 and R11H6.1 presumably code for proteins that function as cytosolic aminopeptidases. In addition to RNAi-treatment for reduction of protein expression peptidase inhibitors were used to assess whether the catalytic activity of the peptidases is important for proper PEPT-1 function. The mammalian homologues LTA4H and CNBP2 were reported to be sensitive to the aminopeptidase inhibitor bestatin (125) (126) which interestingly serves as a substrate of peptide transporters. Another peptidase inhibitor is amastatin which is a tetrapeptide-mimetic and has been used previously to separate peptide hydrolysis from transport since mammalian peptide transporters do not transport tetrapeptides (127). To investigate, whether inhibition of intracellular peptidases by amastatin and bestatin reduced PEPT-1 function with decreased β -Ala-Lys-AMCA uptake as shown for ZC416.6 and R11H6.1 RNAi treatment, different concentrations (0.01, 0.1 and 1 mM) of both peptidase inhibitors were applied to

rff-3(pk1426) *C. elegans*. In Figure 39 the results in transport assay and of PEPT-1 protein levels are shown.

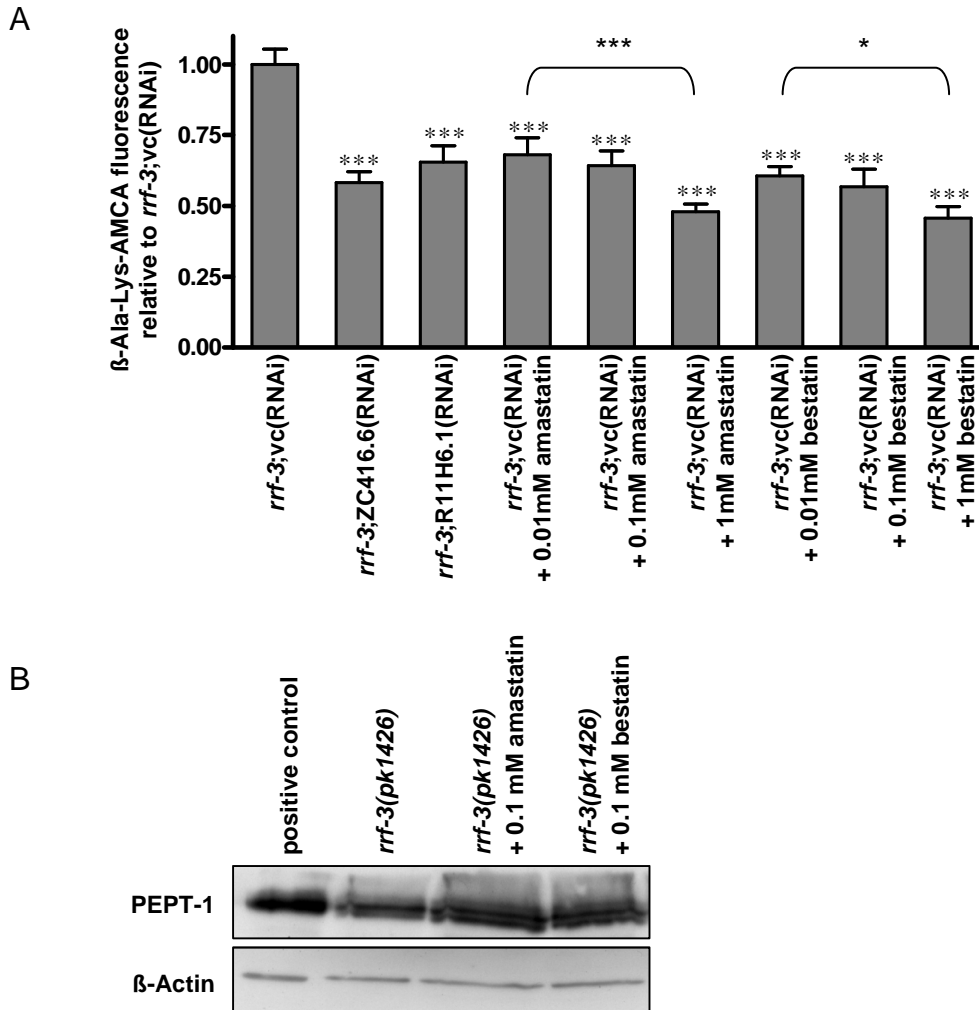


Figure 39: Effect of amastatin/bestatin on dipeptide uptake and PEPT-1 protein level

(A) β -Ala-Lys-AMCA fluorescence intensities of *rff-3(pk1426)* *C. elegans* additionally treated with ZC416.6(RNAi) and R11H6.1(RNAi) or different concentrations of amastatin and bestatin. The fluorescence intensities were determined for the area posterior the pharynx using Leica Confocal software 5.2. Denoted is the fluorescence relative to *rff-3;vc(RNAi)* worms. The experiment was performed two times and each time at least the fluorescence of 10 worms per group was analysed. Statistical analysis was performed by a One-Way-ANOVA with Turkey Post test. Significance (* $p < 0.05$, *** $p < 0.001$) to *rff-3;vc(RNAi)* is denoted. (B) PEPT-1 protein expression of membrane protein lysates of controls and *rff-3(pk1426)* *C. elegans* incubated for 1 hour with 0.1 mM amastatin/bestatin. 20 μ g membrane protein lysates were loaded per lane. Oocytes expressing *C. elegans* PEPT-1 were used as a positive control and β -Actin was used as a loading control.

Animals exposed to amastatin and bestatin showed a concentration-dependent decrease in the uptake of the fluorescent dipeptide β -Ala-Lys-AMCA (Figure 39A)

whereas peptidase inhibitor treatment did not alter PEPT-1 protein levels in lysates (Figure 39B). While bestatin at high concentrations could potentially inhibit β -Ala-Lys-AMCA uptake by competition, transport inhibition at low bestatin concentrations or the amastatin effects cannot be explained by a direct action on PEPT-1 transport function.

Since the two putative peptidases could contribute to intracellular hydrolysis of di- and tripeptides entering the cells via PEPT-1, their inhibition or reduced protein levels could keep dipeptide concentrations high while simultaneously decreasing the intracellular pool of free amino acids. Therefore worms treated with RNAi of ZC416.6 and R11H6.1 were supplemented with free amino acids and β -Ala-Lys-AMCA uptake and PEPT-1 protein expression was determined as well (Figure 40).

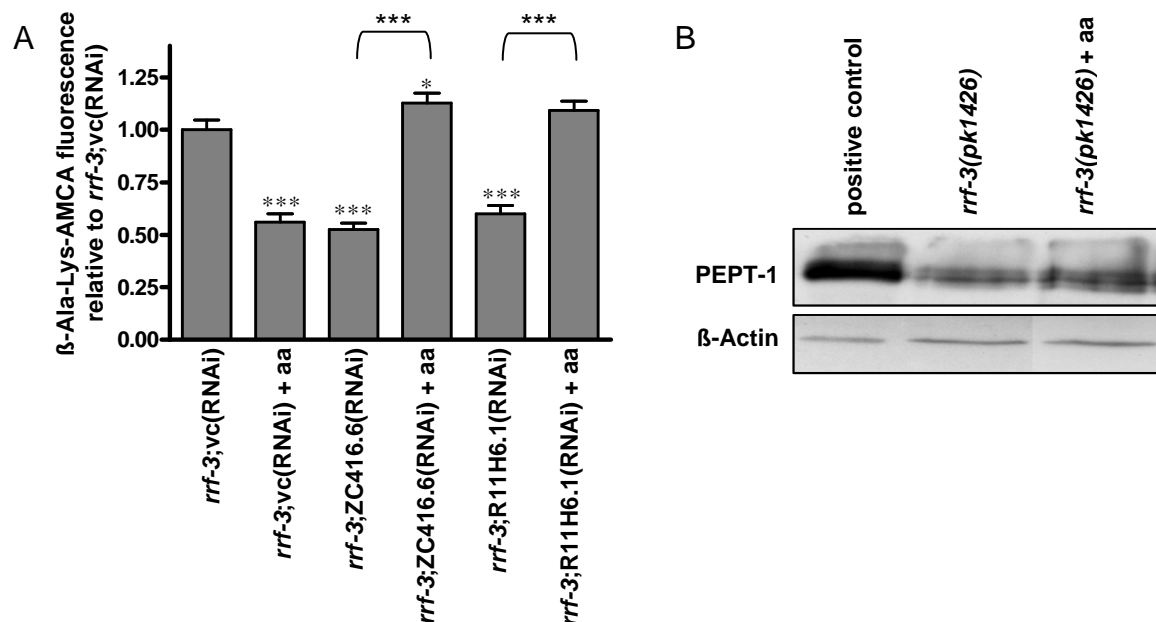


Figure 40: Effect of a free amino acid supplementation on dipeptide uptake and PEPT-1 protein levels

(A) β -Ala-Lys-AMCA fluorescence intensities of *rrf-3(pk1426)* *C. elegans* treated with RNAi of vector control (vc), ZC416.6 and R11H6.1 with and without amino acid (aa) supplementation. The fluorescence intensities were determined for the area posterior the pharynx using Leica Confocal software 5.2. Denoted is the fluorescence relative to *rrf-3;vc*(RNAi) worms. The experiment was performed two times and each time at least the fluorescence of 8 worms per group were analysed. Statistical analysis was performed by a One-Way-ANOVA with Turkey Post test. Significance (* $p < 0.05$, *** $p < 0.001$) to *rrf-3;vc*(RNAi) is denoted. (B) PEPT-1 protein expression of membrane protein lysates of controls and *rrf-3 C. elegans* incubated for 1 hour with amino acids (aa). 20 μ g membrane protein lysates were loaded per lane. Oocytes expressing *C. elegans* PEPT-1 were used as a positive control and β -Actin as a loading control.

Amino acid supplementation in *rrf-3(pk1426)* control worms caused a significantly decreased uptake of the fluorescent dipeptide β -Ala-Lys-AMCA comparable with the impaired uptake induced by RNAi of the dipeptidases ZC416.6 and R11H6.1 (Figure 40A). Nevertheless short-time amino acid substitution did not affect PEPT-1 protein levels (Figure 40B). By contrast when amino acids were supplemented in ZC416.6(RNAi) and R11H6.1(RNAi) treated worms, dipeptide uptake returned to levels comparable to that in control worms. This strongly suggests that these two peptidases contribute to the control of the intracellular pool of amino acids that in turn could affect PEPT-1 transport capacity. It was previously reported that peptide transport in *C. elegans* interferes with the TOR pathway (12). TOR is known to function as the main sensor of intracellular amino acid availability (86) (78) and is known to regulate amino acid transporter expression (89) (91). It therefore appeared reasonable to assume that diminished dipeptidase function and the effects of amino acid supplementation could involve TOR-signalling that feeds back to PEPT-1 protein expression and function.

2.2.3.3. TOR appears to affect PEPT-1 protein levels and function

Since the previous findings suggested that the cellular free amino acid pool may participate in the control of PEPT-1 transport capacity and that this could be possibly mediated by TOR, this link was assessed with gene deletion/RNAi treatment for proteins of the TOR pathway (Figure 41).

While uptake of the reporter dipeptide was completely abolished and PEPT-1 protein was below detection limit in *pept-1;vc*(RNAi) serving as a reference, treatment with *rict-1*(RNAi) - a homologous protein of mammalian rictor - reduced peptide uptake by about 50 % (Figure 41A) and also PEPT-1 protein levels when compared to the *rrf-3(pk1426)* control strain (Figure 41B).

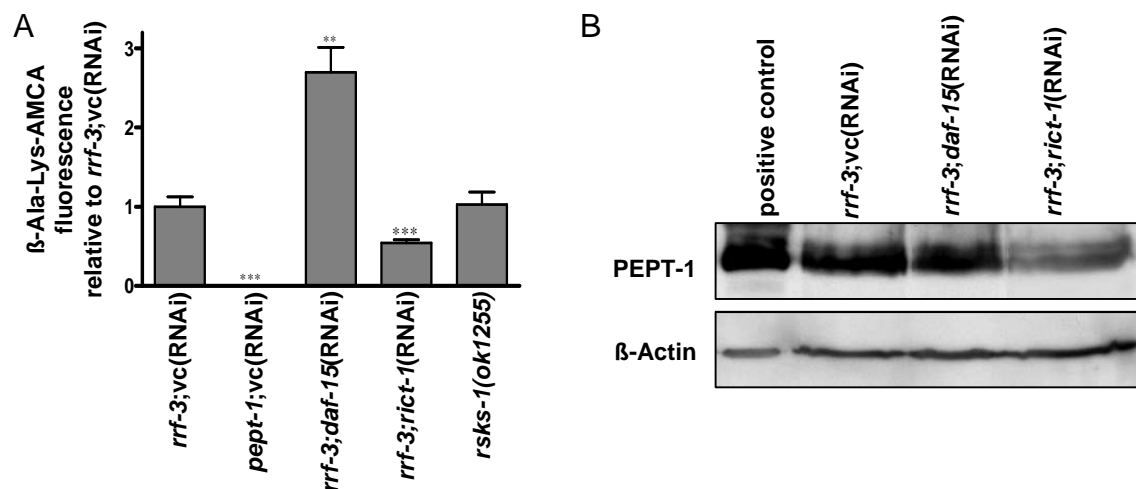


Figure 41: Impaired TOR signalling alters dipeptide uptake and PEPT-1 protein levels

(A) β -Ala-Lys-AMCA fluorescence of *C. elegans* controls (*rrf-3*, *pept-1*) and of worms with knockout/knockdown in the TOR pathway (*daf-15*(RNAi), *ric1*(RNAi), *rsks-1(ok1255)*) was measured. The experiment was performed two times with four technical replicates. Statistical analysis was performed by a Student's *t*-Test. Significance (** $p < 0.01$ and *** $p < 0.001$) to *rrf-3;vc*(RNAi) is denoted. (B) PEPT-1 protein expression in controls and *rrf-3(pk1426)* *C. elegans* with RNAi knockdown of *daf-15* (raptor homologue) and *ric1* (ricor homologue) was measured. 20 μ g membrane protein lysates were loaded per lane. Oocytes expressing *C. elegans* PEPT-1 were used as positive control, whereas β -Actin was used as loading control.

In animals with *rsks-1(ok1255)* knockout, dipeptide uptake remained unaltered. However, when expression of DAF-15, the homologous protein to mammalian raptor was suppressed by RNAi treatment, dipeptide uptake increased to 280 % ($p < 0.01$) of control in the absence of any changes in transporter protein levels. These findings strongly suggest that the *daf-15* and *ric1* encoded proteins participate in control of PEPT-1 transport activity in the intestine.

3. DISCUSSION

3.1. Amino acid homeostasis in *C. elegans*

Protein digestion in the intestinal lumen generates a huge spectrum of oligopeptides which are further cleaved into di- and tripeptides and free amino acids. The intestinal peptide transporter PEPT-1 is responsible for the uptake of large quantities of amino acids in di- and tripeptide bound form, whereas free amino acids are absorbed by a large variety of different amino acid transporters. It was shown for *C. elegans* lacking PEPT-1 that these animals have reduced tissue amino acid levels. Although amino acid levels were reduced the question emerged whether the lack of PEPT-1 was partially compensated by an increased expression of amino acid transport systems. We had previously observed that in *pept-1(lg601)* *C. elegans* some HAT subunit homologues and one PAT homologous gene showed altered mRNA expression levels. It was therefore part of the present project to assess the functional role of these amino acid transporters in wild type and in *pept-1(lg601)* deficient *C. elegans*.

3.1.1. Role of the HSHAT proteins ATGP-1 and ATGP-2 in *C. elegans*

Mammalian HATs are composed of a catalytic multi-transmembrane spanning subunit (light chain, LSHAT) and a type II *N*-glycoprotein subunit (heavy chain, HSHAT) linked by a disulfide bridge (17). In mammals there are two HSHATs referred to as rBAT and 4F2hc. rBAT is mainly found in the apical membrane of proximal tubular and intestinal epithelial cells. 4F2hc is ubiquitously expressed and found in the basolateral membrane of epithelial cells (29). LSHAT members need coexpression with the corresponding HSHAT for proper targeting to the plasma membrane. The LSHAT subunits confer the specific amino acid transport activity of the heteromeric complex. For example rBAT is essential for the cell surface localisation of LSHAT $b^{0,+}AT$, but it is not required for reconstituted $b^{0,+}AT$ transport activity (30). Mutations in human genes as in the case of rBAT cause cystinuria as a renal disease (reviewed by (36)).

In *C. elegans* there are two homologous proteins to mammalian HSHAT known, called ATGP-1 and ATGP-2 (amino acid transporter glycoprotein subunit 1 and 2)

with a protein sequence identity to mammalian proteins of ~30%. Studies in *Xenopus laevis* oocytes revealed that the expression of ATGP-1 alone caused a strong surface expression and weak intracellular localisation of the protein (41). Hence, *C. elegans* ATGP-1 appears to behave like mammalian 4F2hc which localises to the cell surface even in the absence of a light chain (21). The second *C. elegans* HSHAT ATGP-2 resides in the cytosol when expressed in oocytes while coexpression with the LSHAT homologues AAT-1 or AAT-3 resulted in a strong surface expression of the protein complexes. The transport characteristics for *C. elegans* AAT-1/ATGP-2 and AAT-3/ATGP-2 resembled those of the Na⁺-independent mammalian transport system L and to some extent system asc (21). Mammalian system L (LAT2-4F2hc) mediates as a sodium-independent exchanger the transport of large neutral amino acids against smaller neutral ones in the basolateral membrane of intestinal cells. The activity as an exchanger depends on the amount of intracellular amino acid substrates available for efflux (22). In mice it was shown that system asc (asc1-4F2hc) is mainly expressed in brain (128) and gene deletion of *asc-1* in mice resulted in early postnatal lethality (129). In *C. elegans* the distinct membrane localisation (apical versus basolateral) of the ATGP-1 and ATGP-2 proteins is not yet known.

In mice it was shown that gene deletion of *4F2hc* caused lethality during early embryogenesis (130), and malfunction of the basolateral amino acid transport system can obviously not be compensated by other transporters. *C. elegans* with knockouts of *atgp-1(ok388)* and *atgp-2(ok352)* were fully viable as shown here and did not display any alterations of reproduction either. This suggests that they may not have the same function and/or basolateral localisation as the mammalian HSHAT 4F2hc. It may be argued that ATGP-1 and ATGP-2 are therefore more similar to the mammalian apical amino acid transporter heavy subunit rBAT. In humans it was shown that mutations in the system b^{0,+} (b^{0,+}AT-rBAT) which would lead to malabsorption of distinct amino acids can be compensated when these amino acids were provided as peptides and taken up via PEPT-1. In *C. elegans* we did not find any evidence for such a compensation, because alterations in the number of progeny was also not observed in *pept-1;atgp-1(RNAi)* and *pept-1;atgp-2(RNAi)* worms lacking both transport proteins. Surprisingly in *atgp-1(ok388)* knockout animals PEPT-1 protein expression was increased, while peptide transporter protein expression was

found to be decreased in *atgp-2(ok352)* worms. Moreover it seemed that ATGP-1 and ATGP-2 can compensate for each other, because knockout of one heavy subunit homologue led to increased protein expression of the other subunit which may suggest that both transporter subunits have the same membrane localisation and similar function. Although the number of progeny and worm viability was not changed in *atgp-1(ok388)* and *atgp-2(ok352)* knockout animals, intracellular amino acid contents of whole worm lysates of *atgp-1(ok388)* *C. elegans* reflected most likely the compensation by increased protein levels of PEPT-1 and ATGP-2 and transport function. The concentration of only five amino acids (Ala, Asn, Met, Phe, Arg) was found significantly decreased in levels when compared to wild type animals. In *atgp-2(ok352)* worms however the observed amino acid profile revealed that the concentrations of most of the amino acids (10 out of 18) was significantly reduced, while the non-essential amino acids asparagine, glycine and serine showed increased levels. As the amino acid concentration of glutamine and glycine was significantly altered in *atgp-2(ok352)* worms and the predicted mammalian homologue rBAT is responsible for the uptake (intestine) and reabsorption (kidney) of cystine which is rapidly reduced to cysteine, the limiting substrate for the synthesis of intracellular glutathione (101), we assessed tGSH and GSSG levels in *atgp-2(ok352)* worms. GSSG levels were found decreased, while total GSH levels remained unchanged.

Whereas neither the single knockouts nor RNAi double knockdowns in a *pept-1(lg601)* background altered viability and fertility of the worms, a deletion of *atgp-2* in a PEPT-1 deficient background was found to be lethal (Spanier, personal communication). Hence, this double knockout generates an even stronger phenotype than RNAi knockdown of *atgp-2* in a *pept-1(lg601)* background. The lack of one HSHAT seems to be compensated by increased expression of the second subunit, whereas in the case of *atgp-1(ok388)* also PEPT-1 seems to be part of the adaptive compensation mechanism. From the data it may be postulated that the increased uptake of dipeptides in *atgp-1(ok388)* worms may cause an overall cellular amino acid concentration comparable with that of wild type animals. However, it appears that the amino acid transporter subunits in worms are less important for the animals than their mammalian homologues. They also do not seem to play a prominent role for amino acid homeostasis in *pept-1(lg601)* *C. elegans*. Consequently more studies

are needed to assess the function of these amino acid transporters in worms or to identify other proteins that contribute to control of amino acid homeostasis in wild type or PEPT-1 deficient animals.

3.1.2. The LSHAT subunit *aat-6* is necessary for amino acid homeostasis in *pept-1(lg601) C. elegans*

Besides the HAT heavy subunits there are nine *C. elegans* genes encoding for homologues of HAT light subunits. They are named *aat-1* to *aat-9* (amino acid transporter catalytic chain). AAT-1 to AAT-3 are closer related to mammalian transporters (39-45% protein identity) than AAT-4 to AAT-9 (28-31% protein identity). But only AAT-1, AAT-2 and AAT-3 exhibit the conserved cysteine residue which is necessary for the disulfide bridge formed between the light and the heavy chains. It was shown that AAT-1 and AAT-3 together with ATGP-2 can build functional transport systems responsible for the uptake of most neutral amino acids (41). AAT-1 is expressed in the nervous system, the intestine and glandular cells (131). It was postulated that the other six *C. elegans* LSHATs may not need to associate with a heavy subunit for functional expression and membrane targeting (41). In *Xenopus* oocytes expressing AAT-4 and AAT-9 proteins reached the cell membrane without an exogenous heavy chain subunit (41) (42). AAT-9 was shown to perform exclusively an obligatory exchange of aromatic amino acids, whereby it resembles the mammalian transporter TAT1 found in mammals mostly in kidney, skeletal muscle, placenta and heart (43). AAT-9 is expressed in neurons and in body wall muscles of the mouth region in worms.

As shown here, RNAi gene silencing of three LSHATs (*aat-5*, *aat-6* and *aat-7*) in a *pept-1(lg601)* knockout background caused alterations in the number of progeny. These changes were dependent on the absence of the di- and tripeptide transporter, because in a wild type background the number of progeny was not affected by RNAi knockdowns. Amongst the subunits, AAT-6 seemed to be most important for amino acid homeostasis in *pept-1(lg601) C. elegans*, because knockdown of this gene caused a sterile phenotype.

Up to now nothing is known about the function or membrane localisation of AAT-6. Expression of *aat-6* cRNA in *Xenopus laevis* oocytes unfortunately failed

to produce a functional transporter. *C. elegans* AAT-6 has highest protein homology to the HAT light subunit xCT of the cystine/glutamate exchanger system x_c^- (xCT-4F2hc). This transporter mediates the Na^+ -independent, electroneutral exchange of cystine (influx) against glutamate (efflux) at the apical plasma membrane (24). Availability of cystine/cysteine is the rate-limiting step in glutathione synthesis which is the major natural antioxidant, protecting cells from oxidative stress (132). It was shown that transcription of the xCT gene and x_c^- transport activities are induced by oxidative stress, mediated by electrophilic agents, depletion of cystine and by oxygen (133). xCT deficient mice are viable and fertile indicating that the supply of cysteine can be compensated by other routes including di- and tripeptide uptake via PEPT1 during development (134). The same effect was observed for wild type *C. elegans* with RNAi knockdown of *aat-6*, but when additionally PEPT-1 was lacking, a further decrease in adult body length and infertility was observed. The reduced body length development in *pept-1;aat-6(RNAi)* worms could not be diminished even by a 1:100 dilution of *aat-6* dsRNA, whereas the number of progeny increased up to 50 % of that of control worms. These findings suggest that AAT-6, like AAT-9, is a functional amino acid transporter in worms which contributes significantly to amino acid status and even amino acid supplementation could not rescue the sterile phenotype of *pept-1;aat-6(RNAi)* worms. It furthermore was shown here that there was a modest increase of ATGP-1 and ATGP-2 protein levels in *rrf-3;aat-6(RNAi)* and *pept-1;aat-6(RNAi)* worms when compared to those in control animal. This suggests that *C. elegans* compensates the lack of AAT-6 with an increased expression of both heavy subunits, but this seems not to provide sufficient amino acids.

Heteromeric amino acid transport systems are present in all species ranging from yeast to mammals. For worms lacking the peptide transporter the heavy subunits appear not important but the light subunit AAT-6 seems most crucial for growth and reproduction. Silencing of *aat-6* in *pept-1(lg601)* worms resulted in a reduction in adult body length and a sterile phenotype. Further studies are needed to determine the spatial expression of this subunit in worms and how its expression is controlled.

3.1.3. The PAT homologue Y4C6B.2 represents a second amino acid transporter essential for amino acid homeostasis in *pept-1(lg601)* *C. elegans*

Transcriptome data generated from worms deficient in PEPT-1 revealed an 18-fold increase in mRNA expression of the Y4C6B.2 gene suggesting that this homologous protein of proton-coupled amino acid transporter (PAT) class could be necessary for amino acid homeostasis in *pept-1(lg601)* worms. Three *C. elegans* PAT homologues were studied, Y43F4B.7, Y4C6B.2 and T27A1.5.

PAT1 (SLC36A1) was originally identified as the lysosomal amino acid transporter (LYAAT1) in rat brain (46). It is expressed in almost all tissues especially in brain, small intestinal brush border membrane, kidney and colon. In brain PAT1 is mainly found in neuronal lysosomes (46). In apical membranes of the intestine it however mediates the uptake of small neutral amino acids including β -alanine, glycine, L-proline, γ -aminobutyric acid (GABA), α -(methylamino)-isobutyric acid (44) and pharmaceutically relevant compounds such as D-cycloserin or L-azetidine-2-carboxylic acid (45). In lysosomes PAT1 exports the same amino acids as generated by lysosomal proteolysis. It also was shown to mediate the electroneutral cotransport of protons with short-chain fatty acids (47). For zwitterionic substrates transport is energised by an inwardly directed H^+ gradient with a stoichiometry of proton to substrate of one. Function of PAT1 results in an acidification of the cytosol. All substrates transported possess a rather low affinity (135). By contrast, PAT2 (SLC36A2) is a high-affinity transporter with significant functional and sequence similarity to PAT1 (49). It is also responsible for the uptake of alanine, glycine and proline and short-chain fatty acids in a proton symport (47). PAT2 is strongly expressed in brain, heart and lung and with lower expression levels in kidney and muscle. It is not found in lysosomes, unlike PAT1, but it is present in the ER of neurons and in the cell plasma membrane (136). Mutations in mammalian PAT1 and PAT2 are associated with iminoglycinuria (OMIM 242600) an inherited disorder (50) which is characterised by increased excretion of proline, hydroxyproline and glycine in the urine and impaired intestinal transport is observed in some pedigrees (52).

The effects observed for RNAi knockdown of the three PAT homologues (Y4C6B.2, T27A1.5 and Y43F4B.7) in *pept-1(lg601)* worms revealed that only Y4C6B.2 caused a strong phenotype with sterility. With an 18-fold increase in

mRNA in *pept-1(lg601)* worms, the functional Y4C6B.2 protein seems to compensate the lack of PEPT-1 and shows essentiality for reproduction in *pept-1(lg601)* *C. elegans*. By contrast, in wild type animals it seems to play only a minor role. Attempts to express Y4C6B.2 in *Xenopus* oocytes failed to generate a functional transport protein (Kottra, personal communication).

In *Drosophila* two homologous genes to mammalian PAT proteins are found, CG3424 (named *path*) and CG1139. Flies with a homozygote *path* knockout were markedly smaller, approximately 40 % lighter in weight and had a delay in development compared with wild type animals. Homozygous *path*^{-/-} *Drosophila* females also laid no eggs (95). The same effects were observed for *pept-1(lg601)* worms with RNAi gene silencing of Y4C6B.2. Even a 1:10 dilution of the Y4C6B.2 dsRNA still caused a retarded development and smaller adult body size. A sterile phenotype was observed for *pept-1;Y4C6B.2(RNAi)* worms, whereby a dilution of Y4C6B.2 dsRNA could partially rescue the sterile phenotype. But even worms grown on a 1:100 dilution laid significantly less eggs than control worms. In contrast to *Drosophila* the phenotypic effects observed for *C. elegans* all were dependent on the absence of PEPT-1. Since in mammals PAT1 is localised in the apical membrane of intestinal and renal cells it is plausible to assume that the protein is similarly found in brush borders of worm epithelia. When the expression of Y4C6B.2 is decreased in *pept-1* worms via RNAi, it results in a stronger phenotype, because the assumed compensatory uptake of amino acids by Y4C6B.2 is not possible and apparently this transport function cannot be taken over by other transporters. This may also explain why amino acid supplementation failed to rescue the severe phenotypes. Recent data collected in *Drosophila* suggests that PATH is a low capacity transporter that may act as a “transceptor” - a receptor that is structurally related to a transporter (137) for sensing intracellular or extracellular amino acids (95). It is of course tempting to speculate that Y4C6B.2 in worms may also serve as a transceptor and this should be assessed by follow up studies.

3.2. Identification of proteins that can alter PEPT-1 function in *C. elegans*

The intestinal peptide transporter PEPT1 has been intensively studied in various species over the past decades with respect to its kinetics, substrate specificity, dietary and pharmacological importance (for review (138)) and was shown to act as an electrogenic symporter energised by a negative apical membrane potential (139). PEPT1 expression and function is subject to regulation by prolonged exposure to substrates and via activation of protein kinase C (140). Sustained starvation in rats (141) as well as a high protein diet and individual amino acid (142) were shown to increase PEPT1 expression and protein abundance in the apical membrane. In yeast it was shown that imported amino acids and also dipeptides increased the capacity to import peptides via an ubiquitin-dependent proteolytic pathway (143) (144). Li and co-workers (145) have shown that rat PEPT1 promoter is activated by lysine, whereas human PEPT1 is not. Hence, there seem to be species-specific differences in PEPT1 expression control. It is also regulated by cAMP with increasing intracellular levels inhibiting PEPT1 transport activity (146) and decreasing cAMP levels elevating activity (147). When free intracellular Ca^{2+} levels increase PEPT1 activity is diminished and vice versa (148). Hormones such as leptin and insulin were shown to regulate PEPT1 abundance and activity (149) (150) mainly by recruitment of preformed transporters.

Although regulation phenomena of PEPT1 have been studied, little is known about cellular proteins that may directly or indirectly interact with the peptide transporter protein or modulate the transport process. In the present study a RNAi genetic screen of 162 genes known to be expressed in the *C. elegans* intestine was performed to identify PEPT-1 modulator genes/proteins. The screening employed initially a transport assay with a fluorescent reporter substrate and a secondary selection for phenotypic features resembling those of the *pept-1* knockout, such as fat accumulation and fatty acid absorption. In addition to the NHX-2 sodium-proton antiporter – known already to be essential for PEPT-1 function - four PEPT-1 modulating genes with homologues in higher species F26E4.12, C54H2.5, ZC416.6 and R11H6.1 were identified.

3.2.1. Silencing F26E4.12 induces an increased PEPT-1 transporter function

An increased transport function was only obtained by RNAi-treatment for the gene F26E4.12. It is coding for a homologue of a mammalian phospholipid hydroperoxide glutathione peroxidase (PHGPx, GPx4) which is a selenium-dependent member of the glutathione peroxidase (GPx) family with six isozymes. GPx proteins are classified as cytosolic (cGPx or GPx1), gastrointestinal (GI-GPx or GPx2), plasma (pGPx or GPx3), phospholipid hydroperoxide (PHGPx or GPx4), epididymal (GPx5) and olfactory (GPx6) proteins (151). All glutathione peroxidases catalyse the reduction of H_2O_2 or organic hydroperoxides to water or corresponding alcohols by means of reduced glutathione (GSH) as an electron donor (107). There are some differences between PHGPx and the other glutathione peroxidases: PHGPx is a 20-22 kDa monomer protein, whereas the other GPx are tetramers (152). It is a key enzyme in protection of biomembranes exposed to oxidative stress (153). PHGPx uses exclusively phospholipid hydroperoxides as substrates (Figure 42) and can additionally react with hydrogen peroxide and a wide range of lipid hydroperoxides such as those derived from cholesterol and cholesteryl esters (154), as well as thymine hydroperoxides (155).

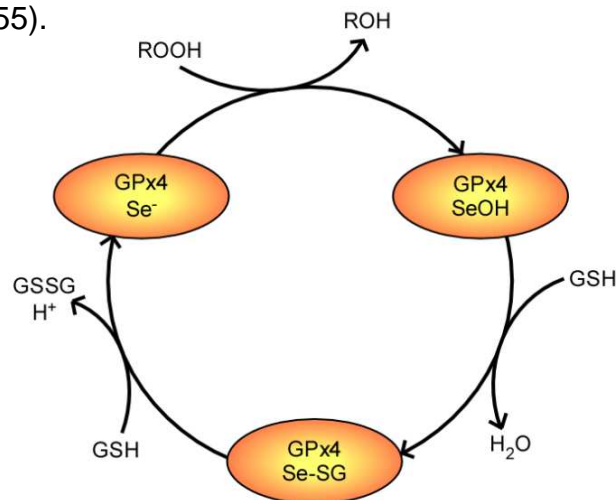


Figure 42: Schema for the catalytic cycle of GPx4

During the catalytic cycle of GPx4, the active selenol ($-\text{Se}^-$) is oxidised by peroxides to selenenic acid ($-\text{SeOH}$) which in turn is reduced with glutathione (GSH) to an intermediate selenodisulfide ($-\text{Se-SG}$). GPx4 is regenerated by a second glutathione molecule, releasing glutathione disulfide (GSSG) (modified from (156)).

PHGPx can use in addition to glutathione also other reducing substrates (157). PHGPx is suggested to act as a regulator of apoptosis, gene expression and eicosanoid biosynthesis. It is synthesised as a long form (23 kDa, targeted to

mitochondria) and a short form (20 kDa, non-mitochondrial, found in cytosol and nucleus), both arising from the same *Gpx4* gene, but with different translation initiation sites (158).

Silencing of F26E4.12 enhanced β -Ala-Lys-AMCA uptake around three-fold without affecting *pept-1* mRNA or protein expression levels. This effect may originate in worms by virtue an improved transporter translocation into the apical membrane either by accelerated membrane delivery or insertion from vesicles. This however could not be assessed as the technique used for membrane protein preparation did not allow distinguishing between membrane-inserted PEPT-1 and PEPT-1 located in transport vesicles. Alternatively, increased dipeptide uptake may also be caused by peroxidation of phospholipids, induced by the lack of the phospholipid hydroperoxide glutathione peroxidase. Enhanced levels of lipid hydroperoxides was shown to disturb the assembly of the membrane and cause changes in fluidity and permeability (159) which could either affect PEPT-1 function or allow increased diffusion of β -Ala-Lys-AMCA into intestinal cells.

Mammalian cytosolic GPx4 was shown to suppress the activity of lipoxygenases (160) and cyclooxygenases (161) and therefore plays an important role in arachidonate and leukotriene metabolism. Until now there are no homologues of lipoxygenases (LOX) and cyclooxygenases (COX) found in *C. elegans* suggesting that these pathways do not exist in worms.

The disruption of the *GPx4* gene caused early embryonic lethality in mice (151) presumably linked to the *GPx4* cytosolic product. However heterozygous *GPx4*^{+/-} mice developed normal and therefore served as a model of deficiency with approximately 50 % decrease of GPx4 in all tissues for all GPx4 isoforms (162), comparable with RNAi knockdown of F26E4.12 in *C. elegans*. For *GPx4*^{+/-} mice lipid peroxidation was increased with higher levels of 4-hydroxynonenal (4-HNE) and oxidative stress (162). In *C. elegans* treated with F26E4.12 RNAi mitochondrial ROS levels were found not to be altered. Lipid peroxidation was shown to play an important role in a variety of cellular processes, e.g. inactivation of membrane enzymes, alterations in functions of ion channels, collapse of membrane potential and reduced mitochondria functions (163). But when lipid hydroperoxides are not detoxified by GPx4 and therefore accumulate they can undergo iron- and oxygen-mediated chain-breaking lipid peroxidation to generate a variety of α,β -unsaturated electrophilic aldehydes amongst those 4-HNE is the

most abundant form (164). It was also shown that lipid hydroperoxides initiate the activation of the transcription factor activator-protein 1 (AP-1) (165) which in turn could induce the transcriptional activation of the peptide transporter gene as shown previously (166). Reduced expression of F26E4.12 might increase the concentration of ROS derived (phospho)lipid hydroperoxides and therefore enhanced levels of 4-HNE are likely. The pathway to dispose 4-HNE is in most tissues the conjugation with glutathione which is catalysed by glutathione transferases (GSTs) (167). Mammalian enzymes with high catalytic efficiency for 4-HNE belong to the alpha class, whereas those in *Drosophila* are classified as sigma and delta and those in *C. elegans* as pi class GSTs (168). In *C. elegans* there are five genes (*gst-5*, *gst-6*, *gst-8*, *gst-10* and *gst-24*) encoding for glutathione transferases which are capable of catalysing 4-HNE conjugation (169). *C. elegans* over-expressing *gst-10* had an increased resistance to paraquat compared with control animals. Also in worms treated with F26E4.12 RNAi an enhanced stress resistance against paraquat was observed which could result from elevated levels of GST-10 (also called CeGSTP2-2). Nonetheless, when metabolic detoxification of 4-HNE is overwhelmed, these aldehydes can form covalent protein-aldehyde adducts. The proteasome in mammals is unable to degrade proteins modified by 4-HNE (170), whereas some data suggest that autophagy is an important mechanism for the removal of protein-4-HNE adducts. In human vascular smooth-muscle cells (VSMC) exposed to autophagy stimulator rapamycin, the removal of protein-aldehyde adducts was accelerated (171). Rapamycin causes decreased activity of TORC1 which in turn activates autophagy and protein degradation and also could activate TORC2. But the mechanism by which 4-HNE or protein-4-HNE adducts elicit autophagy remains unclear. A putative role of F26E4.12 in the complex interplay of lipid peroxidation, autophagy and TOR signalling in peptide transport processes will be discussed in a subsequent paragraph.

3.2.2. The ER cargo transport protein C54H2.5 not only alters PEPT-1 expression and function

RNAi knockdown of C54H2.5 resulted in a significant reduction of uptake of the reporter and also enhanced fat accumulation and increased fatty acid absorption. The ER cargo transport protein encoded by C54H2.5 appears to participate in protein secretion, maturation and the unfolded protein response (116). Trafficking of PEPT-1 from ER to Golgi and to its final membrane destination may - as the previous findings suggest - depend on proper function of the protein encoded by C54H2.5. Homologous genes to C54H2.5 are conserved among a number of species ranging from *S. cerevisiae* to *H. sapiens*. Conserved within this group is the di-lysine motif -KKXX-COOH, which is thought to act as a Golgi to ER retrieval signal for membrane proteins by binding to α -COPI, a protein involved in retrograde transport from the Golgi to ER (172). The best investigated homologue to C54H2.5 is Erv29p of *S. cerevisiae*. Erv29p is an integral membrane protein which is required for the delivery of specific secretory, correctly folded proteins from the ER to the Golgi. Erv29p is enriched in COPII vesicles exiting the ER (173) and it is responsible for loading selected cargo proteins into COPII vesicles for export. Thus Erv29p might also act as a cargo-receptor (174), but it is also important for degradation of soluble misfolded proteins (115). The mammalian homologue SURF-4 interacts with the ER-Golgi intermediate compartment and is crucial for its stability (175). The surfeit locus contains the tightest cluster of mammalian genes so far described, but in invertebrate organisms like *C. elegans* or *D. melanogaster* they are not so tightly clustered (176).

RNAi silencing of C54H2.5 did not significantly alter promoter activity or transcription of *pept-1*, but decreased PEPT-1 protein levels. It was demonstrated for Erv29 Δ cells that the lack of the cargo transport protein interrupted the traffic between ER and Golgi of a subset of proteins. While trafficking of CPY (carboxypeptidase Y) and PrA (proteinase A), both ER quality control substrates was defective in these cells, transit time of invertase and alkaline phosphatase was not affected (115). Here in *C. elegans* it was demonstrated that the amino acid transporter protein ATGP-2 showed as well a distinct reduction in protein levels similar to PEPT-1 after treatment of worms with C54H2.5 RNAi, while the expression of two other proteins, ATGP-1 and PGP-2, was not altered. These data suggest that the C54H2.5 protein in worms may behave like the yeast Erv29

and may control trafficking of a subset of proteins leaving the ER. The PEPT-1 protein and the amino acid transporter subunit ATGP-2 appear to belong to this subgroup and their impaired delivery to the apical membrane may contribute to the changes in phenotypes found in the secondary screens. Although body length development of C54H2.5(RNAi) worms was comparable to control worms, the number of progeny was significantly reduced similar to PEPT-1 deficient *C. elegans*. Besides being responsible for cargo transport of correctly folded proteins from ER to Golgi, yeast Erv29p is also essential for the degradation of misfolded proteins (177) which cause ER stress when accumulating (Figure 43). The ER stress is leading to cellular deployment of the unfolded protein response (UPR). Activation of UPR culminates in three processes: inhibition of protein synthesis, increased expression of ER resident chaperones and degradation of misfolded proteins.

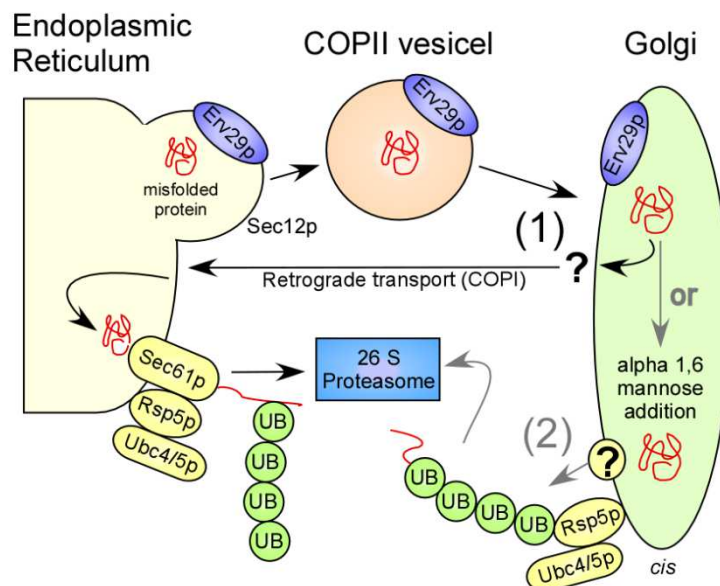


Figure 43: Degradation of misfolded proteins via the HIP pathway

The degradation mechanism via HIP pathway eliminates misfolded proteins by transport them in COPII vesicles, involving Sec12p and the putative cargo receptor Erv29p, from the ER to Golgi. In the cis-Golgi compartment two possibilities could happen. (1) The misfolded protein may be transported back to the ER, where it would enter the cytosol through translocon, ubiquitinated by ubiquitin ligase Rsp5p and then degraded by proteasome. (2) The second possibility is that the misfolded protein is modified by α -1,6 mannose addition in the *cis* Golgi compartment before it is ubiquitinated and degraded by the proteasome (modified from (177)).

When Erv29p was missing in yeast, misfolded protein degradation failed and the substrates were stabilised in the ER which in turn caused ER stress, prolonged UPR activation and thereby ROS accumulation (116). However after silencing of

C54H2.5 in worms, no increase in mitochondrial ROS levels was observed. But there was a significant two-fold increase of the GSH and GSSG concentration which may suppress ROS accumulation. The higher glutathione concentration could also be responsible for the increased stress resistance against paraquat, as compared to control worms. For *Erv29Δ* cells with induced ER stress it was also demonstrated that GSH addition permitted a continued growth and reduced ROS accumulation (116). However, as the silencing of C54H2.5 is very likely to affect numerous other proteins, we did not further investigate its role in peptide transport and associated phenotypic features in worms.

3.2.3. Gene silencing of both aminopeptidases ZC416.6 and R11H6.1 cause altered PEPT-1 expression and protein levels

The gene ZC416.6 in *C. elegans* is coding for an ortholog of the bifunctional leukotriene A₄ hydrolase/aminopeptidase LTA4H. The gene is homologous to mammalian LTA4H as a bifunctional zinc metalloenzyme that mainly resides in the cytosol (178). It catalyses the final step in the biosynthesis of leukotriene B₄ (LTB₄) which originates from arachidonate converted into the unstable epoxide leukotriene A₄ by 5-lipoxygenase. This intermediate is catalyzed by LTA4H to LTB₄ or it is conjugated with glutathione to leukotriene C₄ (LTC₄) (109). For *C. elegans* it was shown that AP-1 (aminopeptidase 1), another *C. elegans* LTA4H homologue than ZC416.6 is unable to use LTA₄ as a substrate (179). Yet, invertebrates like *C. elegans* were shown not to synthesise leukotrienes (111). It may therefore be the aminopeptidase activity expressed by ZC416.6 in *C. elegans* that defines its biological role.

The gene *pes-9* (Cosmid number R11H6.1) encodes a zinc dependent exopeptidase which is homologous to the human cytosolic non-specific dipeptidase 2 (CNDP2, CN2) and the Dug1p protein in *S. cerevisiae*. The mammalian homologue CNDP2 (human cytosolic non-specific dipeptidase or formerly called human tissue carnosinase) was first discovered in 1949 (180) and is ubiquitously expressed in human tissues (181). It is a homodimer (182), a metal-ion dependent dipeptidase (125) and can hydrolyse carnosine (β-alanyl-L-histidine) to L-histidine and β-alanine (183). However, CNDP2 acts more as a

cytosolic non-specific dipeptidase rather than a selective carnosinase, because of its wide range of substrates (112).

RNAi-treatment for the aminopeptidase homologues ZC416.6 and R11H6.1 in *C. elegans* drastically reduced peptide transport and was associated with decreased PEPT-1 protein levels. Since no changes in mRNA levels were observed, either a reduced translation efficiency and/or enhanced PEPT-1 protein degradation must cause this. Reduced peptide transport was associated with phenotypic changes similar to those found in the *pept-1(lg601)* worms such as increased fatty acid uptake and fat accumulation (67). However, neither body size nor brood size were affected significantly like in PEPT-1 deficient animals. Evidence that the intracellular peptidases may participate in the control of peptide transport activity was independently obtained by use of the peptidase inhibitors amastatin and bestatin. Short term treatment of worms with these inhibitors caused a dose-dependent decrease in uptake of the fluorescent dipeptide with no changes in PEPT-1 protein levels. From these findings we may conclude that the activity of intracellular peptidases affects intestinal peptide uptake in the absence of changes of the transporter protein, whereas a long term suppression of expression of the peptidases by RNAi treatment in addition causes decreased PEPT-1 protein levels.

Most of the di- and tripeptides entering the cells via PEPT-1 are rapidly cleaved by cytosolic peptidases to free amino acids that transiently increase the intracellular amino acid pool and that leave the cell via basolateral amino acid transporters. However, most of these basolateral transporters act as exchangers (for review (15)) and therefore amino acid efflux from intestinal cells is counterbalanced by influx of other amino acids from the extracellular space that fill up the intracellular amino acid pool. However, when intracellular peptide hydrolysis capacity is reduced, the intracellular pool of amino acids will be reduced in cells expressing PEPT-1 while short chain peptides accumulate in the cytosol (184). That the level of intracellular amino acids is crucial for proper PEPT-1 function was shown by supplementing free amino acids. Whereas this treatment led to transport inhibition in control worms, in animals with silenced peptidases, supplementation of free amino acids reversed the transport inhibition back to that in wild type worms.

3.2.4. A novel predicted interaction between TORC2 and PEPT-1 may play an important role in transporter expression and function

The mammalian TOR protein complex acts as an intracellular amino acid sensor (78) (87) with the protein components TORC1 and TORC2 displaying negative reciprocal regulation (71). A decrease in cellular free amino acid levels was shown to cause a deactivation of TORC1 which in turn impairs protein translation by dephosphorylation of S6K1 and enhances protein degradation and turnover (83). Inhibited S6K1 in turn activates TORC2 (185). An increased intracellular amino acid concentration induced by amino acid supplementation may thus in reverse activate TORC1 and inactivate TORC2. One part of TORC2 is rictor called RICT-1 in *C. elegans*. In the present study it was shown that inactivation of TORC2 by RNAi gene silencing of *rict-1* caused reduced PEPT-1 protein levels and at the same time impaired transport. In this context it is important to note that, as recently shown, *rict-1(mg451)* *C. elegans* mutants show phenotypic characteristics reminiscent of *pept-1(lg601)* animals with increased body fat, developmental delay, smaller body size and reduced brood size (186) (187). By contrast, RNAi knockdown of *daf-15*, part of TORC1 and antagonist of *rict-1*, increased dipeptide uptake nearly three-fold although here PEPT-1 protein levels appeared unaltered. PEPT-1 activity was not affected by the knockout of *rsks-1* (homologous to mammalian S6K) that acts downstream of TORC1 (188) and *rsks-1(ok1255)* worms did not display a CeTOR phenotype (189). As PEPT-1, RICT-1 and DAF-15 are all expressed in intestinal cells, an interaction of the proteins in controlling PEPT-1 expression level and/or function might be plausible (12) (187) (190) (Figure 44).

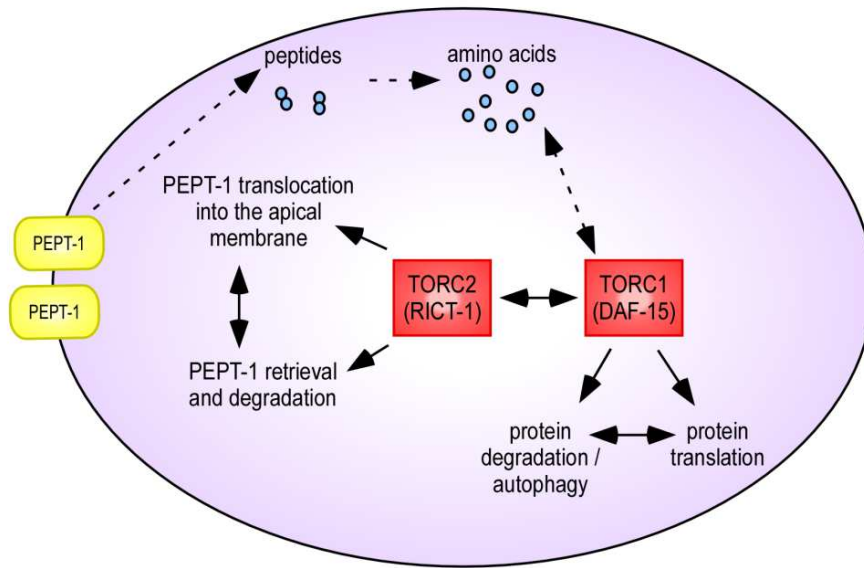


Figure 44: Postulated interaction of TORC2 and PEPT-1 in *C. elegans*

Hence it seems that inactivation of RICT-1 by RNAi gene silencing of *ric1-1* decreases dipeptide uptake via PEPT-1, whereas the lack of DAF-15 could activate RICT-1 by negative reciprocal regulation as shown for mammalian TORC1 and TORC2 (71) and enhance transport function probably by recruitment of preformed transporters located in cytosolic vesicles.

A similar effect was obtained for insulin stimulation on hPEPT1 translocation in Caco-2 cells (149). hPept1 gene expression was not altered by insulin, but the amount of hPEPT1 protein in the apical membrane and the dipeptide uptake were increased. It was shown that this mechanism seemed to be due to a recruitment of hPEPT1 from a preformed cytoplasmic pool (149). Assigned to our postulated hypothesis insulin stimulation activates the insulin-like signalling cascade with inactivation of TORC1 by phosphorylated Akt which in turn activates TORC2 and increases translocation of PEPT-1 into the apical membrane. Inactivation of TORC1 and thereby the activation of TORC2 can be induced by several input signals such as gene silencing of *daf-15* or by increased levels of 4-HNE. When the phospholipid hydroperoxide glutathione peroxidase F26E4.12 is knocked down via RNAi it is presumed that lipid peroxidation generates 4-HNE.

It was shown previously that 4-HNE induces autophagy by inactivation of TORC1 via a yet unknown mechanism (171). The inactivation of TORC1 can cause the activation of TORC2 and may increase the translocation of preformed PEPT-1 from vesicles into the apical membrane with increased dipeptide uptake as observed for F26E4.12 RNAi treated *C. elegans* (Figure 45).

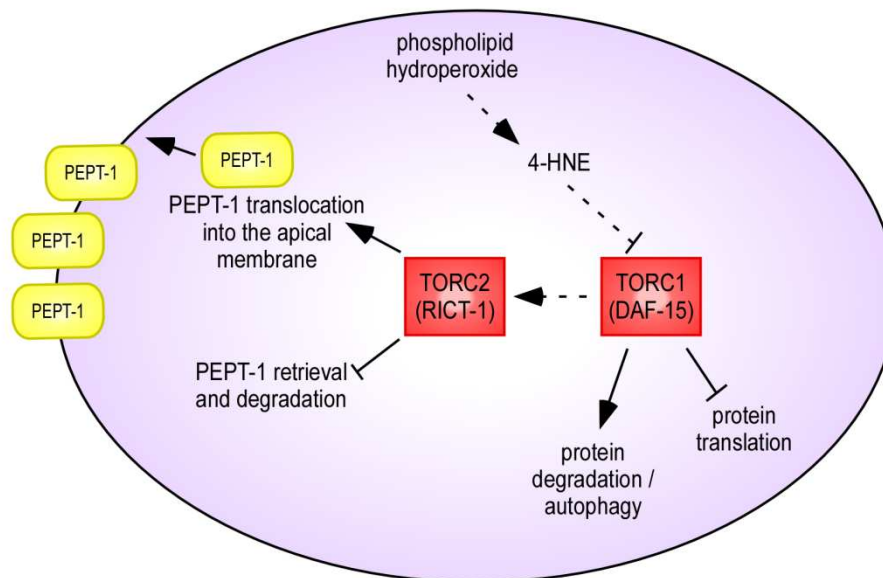


Figure 45: Postulated mechanisms by which increased levels of 4-HNE may alter PEPT-1 presence in the apical membrane

The proposed interplay between TORC1, TORC2 and PEPT-1 was further investigated by supplementing worms with amino acids. It was previously shown that increased intracellular amino acid concentrations activate TORC1 and thereby stimulate protein translation, inhibit protein-turnover and in reverse can lead to an inactivation of TORC2 (Figure 46). Inactivated TORC2 could reduce dipeptide uptake by causing a retrieval of PEPT-1 from the apical membrane into vesicular compartments as shown for PEPT-1 in mammalian models (140). Intracellular amino acid levels may also be altered when intracellular peptidases are inhibited or expression is reduced by silencing. Cytosolic peptidases are considered to be responsible for rapid hydrolysis of absorbed di- and tripeptides with liberated amino acids released into circulation via basolateral efflux systems (191). In this respect, peptidases may increase the driving force for peptide uptake by removing the substrate from the transport equilibrium and thereby contribute to the thermodynamics of the transport process. Any alteration in the capacity for hydrolysis of di- and tripeptides entering the cell, e.g. by RNAi knockdown of the peptidases ZC416.6 and R11H6.1 or by peptidase inhibition

with amastatin or bestatin, would lead consequently to changes in the cellular pool of free amino acids that may be sensed by the TOR pathway (192) and may in turn cause decreased PEPT-1 transport (Figure 46).

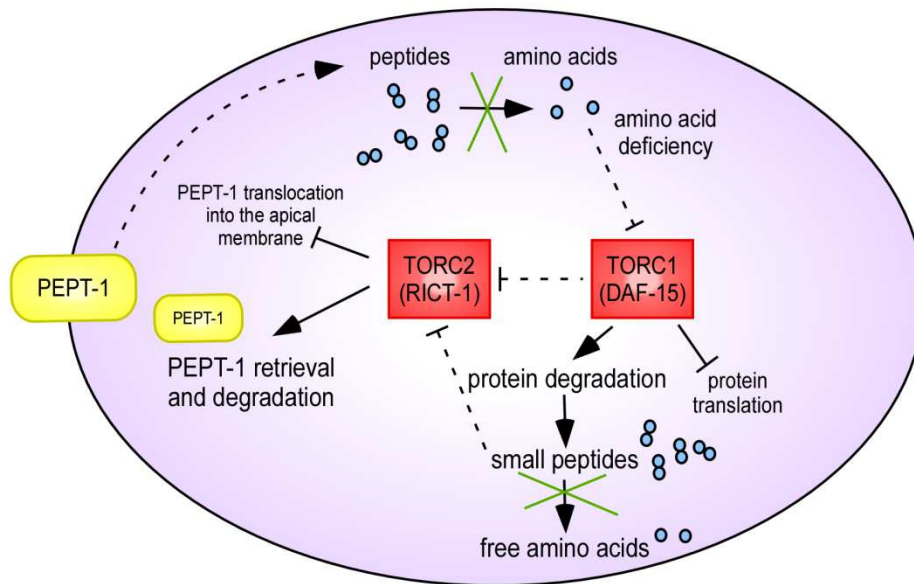


Figure 46: Putative role of cellular aminopeptidases on PEPT-1 and TORC2 signalling

The prime role of TOR in epithelial morphogenesis and in intestinal cell functions has been demonstrated (193) (194) and amino acids such as glutamine, arginine and leucine are considered as input signals for TOR (195) (196) (197). The present data obtained in worms suggest that amino acid homeostasis in epithelial cells is indeed affected by cytosolic peptidases and that a supply-network that involves TORC1 and TORC2 may coordinate the absorption of short chain peptides via PEPT-1.

4. CONCLUSION

The supply of amino acids to the organism is mediated by amino acid and peptide transporters in the apical membrane of epithelial cells. When the di- and tripeptide transporter PEPT-1 is deleted in *C. elegans* amino acid transporters are thought to compensate with increased expression and amino acid uptake to allow growth and reproduction of *C. elegans*. Amongst the various amino acid transporters, two genes were shown to be necessary for amino acid homeostasis in animals lacking PEPT-1. The heterodimeric amino acid transporter light subunit homologue AAT-6 and the proton-coupled amino acid transporter homologue Y4C6B.2 were demonstrated to be essential for the fitness and reproduction of PEPT-1 deficient worms. When the corresponding genes were silenced in a *pept-1(lg601)* background, the worms were significantly smaller and their reproduction failed. Unfortunately the substrate specificity of AAT-6 and Y4C6B.2 in worms are not known and require further investigations for better understanding the role of these proteins for amino acid homeostasis in *pept-1(lg601) C. elegans*.

A genetic screen applied to identify PEPT-1 modulatory genes/proteins in *C. elegans* based on a functional transport assay and associated phenotypic changes in worms revealed the four candidate genes F26E4.12, C54H2.5, ZC416.6 and R11H6.1. The gene F26E4.12 encodes a phospholipid hydroperoxide glutathione peroxidase that when silenced caused increased transport activity. An ER to Golgi cargo transport protein encoded by C54H2.5 not only appears to contribute to PEPT-1 maturation and delivery to the plasma cell membrane, but was also shown to affect other membrane transporter proteins. The remaining two putative cytosolic aminopeptidases encoded by ZC416.6 and R11H6.1 were demonstrated to alter PEPT-1 protein levels and function. Inhibition of the enzymes by peptidase inhibitors also changed PEPT-1 transport function. Since the peptidases most likely affect the intracellular amino acid pool that is sensed by TOR, the role of rictor and raptor homologous proteins on PEPT-1 transport was assessed and it was demonstrated by RNAi treatment that they change transporter function in a reciprocal manner. A model was proposed that involves a coordinated interplay of intracellular amino acid

concentrations affecting TORC1 and TORC2 activity which is translated into altered PEPT-1 transport activity most likely by changes in membrane insertion or retrieval and degradation.

5. METHODS

5.1. General *C. elegans* methods

5.1.1. Cultivation of *C. elegans*

All *C. elegans* strains were grown as mixed population on NGM agar plates seeded with *E. coli* OP50 (1). For RNAi experiments worms were fed with corresponding *E. coli* HT115. The animals were kept at a temperature of 20°C.

5.1.2. Preparation of synchronised *C. elegans* populations

To synchronise populations, a mixed-stage worm culture was washed off the plates with M9 buffer and eggs were prepared by hypochlorite treatment. Synchronized L1 larvae were grown on NGM (RNAi) agar plates with *E. coli* OP50 till the fourth larval state (L4).

5.1.3. Protein extraction and Bradford assay

For protein extraction, equal volumes of glass beads (~600 µm diameter) and worm lysis buffer were added to the samples which were homogenized 3 times for 30 seconds (Fast Prep FP120, Thermo Savant). Samples were cooled between homogenization steps for 1 minute on ice. Protein concentration was determined by following the instructions of Bio-Rad Protein Assay (BIO-RAD Laboratories GmbH, Germany).

5.1.4. RNA interference

RNA interference (RNAi) is a mechanism for gene silencing induced by double-stranded RNA (dsRNA). The dsRNA (>100 bp) is cleaved in the cell into fragments of 21-23 bp by a ribonuclease known as Dicer. These short interfering RNA (siRNA) are bound by the RNA-induced silencing complex (RISC) that recognizes and degrades mRNA corresponding in sequence to siRNA. The RNAi mechanism in *C. elegans* is possible by feeding *E. coli* HT115 (102). These bacteria carry one plasmid encoding for the target gene and a second plasmid which contains an IPTG-inducible T7 polymerase promoter. These plasmids have also an ampicillin and a carbenicillin resistance, what is used for selection. Bacteria are grown in the presence of IPTG to induce the expression of T7

polymerase, which in turn transcribes the dsRNA of the target gene. *E. coli* HT115 bacteria transformed with an empty vector served as a vector control.

5.2. Molecular biological techniques

5.2.1. Single-worm nested PCR

For confirmation of a gene deletion single-worm nested PCR was used. A single worm was incubated in 3 µl worm lyses buffer (2x WLB) and proteinase K for 1 hour at 65°C. The PCR mastermix contained per reaction 15.5 µl dH₂O, 2.5 µl PCR buffer, 2.5 µl dNTPs, 0.3 µl forward and reverse primer and 0.3 µl Taq polymerase. For the first PCR outer primer and for the second PCR inner primer were used. 0.5 µl of the worm lysate (in the first PCR) and 0.5 µl of the first PCR (in the second PCR) served as templates. The PCR program was adapted to primer melting temperature and the length of the built product.

5.2.2. Crossing of *rsks-1(ok1255)* with wild type

The strain *rsks-1(ok1255)* was received by the *C. elegans* gene knockout consortium and was not crossed out with wild type. To exclude the possibility of background mutations, this strain was crossed four times with wild type. In the beginning the approximately 1700 bp long deletion of *rsks-1* was tested by nested PCR. L4 *rsks-1* hermaphrodites and wild type males were placed together in a ratio of 1:3 (first crossing). L4 and males of the F1 generation (all heterozygous) were again put together on one plate with a ratio of 1:3 (second crossing). With homozygous (tested by nested PCR) *rsks-1* hermaphrodites of the second crossing and wild type males two more crossings were performed. In the end an out crossed *rsks-1(ok1255)* knockout strain could be used for experiments.

5.2.3. Cloning of bacteria for RNA interference of *aat-4* and *aat-9*

The RNAi clone library from J. Ahringer lab (70) (198) contains *E. coli* for nearly every *C. elegans* gene. RNAi bacteria for gene knockdown of *aat-4* and *aat-9* were missing. To get a complete overview of the heterodimeric amino acid transporter subunits 1199 bp (*aat-4*) and 1283 bp (*aat-9*) of the genes were

amplified by PCR, cloned into the vector pPD 129.36 and then transformed into *E. coli* HT115.

Preparation of genomic DNA

A mixed population of wild type worms was washed off three agar plates with M9 buffer. In the last washing step 1 ml worm lysis buffer (WLB for gDNA) was added, they were rapidly frozen in liquid nitrogen and stored at -80°C. After unfreezing the worm sample on ice, 10 µl of proteinase K were added and after 30 minutes at 65°C further 5 µl of proteinase K were added. The sample was again kept at 65°C for 30 minutes to allow the degradation of the proteins. After cooling down on 37°C 5 µl RNase A were added followed by a 30 minutes incubation at 37°C. In order to extract and purify the genomic DNA the Presto Spin D Universal Kit (Molzym, Bremen, Germany) was used according to the instructions. The gDNA was stored at 4°C.

Preparation of chemically competent *E. coli* HT115

A 5 ml overnight culture of *E. coli* HT115 in LB medium was prepared. This overnight culture was diluted 1:100 in fresh LB medium with a final volume of 200 ml. The diluted culture was grown to an OD₆₀₀ of 0.35 to 0.38. The cells were then aliquoted into four 50 ml tubes and cooled down on ice. Tubes were centrifuged for 10 minutes with 4000 rpm at 4°C. The supernatant was removed and the bacteria pellet resuspended in 10 ml ice cold 0.1 M CaCl₂ / 0.02 M MgCl₂ solution. The centrifugation and resuspension step was repeated. The cell suspension was kept on ice for 30 minutes. After centrifugation for 10 minutes with 4000 rpm at 4°C 2 ml of an ice cold 0.1 M CaCl₂ / 0.02 M MgCl₂ / 15 % glycerine solution was added. The cells were dispensed in 110 µl aliquots and stored at -80°C.

Amplification of gene fragments by PCR

To amplify parts of the genes of *aat-4* (1199 bp) and *aat-9* (1283 bp) polymerase chain reaction (PCR) was used. The mastermix for each reaction contains 37 µl dH₂O, 5 µl PCR buffer, 5 µl 2 mM dNTPs, 1 µl 100 pM forward and reverse primer and 1 µl Pfu polymerase (proof-reading). As a template 100 ng genomic wild type DNA was used. The PCR program started with a DNA denaturation at 93°C for 2 minutes. In the first step of the amplification cycle the temperature was

kept at 93°C for 30 seconds. In the annealing step the temperature was dropped to 65°C for 30 seconds and in the third step the temperature was maintained at 72°C for 2 minutes. 30 cycles of these three steps were performed.

Agarose gel electrophoresis and gel extraction

After PCR 3 µl loading dye were added to the samples and they were completely loaded to a 1.5 % agarose gel with 3 µl ethidium bromide. A DNA standard (GeneRuler Ladder Mix, Fermentas) was run in parallel to enable sizing of the PCR products. The gel was run at 95 V for approximately one hour. The gel was examined under UV light to compare the DNA fragments with the DNA standard. The bands with the right size were cut out of the gel and DNA was extracted by using the QIAquick Kit (Qiagen).

Ligation of fragments of *aat-4* and *aat-9* with TOPO vector

Cloning of the gene fragments first into the TOPO vector and not directly in pPD 129.36 was necessary to enable later a complete restriction digest of the PCR products of *aat-4* and *aat-9*. The TOPO vector had thymine sticky ends, why it was necessary to affix an adenine tail to the end of the extracted PCR products before doing ligation. This was done by adding 5 µl PCR buffer, 1 µl dATPs and 0.6 µl Taq polymerase to 50 µl PCR product. After 10 minutes of incubation at room temperature ligation could occur. For that 1.5 µl fragment with adenine tail, 0.3 µl TOPO vector and 0.25 µl salt solution were incubated for 30 minutes at room temperature.

Transformation of the TOPO vector constructs in Top10F'

To aggrandise the ligated vector-fragment-construct, it was transformed into competent Top10F' *E. coli*. For the transformation 40 µl dH₂O and 100 µl competent cells were added to the ligation mix. It was incubated for 30 minutes on ice and a 45 seconds heat shock at 42°C followed. After cooling down on ice, 450 µl DYT medium was added. The incubation at 37°C took 1 hour. To concentrate the *E. coli*, the sample was centrifuged 5 minutes at 3000 rpm. The cell pellet was resuspended in 200 µl supernatant and plated on LB-plates with ampicillin, X-Gal (5-bromo-4-chloro-3-indolyl-β-D-galactoside) and IPTG (Isopropyl-β-D-thiogalactopyranosid). The plates were incubated over night at 37°C. IPTG and X-Gal were used to detect successful ligation of the PCR product

into TOPO vector. The TOPO vector had a *lacZ* gene sequence in which the multiple cloning site was located in. When a successful ligation took place the *lacZ* gene sequence was interrupted by the insert of the fragment. So no β -galactosidase could be expressed and the bacteria colony was white. In case of an unsuccessful ligation the vector re-ligated with itself and the gene sequence for β -galactosidase was intact. IPTG could induce it and β -galactosidase was expressed. The β -galactosidase hydrolysed X-Gal and the colonies turned blue.

Restriction of the TOPO vector

Some white colonies were picked from the plates, cultured over night and the plasmid DNA was extracted using the QIAprep Spin Miniprep Kit (Qiagen) according to the instructions. For cutting the gene fragments out of the TOPO vector 5 μ l DNA, 0.5 μ l PstI, 0.5 μ l Sall, 2 μ l appropriate buffer and 12 μ l dH₂O were incubated 1 hour at 37°C. Then the two different fragments (PCR product and vector) were separated by gel electrophoresis and the gene fragments were extracted out of the gel.

Ligation of the gene fragments with the vector pPD129.36

Before ligation, the vector pPD 129.36 was also restricted with the endonucleases PstI and Sall to get the complementary sticky ends to the restricted gene fragments of *aat-4* and *aat-9*. Ligation of the gene fragments with the pPD 129.36 vector was carried out in an insert:vector proportion of 3:1. Gene fragments and vector were mixed with 1.5 μ l T4 DNA ligase, buffer and dH₂O and incubated 1.5 hours at room temperature.

Sequencing

The plasmid DNA of pPD 129.36 with ligated *aat-4/aat-9* gene fragment was sequenced by GATC (Konstanz, Germany). The sequence generated by GATC was aligned against the original gene sequence and was 100% identical.

Transformation of the plasmid in *E. coli* HT115

The positive sequenced plasmids were transformed into competent HT115 *E. coli* to generate RNAi bacteria for *aat-4* and *aat-9* gene silencing. For control, DNA was extracted, restricted with PstI and Sall and separated on a gel. Positive bacteria were frozen in 1 volume glycerol and stored at -80°C.

5.2.4. mRNA-expression levels of *C. elegans*

RNA preparation and cDNA synthesis

Synchronised L1 larvae were grown on RNAi agar plates until they reached the L4 larval stage. They were washed off the plates with M9 buffer, frozen in liquid nitrogen and total RNA was isolated from each *C. elegans* sample using a combination of TRIZOL® (Invitrogen, Germany) extraction till the ethanol precipitation step followed by purification via RNeasy Mini Kit (Qiagen, Germany). RNA concentrations were measured at the NanoDrop (NanoDrop ND 1000, PeqLab). And RNA quality was visualised by gel electrophoresis with a special RNA gel. 2 µg RNA was reverse transcribed using the Transcriptor High Fidelity cDNA Syntheses Kit (Roche, Germany).

Real-time RT-PCR

Quantitative real-time PCR (qPCR) was performed using a LightCycler (Roche, Germany) with 12.5 ng of cDNA per PCR reaction and the FastStart SYBR Green Kit (Roche, Germany). Cycle parameters were annealing at 60°C for 10 s, extension at 72°C for 20 s and melting at 95°C for 15 s. Specificity of PCR products was controlled by melting curve analysis and by agarose gel electrophoresis. Primers were designed using the program Light Cyclor Probe Design (Roche, Germany). For quantification a housekeeping gene (*ama-1*) was measured for each sample. The primer efficiency was calculated using the LinRegPCR Interface (199), a method that is based on calculation of the average amplification efficiency of a primer pair in all PCRs in an experiment in combination with the corresponding cycle threshold (C_T) value. Final analysis and normalisation of the results were done by qPCR software (200).

5.3. Assays for developmental and progeny studies

5.3.1. Body length and developmental studies

Growth and development of *C. elegans* grown on various RNAi bacteria were investigated. Synchronised L1 larvae ($t=0$) were transferred to RNAi NGM plates and photographed every 24 hours until they reached adulthood. The body size of

eight worms per day and group was calculated using the program Motic Images Plus 2.0.

5.3.2. Number of progeny

36 L4 larvae of every experimental group were separated on 12-well (RNAi) agar plates. The hatched larvae of each individual worm were counted.

5.3.3. Amino acid supplementation studies

Synchronised L1 larvae were grown on RNAi agar plates with RNAi bacteria and supplemented with 150 µl amino acids (mixture 1:1 of MEM (100x) non-essential amino acids and MEM amino acids (50x) without L-glutamine). Either every day pictures were taken for measuring body length development and brood size assay was performed, or β -Ala-Lys-AMCA uptake was determined with L4 larvae.

5.3.4. Resistance to oxidative stress induced by paraquat

Paraquat (N,N'-dimethyl-4,4'-bipyridinium dichloride) catalyses the formation of reactive oxygen species (ROS) and thus induces oxidative stress. Synchronised L1 larvae were grown on RNAi agar plates until they reached L4 larval stage. 30 worms were transferred to fresh plates, which contained 100 µl of a 50 mM paraquat solution. Daily living worms (responding to a mechanical stimulus) were counted. Until all *C. elegans* were dead, they were transferred every third day to freshly prepared RNAi plates containing paraquat.

5.4. Uptake experiments and staining assays

5.4.1. Fluorescent dipeptide β -Ala-Lys-AMCA uptake assay (Screen)

Synchronised *rrf-3* L1 larvae were grown on control RNAi bacteria (vector control, *pept-1*) or on RNAi bacteria expressing individual dsRNA for 162 intestinal expressed genes for 3 days until control worms reached the L4 larval stage. As an additional control synchronised *pept-1* knockout L1 larvae were grown on vector control RNAi bacteria for 5 days until they reached L4 larval stage. These controls (*rrf-3;vc*(RNAi), *rrf-3;pept-1*(RNAi), *pept-1;vc*(RNAi) and *rrf-3;vc*(RNAi) without addition of β -Ala-Lys-AMCA) were included in each experiment of the β -Ala-Lys-AMCA uptake assay.

After 3 days (5 days in the case of *pept-1;vc*(RNAi) control) the worms were washed off the plates with M9 buffer. A final concentration of 0.25 mM β -Ala-Lys-AMCA was added and the samples were incubated for 3 hours at 20°C. Afterwards 0.5 ml liquid *E. coli* OP50 culture was added and samples were incubated for 1 hour to wash the β -Ala-Lys-AMCA out of the intestinal lumen. After 4-6 washing steps with M9 buffer the worms were placed on empty NGM agar plates. Images were taken and exemplarily body length of two worms per control/RNAi construct was measured. 4 times 20 worms per control/RNAi construct were transferred by hand from the NGM agar plate into one well of a black 384-well plate. Hence, for each control/RNAi construct four replicates were performed. In case of *rrf-3;vc*(RNAi) worms without β -Ala-Lys-AMCA addition only two wells were measured. Fluorescent signals were detected at 340/445 nm using a Varioskan (Thermo Electron Corporation, USA). Each well was measured 10 times (10 technical replicates) with shaking in between. Fluorescence intensity was calculated relative to the mean of the control (for detailed description of the calculation see the appendix 8.4.2.). Each experiment was repeated 2-4 times independently on biological replicates.

Visualisation of the β -Ala-Lys-AMCA uptake by using a confocal microscope

To confirm selected data sets from the β -Ala-Lys-AMCA screen detected by the fluorescence plate reader, the β -Ala-Lys-AMCA uptake was visualised with a Leica TCS SP2 Confocal System coupled to a DM IRB microscope (Leica, Germany). L4 larvae were washed off agar plates and were washed 2 more times with M9 buffer. The worms were incubated in M9 buffer containing 1 mM β -Ala-Lys-AMCA for 3 hours. Alternatively, the worms were preincubated with different concentrations (1 mM, 0.1 mM, 0.01 mM) bestatin or amastatin for 10 minutes and then 1 mM β -Ala-Lys-AMCA was added. Coincubation lasted for 3 hours. Afterwards worms were washed several times with M9 buffer, anaesthetised and loaded to an object slide. Picture series were taken with 10 horizontal z-slices. The fluorescence intensities of at least 10 worms per experiment were determined for the area posterior the pharynx using Leica Confocal Software 5.2.

5.4.2. Labelling *C. elegans* with a fluorescent free fatty acid probe

To determine time-dependent fatty acid uptake in *C. elegans*, L4 larvae were labeled with the fatty acid analog 4,4-difluoro-5-methyl-4-bora-3a,4a-diaza-3-indacene-dodecanoic acid (BODIPY 500/510 C1,C12, Invitrogen, Molecular Probes, Germany). BODIPY-C12 was dissolved in 100% DMSO at a concentration of 2.4 μ M. L4 larvae were incubated for 10 minutes in M9 buffer containing a final concentration of 20 nM BODIPY-C12 (and 0.1% DMSO). Worms were washed several times in M9 buffer before loading to an object slide. The BODIPY fluorescence was visualized using a Leica TCS SP2 Confocal System coupled to a DM IRB microscope (Leica, Germany).

5.4.3. Sudan Black B fat staining

For visualization of intestinal and hypodermal fat in *C. elegans* Sudan Black B staining is a common method and was prepared according to an established protocol (201). For visualization of the black-blue stained fat granules we used a Leica DM IRB microscope (Leica, Germany) with a digital camera.

5.4.4. Measurement of mitochondrial ROS levels

To determine ROS (reactive oxygen species) production in mitochondria the dye CM-H₂XRos was used. This dye enters active respiring cells, accumulates in mitochondria and is oxidised there by ROS. CM-H₂XRos, when oxidised, creates a fluorescent conjugate with thiol groups of proteins and peptides, which can be detected with an absorption maximum at 578 nm and an emission at 590-650 nm. Emitted fluorescence directly corresponds to the amount of ROS generated in mitochondria (202). Synchronised *C. elegans* were grown on RNAi agar plates until they reached L3 larval stage. Then they were transferred to fresh RNAi plates. These plates contained heat killed (3 hours, 60°C) RNAi bacteria and a final concentration of 0.5 μ M CM-H₂XRos. The worms were grown on these plates for 24 hours, then washed off the plates with M9 buffer and anesthetised with 5 mM levamisol. Pictures of at least 10 worms per experiment were taken at the confocal laser scanning microscope.

5.5. Proteobiochemical methods

5.5.1. Membrane protein extraction *Xenopus laevis* oocytes

To obtain PEPT-1 in higher yield, *Xenopus* oocytes were injected with *pept-1* cRNA (16). Five days after injection the oocytes were homogenized in an equal volume of lysis buffer (20 mM HEPES, 10 mM KCl, 1.5 mM MgCl₂, 1 mM DTT and 5 µl PMSF). The solution was centrifuged for 5 minutes (9000 x g at 4°C). The supernatant contained the *C. elegans* PEPT-1 protein and was used as positive control for western blot analysis.

5.5.2. Membrane protein extraction and protein detection

A mixed worm population was washed off NGM agar plates with M9 buffer and was frozen in liquid nitrogen. 100 µl of membrane extraction buffer (0.1 M Tris/HCl, 0.5 M NaCl, 12.5% glycerol, 2 µM EDTA and 1.25 mM DTT) and glass beads were added and the samples were homogenized 5 times for 30 seconds (Fast Prep FP120, Thermo Savant, USA). The samples were centrifuged for 2.5 minutes with 9000 rpm at 4°C. Supernatants were centrifuged for 45 minutes with 14000 rpm at 4°C. The pellets were resuspended in 50 µl storage buffer (100 mM NaCl, 10 mM HEPES-Na, 150 mM EDTA, 1mM DTT, 1:500 mPIC). Protein concentration was determined by Bradford assay. To the samples probe buffer (8% SDS, 20% glycerol, 20% mercaptoethanol, 0,4% bromphenolblue, 250 mM Tris/HCl) was added in a ratio 1:4. After 2 minutes denaturation at 42°C membrane proteins were separated by SDS-PAGE and blotted onto a nitrocellulose membrane. To control the accurate protein transfer, the membrane was stained with Ponceau S. After 1 hour incubation in 5 % blocking solution (1x PBS, 1 % Tween 20, 5 % skimmed milk powder) the primary antibody was added to the membrane. The anti-CePEPT-1 antibody is directed against the C-terminal PEPT-1 peptide NH₂-CKGFHPDEKDTFDMHF-COOH that was used to immunize three rabbits. The serum after immunization day 130 was collected per animal and each serum was monospecifically enriched. The monospecific anti-CePEPT-1 from animal 1 was used in a 1:5000 dilution. The membrane was washed 30 minutes with blocking solution, afterwards the secondary antibody was added. After several washing steps with blocking solution and PBS, ECL solution 1 (0.1 M Tris/HCl (pH 8,6), 2.5 mM luminal sodium salt, 0.396 mM

p-coumaric acid) and ECL solution 2 (0.1 M Tris/HCl (pH 8,6), 0.0192 % hydrogen peroxide solution) were added and the chemiluminescence was detected with a radiographic film.

5.6. Others

5.6.1. promoter *pept-1::gfp* expression analysis

To investigate *pept-1* expression, a *C. elegans* strain with a *pept-1* promoter-GFP construct (BR2875) was used (12). L4 larvae were transferred to RNAi NGM agar plates. The GFP fluorescence in L4 larvae of the F1 generation were individually visualized using a Leica TCS SP2 Confocal System coupled to a DM IRB microscope (Leica, Germany). Laser intensity was calibrated once and was not changed throughout the experiment. A series of 10 vertical z-sections was taken for each single worm. Images with maximum fluorescence were calculated based on all sections using the Leica confocal software.

5.6.2. Measurement of glutathione levels

The assay was adapted to the protocol described by Rahman et al. (203).

Sample preparation

Synchronised worms were grown on RNAi agar plates until they reached L4 larval stage. They were washed off the plates with M9 buffer and 100 µl worm pellet aliquots were transferred to new tube. There 1 volume nematode extraction buffer (NEB) was added. They were shock frozen in liquid nitrogen and stored at -80°C. For use the samples were thawed on ice, 100 µl NEB and 1 volume glass beads were added. A homogenisation step three times for 30 seconds followed. Between runs the samples were cooled on ice. Glass beads were again washed with 100 µl NEB and after centrifugation for 2 minutes at 2000 rpm the supernatant was transferred to a new tube. Protein concentration for each sample was determined by using the Bradford method.

GSH and GSSG standard curve

For the standard curve different concentrations (0.825 µM, 1.65 µM, 3.3 µM, 6.6 µM, 8.8 µM, 13.2 µM and 26.4 µM) of GSH and GSSG were prepared by diluting the standard solution of GSH and GSSG with KPE.

Measurement of tGSH

The total GSH content was measured in a 96-well-plate on the basis of chromophore formation. The formation of TNB (5-thio-2-nitro-benzoate) was determined spectrophotometrically at 412 nm (Varioskan, Thermo Electron Corporation) after 5 and after 10 minutes (Figure 48). 20 μl of the sample/standard/KPE buffer were put in a well. For each sample/standard/KPE buffer two replicates were measured. 1 volume glutathione reductase (GTR) and 1 volume DTNB (2,2'-dinitro-5,5'-dithio-dibenzoic acid) were mixed and 120 μl of this mixture were added to each well. A first reading was started directly after adding the GTR-DTNB-solution ($t=0$). Every ten seconds 60 μl NADPH were added to one well.

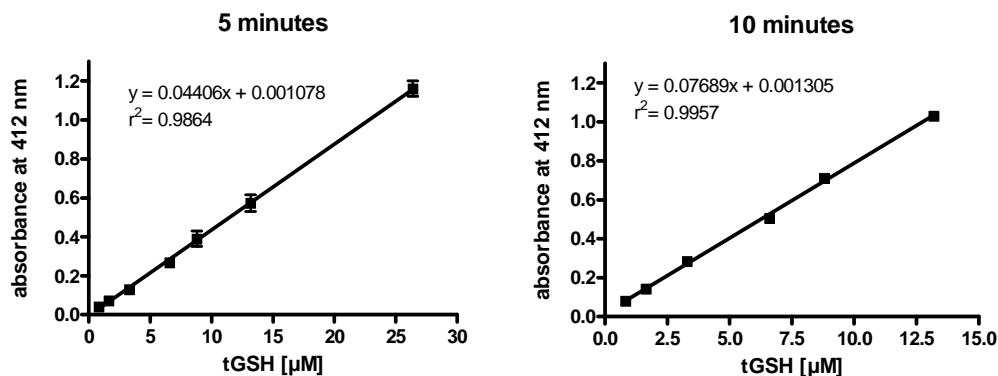


Figure 47: tGSH standard curve for 5 and 10 minutes

For the standard curve a linear regression of known tGSH concentrations (0.825 μM , 1.65 μM , 3.3 μM , 6.6 μM , 8.8 μM , 13.2 μM and 26.4 μM) was performed. 26.4 μM was not measurable after 10 minutes, because the absorption was considerably higher than 1 and thus was outside the linear area of the photometer. Slope and correlation coefficient are given for both curves. Each standard curve was performed at least two times.

The reaction started and the first measurement was performed after 5 minutes ($t=5$) and the second one after 10 minutes ($t=10$). For calculation of tGSH content in the worm samples first the measured KPE buffer value (blank) at each time point was subtracted of every measured sample. Afterwards $t=0$ was subtracted from $t=5$ and $t=10$ and the resulting values were given to the standard curve to determine tGSH concentration. For the last step the tGSH concentration was calculated in relation to protein concentration.

Measurement of GSSG

200 μl homogenised worm sample/standard and 4 μl 2-vinylpyridine were incubated for one hour in a fume hood and were mixed gently to ensure

derivatisation of GSH (Figure 49). 12 μl of TEA were added to remove the excess of 2-vinylpyridine, as it inhibits the glutathione reductase and the solution was kept 10 minutes at room temperature. The derivated samples were measured using the same method as for tGSH.

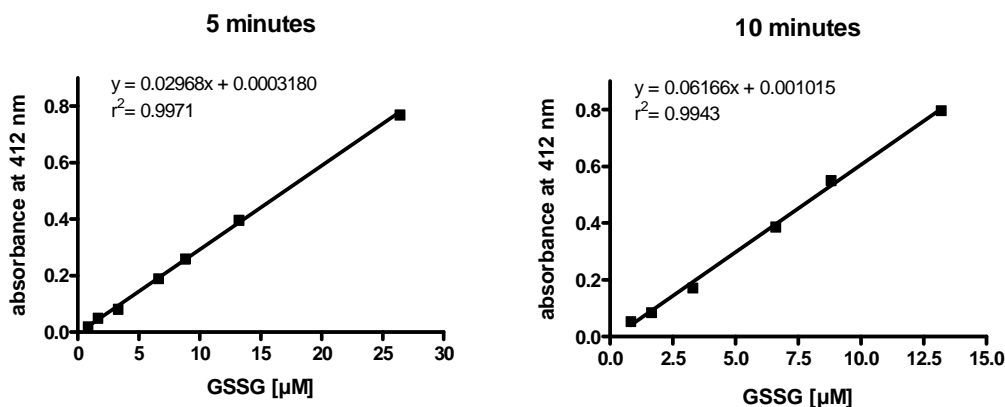


Figure 48: GSSG standard curve for 5 and 10 minutes

For the standard curve a linear regression of known GSSG concentrations (0.825 μM , 1.65 μM , 3.3 μM , 6.6 μM , 8.8 μM , 13.2 μM and 26.4 μM) was performed. 26.4 μM was not measurable after 10 minutes, because the absorption was considerably higher than 1 and thus was outside the linear area of the photometer. Slope and correlation coefficient are given for both curves. Each standard curve was performed at least two times.

Calculation of GSSG concentration in worm samples was the same like for tGSH concentration.

GSH values were calculated using the difference between tGSH and GSSG.

$$[\text{GSH}] = [\text{tGSH}] - 2 [\text{GSSG}]$$

5.7. Statistical analysis

Statistical analysis was performed by using GraphPad Prism 4.01. In most cases the Student's *t*-Test was used to show statistical significance between two groups (control vs. treatment). Otherwise One-way-ANOVA with Turkey Post test was used to compare more than two groups. Most values are given \pm SEM. For life span analysis Kaplan-Meier survival curves are shown and comparison of these curves was determined by using log rank test. For standard curves a linear regression was performed.

6. MATERIALS

6.1. *C. elegans* strains and *E. coli* bacteria

C. elegans strains

The stocks were purchased from Caenorhabditis Genetics Center (CGC) University of Minnesota, Minneapolis, USA.

Table 4: *C. elegans* strains

Strain	Genotype	Reference
N2 var <i>Bristol</i>	wild type	
BR2742	<i>pept-1(lg601)X</i>	(12)
BR2875	<i>ppept-1::GFP;rol-6(su1006)</i>	
NL2099	<i>rrf-3(pk1426)</i>	(204)
RB1206	<i>rsk-1(ok1255)III</i>	
RB767	<i>atgp-2(ok532)II</i>	
VC207	<i>atgp-1(ok388)IV</i>	

Escherichia coli strains

Table 5: *E. coli* strains

Strain	Genotype	Reference
<i>E. coli</i> OP50	<i>ura⁻</i>	(1)
<i>E. coli</i> HT115	<i>F⁻, mcrA, mcrB, IN(rrnD-rrnE)1, lambda⁻, rnc14::Tn10(DE3 lysogen:lacUV5 promoter-T7 polymerase, RNAse III minus</i>	(205)
<i>E. coli</i> Top10F'	<i>F'[lacI^q Tn10(tet^R)] mcrA Δ(mrr-hsdRMS-mcrBC) φ80lacZΔM15 ΔlacX74 deoR nupG recA1 araD139 Δ(ara-leu)7697 galU galK rpsL(Str^R) endA1 λ⁻</i>	

Table 6: Used RNAi bacteria for amino acid homeostasis investigations

Cosmid number	silenced gene
F27C8.1	<i>aat-1</i>
F07C3.7	<i>aat-2</i>
F52H2.2	<i>aat-3</i>
T13A10.10	<i>aat-4</i>
C55C2.5	<i>aat-5</i>
T11F9.4	<i>aat-6</i>
F54D12.3	<i>aat-7</i>
F28F9.4	<i>aat-8</i>
Y53H1C.1	<i>aat-9</i>
F26D10.9	<i>atgp-1</i>
C38C6.2	<i>atgp-2</i>
Y4C6b.2	
T27A1.5	
Y43F4B.7	

Further RNAi bacteria (for selection of PEPT-1 modulators) are summarised in the appendix (Table 16).

6.2. Chemicals, reagents and kits

The chemicals and reagents were purchased from:

Sigma-Aldrich, Steinheim (D); Biotrend, Köln (D); Roth, Karlsruhe (D); Merck, Darmstadt (D); Biorad, Munich (D); Serva, Heidelberg (D); Gibco BRL, Karlsruhe (D); USB, Cleveland, Ohio (USA); JT Baker, Phillipsburg (USA); Fermentas, St. Leon-Roth (D); Heirler Cenovis GmbH, Radolfzell (D)

Table 7: Chemicals and reagents

Name	Company
2-vinylpyridine	Sigma-Aldrich
Agarose GTQ	Roth
Amastatin	Bachem
Bestatin	Peptides International
CM-H ₂ XRos	Invitrogen

DTNB	Sigma-Aldrich
Gene ruler Ladder Mix	Fermentas
Glutathione oxidised (GSH)	Sigma-Aldrich
Glutathione reduced (GSSG)	Sigma-Aldrich
Glutathione reductase	Sigma-Aldrich
IPTG	Sigma-Aldrich
Levamisol	Sigma-Aldrich
Ligase buffer	Fermentas
Loading Dye	Fermentas
MEM (100x) non-essential amino acids	Gibco BRL
MEM amino acids (50x) without L-glutamine	Gibco BRL
MOPS	Roth
NADPH	Sigma-Aldrich
Optiphase supermix Scintillator	Fisher
Paraformaldehyde	Sigma-Aldrich
Paraquat	Sigma-Aldrich
PCR loading dye	Promega
Pfu-polymerase	Promega
Protease inhibitor cocktail tablets	Roche
Restriction enzymes (PstI, Sall)	Fermentas
β -Ala-Lys-AMCA	Biotrend
Sudan Black B	Sigma-Aldrich
T4-DNA-Ligase	Fermentas
TOPO vector	Invitrogen
Trisethanolamine (TEA)	Sigma-Aldrich
Trizol	Invitrogen
X-Gal	Roth

Table 8: Kits

Kit	Company	Use
Presto Spin D Universal Kit	Molzym	gDNA extraction
QIAprep Spin Miniprep Kit	Qiagen	plasmid DNA extraction
QIAquick Kit	Qiagen	gel extraction
QIAquick RNeasy Mini Kit	Qiagen	RNA extraction
Transcriptor High Fidelity cDNA Synthese kit	Roche	cDNA synthesis

6.3. Buffers and media

Table 9: Buffers and media for general *C. elegans* handling

Chemicals	Amount	Company	Chemicals	Amount	Company
Bleach solution			Nystatin		
NaOCl (12 %)	0.5 ml	Roth	Nystatin	4 g	Sigma
5 M KOH	1.25 ml	Roth	Ethanol	200 ml	J.T. Baker
dH ₂ O	23.25 ml		Ammoniumacetate	200 ml	Roth
M9 buffer			NGM-agar		
KH ₂ PO ₄	3 g	Roth	NaCl	3 g	Roth
NaH ₂ PO ₄	6 g	Roth	Peptone	2.5 g	Sigma
NaCl	5 g	Roth	Agar-agar	17 g	Serva
dH ₂ O	ad 1 l		dH ₂ O	ad 1 l	
1M MgSO ₄	1 ml	Sigma	1M CaCl ₂	0.5 ml	Roth
Potassium-phosphat buffer			1M MgSO ₄	1 ml	Sigma
KH ₂ PO ₄	108.53 g	Roth	Potassiumphosphate buffer, pH 6,0	25 ml	
K ₂ HPO ₄	35.28 g	Roth	Nystatin	13 ml	Roth
dH ₂ O	ad 1 l		Cholesterol	1 ml	Sigma
5M KOH	pH 6.0	Roth		<u>for RNAi</u>	
DYT-media			1M IPTG	1 ml	Sigma
Peptone	16 g	Sigma	Carbenicillin	1 ml	Sigma
Bacto Yeast Extract	10 g	Sigma			
NaCl	5 g	Roth			
dH ₂ O	ad 1 l				

Table 10: Buffers and media for molecular biological techniques

Chemicals	Amount	Company	Chemicals	Amount	Company
Worm lysis buffer 1 (WLB1)			LB-agar		
1M Tris/HCl	5 ml		LB-Broth	20 g	Roth
1M NaCl	10 ml	Roth	Agar-agar	15 g	Serva
Glycerol	4 ml	Roth	dH ₂ O	ad 1 l	
1mM EDTA	100 µl	Sigma	<u>for LB-Amp. plates</u>		
dH ₂ O	ad 50 ml		Ampicillin	1 ml	Sigma
1.5 % agarose gel			1 M Tris/HCl		
Agarose	1.2 g	Roth	Tris	121 g	Roth
1x TAE buffer	80 ml		HCl conc.	70 ml	Merck
Ethidium bromide	3 µl	Roth	dH ₂ O	ad 1l	
PCR-buffer			2x WLB (for worm lysis)		
1M KCl	10 ml	Roth	1M KCl	100 µl	Roth
1M Tris	2 ml	Roth	1M Tris. pH 8	100 µl	Roth
10 % Tween 20	0.5 ml	Sigma	50 mM MgCl ₂	100 µl	Roth
10 % Nonidet	0.5 ml	USB	Tween 20	3 µl	Sigma
10 mg/ml BSA	0.5 ml	Roth	Gelatine 0.1 %	200 µl	Sigma
1M MgCl ₂	0.4 ml	Roth	dH ₂ O	ad 2 ml	
Worm lysis buffer (gDNA)			RNA gel		
0.2M NaCl	200 µl	Roth	Agarose	0.8 g	Roth
0.1M Tris/HCl	100 µl		DEPC-water	65 ml	Roth
50 mM EDTA	200 µl	Sigma	Formaldehyde 37 %	6.6 ml	Roth
0.5 % SDS	500 µl	Roth	10x MOPS	8 ml	Roth
LB-media			Loading dye with ethidium bromide	3 µl	Fermentas
LB-Broth	20 g	Roth	50x TAE buffer		
dH ₂ O	ad 1 l		Tris	242 ml	Sigma
			Acetic acid	57.1 ml	Fluka
			0.5M EDTA, pH 8	100 ml	Sigma
			dH ₂ O	ad 1 l	

Table 11: Buffers and media for proteobiochemical methods

Chemicals	Amount	Company	Chemicals	Amount	Company
PBS			Resolving gel (15 %)		
NaCl	0.8 %	Roth	3x resolving gel buffer	1.5 ml	
KCl	0.02 %	Roth	30 % Acrylamide	2.25 ml	Roth
Na ₂ HPO ₄	0.144 %	Roth	dH ₂ O	0.75 ml	
KH ₂ PO ₄	0.024 %	Merck	10 % APS	50 µl	Serva
NaOH/HCl	pH 7.4	Merck	TEMED	5 µl	Sigma
2x Transfer buffer			Stacking gel		
Tris	0.48%	Roth	3x stacking gel buffer	1.7 ml	
Glycine	2.24%	Merck	30 % Acrylamide	300 µl	Roth
SDS	0.04%	Roth	10 % APS	20 µl	Serva
Methanol	40%	Merck	TEMED	1.5 µl	Sigma
Stacking gel buffer			3x Resolving gel buffer		
Tris/HCl, pH 6.8	0.139 M		Tris/HCl, pH 8.8	1.126 M	
SDS	0.1 %	Roth	SDS	0.3 %	Roth
Membrane extraction buffer (MEB)			Blocking solution (5 %)		
WLB1	4 ml		skim milk powder	5 g	Heirler
1M DTT	5 µl	Roth	Tween 20	1 ml	Sigma
HisPic	10 µl	Sigma	1x PBS	99 ml	
Storage buffer			4x SDS probe buffer		
1 M NaCl	100 µl	Roth	SDS	8 %	Roth
1 M HEPES	10 µl	Roth	Glycerol	20 %	Roth
0.5 M EDTA	300 µl	Sigma	β-Mercaptoethanol	20 %	Merck
Glycerole	100 µl	Roth	Bromphenolblue	0.4 %	Roth
1 M DTT	1 µl	Roth	Tris/HCl, pH 6.8	250 mM	
100% HisPic	2 µl	Sigma			
SDS running buffer					
Tris	25 mM	Roth			
Glycine	192 mM	Merck			
SDS	0.1 %	Roth			

Table 12: Buffers and media for other experiments

Chemicals	Amount	Company	Chemicals	Amount	Company
Potassium phosphate EDTA buffer (KPE)			Nematode extraction buffer (NEB)		
A: KH_2PO_4	16 mM	Roth	Na_2EDTA	4.13 mM	Roth
Na_2EDTA	5 mM	Roth	Potassium phosphate buffer	82.64 mM	
B: K_2HPO_4	84 mM	Roth	KCl	50 mM	Roth
Na_2EDTA	5 mM	Roth	MgCl_2	2.5 mM	Roth
			Triton X-100	0.1 %	Sigma
Mix A and B in a ratio of 1:1.18 before use and adjust to pH 7.5.			Sulfosalicylic acid	1 %	Roth
			Protease inhibitor	20 μl	
DTNB			NADPH		
DTNB	0.002 g	Roth	20 mM NADPH	28.75 μl	Sigma
KPE	3 ml		KPE	971.43 μl	
Glutathione-Reductase			Glutathione reduced (GSH)		
GT-Reductase (600 U/ml)	20 μl	Sigma	GSH	1 mg	Sigma
KPE	6 ml		KPE	1 ml	
Glutathione oxidised (GSSG)			<u>working solution:</u>		
GSSG	2 mg	Sigma	dilution of stock solution 1:100 with KPE		
KPE	1 ml		<u>standard solution:</u>		
<u>working solution:</u>			800 μl working solution + 200 μl working solution		
dilution of stock solution 1:200 with KPE					
<u>standard solution:</u>			Triethanolamine (TEA)		
800 μl working solution + 200 μl working solution			TEA	10 μl	Sigma
			KPE	50 μl	
2-Vinylpyridin (2-VP)					
2-VP	10 μl	Aldrich			
KPE	90 μl				

6.4. Plasmids, oligonucleotides and antibodies

Plasmids

The vector pPD129.36 used for cloning RNAi bacteria contains two T7 polymerase promoter sides around the multiple cloning side, an *ori* (origin of replication) and an ampicillin resistance. The backbone size is about 2790 bp.

Oligonucleotides

Table 13: Oligonucleotides

Oligonucleotides for cloning, restriction cut sides for endonucleases were incorporated into the 5' end and these areas are underlined.

Name	Sequence in 5'-3' orientation	Enzymes	Use
aat-4_for	<u>GGTCGACT</u> GCGCTTGAAGAACGGATCA	Sall	Cloning in pPD 129.36
aat-4_rev	G <u>CTGCAG</u> ATTCCAGCTTCTGCTGCTGTT	PstI	Cloning in pPD 129.36
aat-6_for_RT	TCGGTTCGGCTTATCAC		mRNA expression
aat-6_rev_RT	TCGCAAGTGAGGCAAG		mRNA expression
aat-9_for	<u>GGTCGAC</u> ACTCGGCGATGTCCATGAAA	Sall	Cloning in pPD 129.36
aat-9_rev	G <u>CTGCAG</u> AGCCGCAACACGACATCAA	PstI	Cloning in pPD 129.36
ama_LC_for	GTGCCGAGACAACATC		mRNA expression
ama_LC_rev	GAGTCTGGATGGGTACTG		mRNA expression
PAT_LC_for	CATCAATTCAGAATATAAATATCCAAACA		mRNA expression
PAT_LC_rev	TTGGAACTACTAAAGCCATC		mRNA expression
pept-1_for	GCAACACACTGTACGGAAC		Screenin for <i>pept-1</i> deletion
pept-1_rev	CCAGTGGGTGCACCACAAGG		Screening for <i>pept-1</i> deletion
pept-1_LC_for	ACTATGGAATGAGAACGGT		mRNA expression
pept-1_LC_rev	CTTGTCCGATTGCGTAT		mRNA expression
rsks-1_for1	GAGATGCGGAAGCTATGCTC		Screening for <i>rsks-1</i> deletion
rsks-1_for2	ATTCAACTGTGTGCCAGTGC		Screening for <i>rsks-1</i> deletion
rsks-1_rev1	GTTGAATTCCTGCTCCTCCA		Screening for <i>rsks-1</i> deletion
rsks-1_rev2	TGGGGCTTCACTATTTGGTC		Screening for <i>rsks-1</i> deletion

Antibodies**Table 14: Antibodies**

Name	Animal	Incubation period	Dilution	Company
Anti-goat IgG	rabbit	1 hour	1:10000	Sigma
Anti-rabbit IgG	goat	1 hour	1:10000	Sigma
ATGP-1	rabbit	over night	1:500	gift from F. Verrey
ATGP-2	rabbit	over night	1:500	gift from F. Verrey
PEPT-1	rabbit	1 hour	1:5000	Pineda
PGP-2	rabbit	over night	1:1000	gift from G. Hermann
β -Actin	goat	1 hour	1:1000	Sigma

6.5. Instruments**Table 15: Instruments**

Instrument	Company
1450 Microbeta Trilux Scintillation Counter	Wallace
AS-Analyser	
Confocal microscope Leica DM IRBE	Leica
Fast prep FP120 BIO101	Thermo Savant
Light Cycler [®]	Roche
Microscope Leica KL1500	Leica
NanoDrop ND-1000 Spectrophotometer	PeqLab
Thermocycler	Biometra
Varioskan	Thermo Elektron Corporation, Waltham

7. REFERENCES

1. **Brenner, S.** The genetics of *Caenorhabditis elegans*. *Genetics* 77 (1). 1974, pp. 71-94.
2. **The C. elegans sequencing consortium.** Genome sequence of the nematode *C. elegans*: a platform for investigating biology. *Science* 282. 1998, pp. 2012-2018.
3. **Sulston J E, Horvitz H R.** Post-embryonic Cell Lineages of the Nematode, *Caenorhabditis elegans*. *Dev Biol* 56. 1977, pp. 110-156.
4. **Corsi, A K.** A biochemist's guide to *Caenorhabditis elegans*. *Anal Biochem* 359. 2006, pp. 1-17.
5. **Cassada R, Russell D.** The dauerlarva, a post-embryonic developmental variant of the nematode *C. elegans*. *Dev Biol* 46. 1975, pp. 326-342.
6. **McGhee, J D.** The *C. elegans* intestine. *Wormbook*. 27 March 2007, pp. The *C. elegans* Research Community, <http://www.wormbook.org>.
7. **Avery L, Shtonda BB.** Food transport in the *C. elegans* pharynx. *J Exp Biol* 206(Pt 14). 2003, pp. 2441-2457.
8. **Sulston J E, Schierenberg E, White J G, Thomson J N.** The embryonic cell lineage of the nematode *Caenorhabditis elegans*. *Dev Biol* 100. 1983, pp. 64-119.
9. **Winston W M, Molodowitch C, Hunter C P.** Systemic RNAi in *C. elegans* requires the putative transmembrane protein SID-1. *Science* 295. 2002, pp. 2456-2459.
10. **Fei Y-J, Liu J C, Inoue K, Zhuang L, Miyake K, Miyauchi S, Ganapathy V.** Relevance of NAC-2, an Na⁺-coupled citrate transporter, to life span, body size and fat content in *Caenorhabditis elegans*. *Biochem J* 379. 2004, pp. 191-198.
11. **Nehrke, K.** A reduction in intestinal cell pHi due to loss of the *Caenorhabditis elegans* Na⁺/H⁺ exchanger NHX-2 increases life span. *J Biol Chem* 278(45). 2003, pp. 44657-44666.
12. **Meissner B, Boll M, Daniel H, Baumeister R.** Deletion of the intestinal peptide transporter affects insulin and TOR signaling in *Caenorhabditis elegans*. *J Biol Chem*, 279 (53). 2004, pp. 36739-36745.

13. **Lehane, M J.** Peritrophic matrix structure and function. *Annu. Rev. Entomol.* 42. 1997, pp. 525–550.
14. **Freeman H J, Kim Y S.** Digestion and absorption of protein. *Annu Rev Med* 29. 1978, pp. 99-116.
15. **Bröer, S.** Amino Acid Transport Across Mammalian Intestinal and Renal Epithelia. *Physiol Rev.* 2006, pp. 249-286.
16. **Milne, D M.** Disorders of Amino-Acid Transport. *Brit. med. J,* 1. 1964, pp. 327-336.
17. **Chillarón J, Roca R, Valencia A, Zorzano A, Palacín M.** Heteromeric amino acid transporters: biochemistry, genetics and physiology. *Am J Physiol Renal Physiol.* 2001, 281, pp. 995-1018.
18. **Chairoungdua A, Kanai Y, Matsuo H, Inatomi J, Kim D K, Endou H.** Identification and Characterization of a Novel Member of the Heterodimeric Amino Acid Transporter Family Presumed to be Associated with an Unknown Heavy Chain. *J Biol Chem.* 2001, pp. 49390-49399.
19. **White, M F.** The transport of cationic amino acids across the plasma membrane of mammalian cells. *Biochem. Biophys. Acta* 822. 1985, pp. 355-374.
20. **Christensen, N H.** Role of amino acid transport and countertransport in nutrition and metabolism. *Physiol Rev,* 70. 1990, pp. 43-77.
21. **Mastroberardina L, Spindler B, Pfeiffer R, Skelly P J, Loffing J, Shoemaker C B, Verrey F.** Amino-acid transport by heterodimers of 4F2hc/CD98 and members of a permease family. *Nature* 395. 1998, pp. 288-291.
22. **Verrey, F.** System L: heteromeric exchangers of large, neutral amino acids involved in directional transport. *Eur J Physiol* 445. 2003, pp. 529-533.
23. **Fukasawa Y, Segawa H, Kim J Y, Chairoungdua A, Kim DK, Matsuo H, Cha SH, Endou H, Kanai Y.** Identification and characterization of a Na(+)-independent neutral amino acid transporter that associates with the 4F2 heavy chain and exhibits substrate selectivity for small neutral D- and L-amino acids. *J Biol Chem* 275. 2000, pp. 9690-9698.
24. **Bridges C C, Zalups R K.** Cystine and Glutamate Transport in Renal Epithelial Cells Transfected with Human System xc⁻. *Kidney Int.* 68(2). 2005, pp. 653-664.
25. **Winkle van L J, Campione A L, Gorman J M.** Na⁺-independent transport of basic and zwitterionic amino acids in mouse blastocysts by a shared system and by processes which distinguish between these substrates. *J Biol Chem,* 263. 1988, pp. 3150-3163.

26. **Matsuo H, Kanai Y, Kim JY, Chairoungdua A, Kim DK, Inatomi J, Shigeta Y, Ishimine H, Chaekuntode S, Tachampa K, Choi HW, Babu E, Fukuda J, Endou H.** Identification of a novel Na⁺-independent acidic amino acid transporter with structural similarity to the member of a heterodimeric amino acid transporter family associated with unknown heavy chains. *J Biol Chem*, 277 (23). 2002, pp. 21017-21026.
27. **Young J D, Mason D K, Fincham D A.** Topographical similarities between harmaline inhibition sites on Na⁺-dependent amino acid transport system ASC in human erythrocytes and Na⁺-independent system asc in horse erythrocytes. *J Biol Chem*, 263 (1). 1988, pp. 140-143.
28. **Palacín M, Nunes V, Font-Llitjós M, Jiménez-Vidal M, Fort J, Gasol E, Pineda M, Feliubadaló L, Chillarón J, Zorzano A.** The Genetics of Heteromeric Amino Acid Transporters. *Physiology*. 2005, pp. 112-124.
29. **Bröer S, Wagner C.** Structure-Function Relationships of Heterodimeric Amino Acid Transporters. *Cell Biochemistry and Biophysics*. 2002, Vol. 36.
30. **Reig N, Chillarón J, Bartoccini P, Fernández E, Bendahan A, Zorzano A, Kanner B, Palacín M, Bertran J.** The light subunit of system b_{0,+} is fully functional in the absence of the heavy subunit. *The EMBO Journal*. 2002, pp. 4906-4914.
31. **Fernández E, Jiménez-Vidal M, Calvo M, Zorzano A, Tebar F, Palacín M, Chillarón J.** The Structural and Functional Units of Heteromeric Amino Acid Transporters. *The Journal of Biological Chemistry*. 2006, Vol. Vol 281, pp. 26552-26561.
32. **Palacín M, Borsani G, Sebastio G.** The nuclear bases of cystinuria and lysinuric protein intolerance. *Curr Opin Genet Develop* 11. 2001b, pp. 328-335.
33. **Palacín M, Bertran M, Chillarón J, Estévez R, Zorzano A.** Lysinuric protein intolerance: mechanisms of pathophysiology. *Molecular Genetics and Metabolism* (81). 2004, pp. 27-37.
34. **Calonge M J, Gasparini P, Chillaron J, Chillon M, Gallucci M, Roussaud F, Zelante L, Testar X, Dallaspiccola B, Di Silverio F, Barcelo P, Estivill X, Zorzano A, Nunes V, Palacin M.** Cystinuria caused by mutations in rBAT, a gene involved in the transport of cystine. *Nature Genet* 6. 1994, pp. 420-425.
35. **Calonge M J, Volpini V, Biseeglia L, Rousaud F, de Sanctis L, Beccia E, Zelante L, Testar X, Zorzano A, Estivill X, Gasparini P, Nunes V, Palacin M.** Genetic heterogeneity in cystinuria: the rBAT gene is linked to type I but not to type III cystinuria. *Proc Nat Acad Sci USA* 92. 1995, pp. 9667-9671.

36. **Palacin M, Goodyer P, Nunes V, Gasparini P.** Cystinuria. *Metabolic and Molecular Basis of Inherited Diseases (8th ed.)*. 2001a, pp. 4909-4932.
37. **Feliubadaló L, Font M, Purroy J, Rousaud F, Estivill X, Nunes V, Golomb E, Centola M, Aksentijevich I, Kreiss Y, Goldman B, Pras M, Kastner DL, Pras E, Gasparini P, Bisceglia L, Beccia E, Gallucci M, de Sanctis L, Ponzzone A, Rizzoni GF, Zelante L, Bassi M.** Non-type I cystinuria caused by mutations in SLC7A9, encoding a subunit (bo,+AT) of rBAT. *Nature Genet.* 23(1). 1999, pp. 52-57.
38. **Rosenberg L E, Downing S, Durant J L, Segal S.** Cystinuria: biochemical evidence for three genetically distinct diseases. *J Clin Invest* 45. 1966, pp. 365-371.
39. **Simell, O.** Lysinuric protein intolerance and other cationic aminoacidurias. *Metabolic and Molecular Bases of Inherited Diseases (8th ed.)*. 2001, pp. 4933-4956.
40. **Rajantie J, Simell O, Perheentupa J.** Basolateral-membrane transport defect for lysine in lysinuric protein intolerance. *Lancet* 1. 1980, pp. 1219-1221.
41. **Veljkovic E, Stasiuk S, Skelly P J, Shoemaker C B, Verrey F.** Functional Characterization of *Caenorhabditis elegans* Heteromeric Amino Acid Transporters. *J Biol Chem.* 2004 II, pp. 7655-7662.
42. **Veljkovic E, Bacconi A, Stetaks A, Hajnal A, Stasiuk S, Skelly P J, Forster I, Shoemaker C B, Verrey F.** Aromatic Amino Acid Transporter AAT-9 of *Caenorhabditis elegans* Localizes to Neurons and Muscle Cells. *J Biol Chem, Vol* 279, No 47. 2004 I, pp. 49268-49273.
43. **Kim D K, Kanai Y, Chairoungdua A, Matsuo H, Cha S H, Endou H.** Expression cloning of a Na⁺-independent aromatic amino acid transporter with structural similarity to H⁺/monocarboxylate transporters. *J Biol Chem* 276. 2001, pp. 17221-17228.
44. **Dorn M, Weiwad M, Markwardt F, Laug L, Rudolph R, Brandsch M, Bosse-Doenecke E.** Identification of Disulfide Bridge Essential for Transport Function of the Human Proton-Coupled Amino Acid Transporter hPAT1. *J Biol Chem.* 2009, pp. 1-20.
45. **Metzner L, Kalbitz J, Brandsch M.** Transport of pharmacologically active proline derivatives by the human proton-coupled amino acid transporter hPAT1. *J Pharmacol Exp Ther* 309 (1). 2004, pp. 28-35.
46. **Sagné C, Agulhon C, Ravassard P, Darmon M, Hamon M, El Mestikawy S, Gasnier B, Giros B.** Identification and characterization of a lysosomal

transporter for small neutral amino acids. *Proc. Natl. Acad. Sci. U.S.A* 98. 2001, pp. 7206-7211.

47. **Foltz M, Boll M, Raschka L, Kottra G, Daniel H.** A novel bifunctionality: PAT1 and PAT2 mediate electrogenic proton/amino acid and electroneutral proton/fatty acid symport. *FASEB J* 18. 2004, pp. 1758-1760.

48. **Bröer, S.** Apical Transporters for Neutral Amino Acids: Physiology and Pathophysiology. *Physiol* 23. 2008, pp. 95-103.

49. **Boll M, Foltz M, Anderson C M, Oechsler C, Kottra G, Thwaites D T, Daniel H.** Substrate recognition by the mammalian proton-dependent amino acid transporter PAT1. *Mol Membr Biol* 20. 2003, pp. 261-269.

50. **Anderson C M, Grenade D S, Boll M, Foltz M, Wake K A, Kennedy D J, Munck L K, Miyauchi S, Taylor P M, Campbell F C, Munck B G, Daniel H, Ganapathy V, Thwaites D T.** H⁺/amino acid transporter 1 (PAT1) is the imino acid carrier: an intestinal nutrient/drug transporter in human and rat. *Gastroenterology* 127. 2004, pp. 1410-1422.

51. **Chesney, R W.** Iminoglycinuria. *The Metabolic and Molecular Bases of Inherited Diseases (8th ed.)*. 2001, pp. 4971-4982.

52. **Thier S O, Alpers D H.** Disorders of intestinal transport of amino acids. *Am J Dis Child* 117. 1969, pp. 13-23.

53. **Daniel, H.** Molecular and Integrative Physiology of Intestinal Peptide Transport. *Annu Rev Physiol* 66. 2004, pp. 361-384.

54. **Fei YJ, Kanai Y, Nussberger S, Ganapathy V, Leibach FH, Romero MF, Singh SK, Boron WF, Hediger MA.** Expression cloning of a mammalian proton-coupled oligopeptide transporter. *Nature* 368(6471). 1994, 563-6.

55. **Freeman T C, Bentsen B S, Thwaites D T, Simmons N L.** H⁺/di-tripeptide transporter (PepT1) expression in the rabbit intestine. *Pflugers Arch* 430. 1995, pp. 394-400.

56. **Thwaites D T, Anderson C M H.** H⁺-coupled nutrient, micronutrient and drug transporters in the mammalian small intestine. *Exp Physiol* 92. 2007, pp. 603-619.

57. **Rubio-Aliaga I, Daniel H.** Mammalian peptide transporters as targets of drug delivery. *Trends Pharmacol Sci* 23. 2002, pp. 434-440.

58. **Rubio-Aliaga I, Daniel H.** Peptide transporters and their roles in physiological processes and drug disposition. *Xenobiotica* 38(7-8). 2008, pp. 1022-1042.

59. **Daniel H, Spanier B, Kottra G, Weitz D.** From Bacteria to Man: Archaic Proton-Dependent Peptide Transports at Work. *Physiology* 21. 2005, pp. 93-102.
60. **Thwaites D T, Ford D, Glanville M, Simmons N L.** H⁺/solute-induced intracellular acidification leads to selective activation of apical Na⁺/H⁺ exchange in human intestinal epithelial cells. *J Clin Invest* 104. 1999, pp. 629-635.
61. **Thwaites D T, Kennedy D J, Raldua D, Anderson C M H, Mendoza M E, Bladen C L, Simmons N L.** H⁺/dipeptide absorption across the human intestinal epithelium is controlled indirectly via a functional Na⁺/H⁺ exchanger. *Gastroenterology* 122. 2002, pp. 1322-1333.
62. **Anderson C M H, Thwaites D T.** Indirect regulation of the intestinal H⁺-coupled amino acid transporter hPAT1 (SLC36A1). *J Cell Physiol* 204. 2005, pp. 604-613.
63. **Nabulsi N B, Smith D E, Kilbourn M R.** [¹¹C]Glycylsarcosine: synthesis and in vivo evaluation as a PET tracer of PepT2 transporter function in kidney of PepT2 null and wild-type mice. *Bioorg Med Chem* 13. 2005, pp. 2993-3001.
64. **Lu H, Klaassen C.** Tissue distribution and thyroid hormone regulation of Pept1 and Pept2 mRNA in rodents. *Peptides* 27(4). 2006, pp. 850-857.
65. **Chen X Z, Zhu T, Smith D E, Hediger M A.** Stoichiometry and kinetics of the high-affinity H⁺-coupled peptide transporter PepT2. *J Biol Chem* 274. 1999, 2773-2779, pp. 2773-2779.
66. **Fei Y-J, Fujita T, Lapp D F, Ganapathy V, Leibach F H.** Two oligopeptide transporters from *Caenorhabditis elegans* molecular cloning and functional expression. *Biochem J* 332. 1998, pp. 565-572.
67. **Spanier B, Lasch K, Marsch S, Benner J, Liao W, Hu H, Kienberger H, Eisenreich W, Daniel H.** How the Intestinal Peptide Transporter PEPT-1 Contributes to an Obesity Phenotype in *Caenorhabditis elegans*. *PLOS one* 4(7). 2009, p. e6279.
68. **Rual JF, Ceron J, Koreth J, Hao T, Nicot AS, Hirozane-Kishikawa T, Vandenhoute J, Orkin SH, Hill DE, van den Heuvel S, Vidal M.** Toward improving *Caenorhabditis elegans* phenome mapping with an ORFeome-based RNAi library. *Genome Res.* (10B). 2004, pp. 2162-2168.
69. **Fei Y-J, Romero M F, Krause M, Liu J-C, Huang W, Ganapathy V, Leibach F H.** A Novel H⁺-coupled Oligopeptide Transporter (OPT3) from *Caenorhabditis elegans* with a Predominant Function as a H⁺ Channel and an Exclusive Expression in Neurons. *J Biol Chem* 275(13). 2000, pp. 9563-9571.

70. **Fraser A G, Kamath R S, Zipperlen P, Martinez-Campos M, Sohrmann M, Ahringer J.** Functional genomic analysis of *C. elegans* chromosome I by systematic RNA interference. *Nature*, Vol 408. 2000, pp. 325-330.
71. **Das F, Ghosh-Choudhury N, Mahimainathan L, Venkatesan B, Feliars D, Riley D J, Kasinath B S, Choudhury G G.** Raptor-ricTOR axis in TGFbeta-induced protein synthesis. *Cell Signal* 20(2). 2008, pp. 409-423.
72. **Fumarola C, La Monica S, Alfieri R R, Borra E, Guidotti G G.** Cell size reduction induced by inhibition of the mTOR/S6K-signaling pathway protects Jurkat cells from apoptosis. *Cell Death Differ* 12(10). 2005, pp. 1344-1357.
73. **Hara K, Maruki Y, Long X, Yoshino K, Oshiro N, Hidayat S, Tokunaga C, Avruch J, Yonezawa K.** Raptor, a binding partner of target of rapamycin (TOR), mediates TOR action. *Cell* 110(2). 2005, pp. 177-189.
74. **Lang C H, Frost R A.** Endotoxin disrupts the leucine-signaling pathway involving phosphorylation of mTOR,4E-BP1,and S6K1 in skeletal muscle. *J Cell Physiol* 203(1). 2005, pp. 144-155.
75. **Sarbassov D D, Guertin D A, Ali S M, Sabatini D M.** Phosphorylation and regulation of Akt/PKB by the rictor-mTOR complex. *Science* 307(5712). 2005, pp. 1098-1101.
76. **Jozwiak J, Jozwiak S ,Grzela T ,Lazarczyk M.** Positive and negative regulation of TSC2 activity and its effects on downstream effectors of the mTOR pathway. *Neuromolecular Med* 7(4). 2005, pp. 287-296.
77. **Hardie, D G.** The AMP-activated protein kinase pathway--new players upstream and downstream. *J Cell Sci* 117(Pt 23). 2004, pp. 5479-5487.
78. **Sancak Y, Peterson T R, Shaul Y D, Lindquist R A, Thoreen C C, Bar-Peled L, Sabatini D M.** The Rag GTPases bind raptor and mediate amino acid signaling to mTORC1. *Science* 320(5882). 2008, pp. 1496-1501.
79. **Martin D E, Hall M N.** The expanding TOR signaling network. *Curr Opin Cell Biol* 17(2). 2005, pp. 158-166.
80. **Proud, C G.** Regulation of mammalian translation factors by nutrients. *Eur J Biochem* 269(22). 2002, pp. 5338-5349.
81. **Patel J, Wang X, Proud C G.** Glucose exerts a permissive effect on the regulation of the initiation factor 4E binding protein 4E-BP1. *Biochem J* 358(Pt 2). 2001, pp. 497-503.
82. **Hara K, Yonezawa K, Weng Q P, Kozlowski M T, Belham C, Avruch J.** Amino acid sufficiency and mTOR regulate p70 S6 kinase and eIF-4E BP1

through a common effector mechanism. *J Biol Chem* 273(23). 1998, pp. 14484-14494.

83. **Beugnet A, Tee A R, Taylor P M, Proud C G.** Regulation of targets of mTOR (mammalian target of rapamycin) signalling by intracellular amino acid availability. *Biochem J* 372(Pt 2). 2003, pp. 555-566.

84. **Ishiguro H, Katano Y, Nakano I, Ishigami M, Hayashi K, Honda T, Goto H, Bajotto G, Maeda K, Shimomura Y.** Clofibrate treatment promotes branched-chain amino acid catabolism and decreases the phosphorylation state of mTOR, eIF4E-BP1, and S6K1 in rat liver. *Life Sci* 79(8). 2006, pp. 737-743.

85. **Nicklin P, Bergman P, Zhang B, Triantafellow E, Wang H, Nyfeler B, Yang H, Hild M, Kung C, Wilson C, Myer V E, MacKeigan J P, Porter J A, Wang Y K, Cantley L C, Finan P M, Murphy L O.** Bidirectional transport of amino acids regulates mTOR and autophagy. *Cell* 136(3). 2009, pp. 521-534.

86. **Long X, Lin Y, Ortiz-Vega S, Yonezawa K, Avruch J.** Rheb binds and regulates the mTOR kinase. *Curr Biol* 15(8). 2005, pp. 702-713.

87. **Long X, Ortiz-Vega S, Lin Y, Avruch J.** Rheb binding to mammalian target of rapamycin (mTOR) is regulated by amino acid sufficiency. *J Biol Chem* 280(25). 2005 II, pp. 23433-23436.

88. **Wang X, Proud C G.** Nutrient control of TORC1, a cell-cycle regulator. *Trends Cell Biol* 19(6). 2009, pp. 260-267.

89. **Liu X M, Reyna S V, Ensenat D, Peyton K J, Wang H, Schafer A I, Durante W.** Platelet-derived growth factor stimulates LAT1 gene expression in vascular smooth muscle: role in cell growth. *FASEB J* 18(6). 2004, pp. 768-770.

90. **Rajan D P, Kekuda R, Huang W, Devoe L D, Leibach F H, Prasad P D, Ganapathy V.** Cloning and functional characterization of a Na(+)-independent, broad-specific neutral amino acid transporter from mammalian intestine. *Biochim Biophys Acta* 1463(1). 2000, pp. 6-14.

91. **Peyrollier K, Hajduch E, Blair A S, Hyde R, Hundal H S.** L-leucine availability regulates phosphatidylinositol 3-kinase, p70 S6 kinase and glycogen synthase kinase-3 activity in L6 muscle cells: evidence for the involvement of the mammalian target of rapamycin (mTOR) pathway in the L-leucine-induced up-regulation. *Biochem J* 350(Pt 2). 2000, pp. 361-368.

92. **Edinger A L, Thompson C B.** Akt maintains cell size and survival by increasing mTOR-dependent nutrient uptake. *Mol Biol Cell* 13(7). 2002, pp. 2276-2288.

93. **Hennig K M, Colombani J, Neufeld T P.** TOR coordinates bulk and targeted endocytosis in the *Drosophila melanogaster* fat body to regulate cell growth. *J Cell Biol* 173(6). 2006, pp. 963-974.
94. **Wu B, Ottow K, Poulsen P, Gaber R F, Albers E, Kielland-Brandt M C.** Competitive intra- and extracellular nutrient sensing by the transporter homologue Ssy1p. *J Cell Biol* 173(3). 2006, pp. 327-331.
95. **Goberdhan D C I, Meredith D, Boyd C A R, Wilson C.** PAT-related amino acid transporters regulate growth via a novel mechanism that does not require bulk transport of amino acids. *Devel* 132. 2005, pp. 2365-2375.
96. **Nakamura E, Sato M, Yang H, Miyagawa F, Harasaki M, Tomita K et al.** 4F2 (CD98) heavy chain is associated covalently with an amino acid transporter and controls intracellular trafficking and membrane topology of 4F2 heterodimer. *J Biol Chem* 274. 1999, pp. 3009-3016.
97. **Feliubadalo L, Font M, Purroy J, Rousaud F, Estivill X, Nunes V, et al.** Non-type I cystinuria caused by mutations in SLC7A9, encoding a subunit (b0,+AT) of rBAT. *Nature Genet.* 1999, pp. 52-57.
98. **Jonassen T, Davis D E, Larsen P L, Clarke C F.** Reproductive fitness and quinone content of *Caenorhabditis elegans* clk-1 mutants fed coenzyme Q isoforms of varying length. *J Biol Chem* 278(51). 2003, pp. 51735-51742.
99. **Asatoor A M, Freedman P S, Gabriel J R, Milne M D, Prosser D I, Roberts J T, Willoughby C P.** Amino acid imbalance in cystinuria. *J Clin Pathol* 27(6). 1974, pp. 500-504.
100. **Brooks K K, Liang B, Watts J L.** The influence of bacterial diet on fat storage in *C. elegans*. *PLoS One* 4(10). 2009, p. e7545.
101. **Fernández E, Carrascal M, Rousaud F, Abián J, Zorzano A, Palacín M, Chillarón J.** rBAT-b(0,+AT) heterodimer is the main apical reabsorption system for cystine in the kidney. *Am J Physiol Renal Physiol* 283(3). 2002, F540-548.
102. **Kamath R S, Martinez-Campos M, Zipperlen P, Fraser A G, Ahringer J.** Effectiveness of specific RNA-mediated interference through ingested double-stranded RNA in *C. elegans*. *Genome Biol.* 2 (1). 2000, pp. 0002.1-0002.12.
103. **Boll M, Daniel H, Gasnier B.** The SLC36 family: proton-coupled transporters for the absorption of selected amino acids from extracellular and intracellular proteolysis. *Pflugers Arch* 447(5). 2004, pp. 776-779.
104. **Pauli F, Liu Y, Kim Y A, Chen P-J, Kim S K.** Chromosomal clustering and GATA transcriptional regulation of intestine-expressed genes. *Development* 133. 2005, pp. 287-295.

105. **Groneberg DA, Döring F, Eynott PR, Fischer A, Daniel H.** Intestinal peptide transport: ex vivo uptake studies and localization of peptide carrier PEPT1. *Am J Physiol Gastrointest Liver Physiol* 281(3). 2001, G697-704.
106. **Kennedy DJ, Leibach FH, Ganapathy V, Thwaites DT.** Optimal absorptive transport of the dipeptide glycylsarcosine is dependent on functional Na⁺/H⁺ exchange activity. *Pflugers Arch* 445(1). 2002, 139-46.
107. **Margis R, Dunand C, Teixeira F K, Margis-Pinheiro M.** Glutathione peroxidase family - an evolutionary overview. *FEBS J* 275(15). 2008, pp. 3959-3970.
108. **Herbette S, Roeckel-Drevet P, Drevet J R.** Seleno-independent glutathione peroxidases. *FEBS J* 274. 2007, pp. 2163-2180.
109. **Rudberg P C, Tholander R, Thunnissen M M G M, Samuelsson B, Haeggström J Z.** Leukotriene A4 hydrolase: Selective abrogation of leukotriene B4 formation by mutation of aspartic acid 375. *PNAS* 99(7). 2002, pp. 4215-4220.
110. **Orning L, Gierse J K, Fitzpatrick F A.** The bifunctional enzyme leukotriene-A4 hydrolase is an arginine aminopeptidase of high efficiency and specificity. *J Biol Chem* 269. 1994, pp. 11269-11273.
111. **Morgan E L, Maskrey B H, Rowley A F.** At what stage in metazoan evolution did leukotriene generation first appear?--key insights from cartilaginous fish. *Dev Comp Immunol* 29(1). 2005, pp. 53-59.
112. **Lenney, J F.** Human cytosolic carnosinase: evidence of identity with prolinase, a non-specific dipeptidase. *Biol Chem Hoppe Seyler* 371(2). 1990, pp. 167-171.
113. **Ganguli D, Kumar C, Kumar-Bachhawat A.** The Alternative Pathway of Glutathione Degradation Is Mediated by a Novel Protein Complex Involving Three New Genes in *Saccharomyces cerevisiae*. *Genetics* 175. 2007, pp. 1137-1151.
114. **Reeves J E, Fried M.** The surf-4 gene encodes a novel 30 kDa integral membrane protein. *Mol Membr Biol* 12. 1995, pp. 201-208.
115. **Caldwell S R, Hill K J, Cooper A A.** Degradation of endoplasmic reticulum (ER) quality control substrates requires transport between the ER and Golgi. *J Biol Chem* 276(26). 2001, pp. 23296-23303.
116. **Haynes C M, Titus E, Cooper A.** Degradation of Misfolded Proteins Prevents ER-Derived Oxidative Stress and Cell Death. *Mol Cell* 15. 2004, pp. 767-776.
117. **Washburn M P, Koller A, Oshiro G, Ulaszek R R, Plouffe D, Deciu C, Winzeler E, Yates J R 3rd.** Protein pathway and complex clustering of correlated

mRNA and protein expression analyses in *Saccharomyces cerevisiae*. *PNAS USA* 100(6). 2003, pp. 3107-3112.

118. **Bedard K, Krause K H.** The NOX family of ROS-generating NADPH oxidases: physiology and pathophysiology. *Physiol Rev* 87(1). 2007, pp. 245-313.

119. **Kohen R, Nyska A.** Oxidation of biological systems: oxidative stress phenomena, antioxidants, redox reactions, and methods for their quantification. *Toxicol Pathol* 30(6). 2002, pp. 620-650.

120. **Chávez V, Mohri-Shiomi A, Maadani A, Vega L A, Garsin D A.** Oxidative stress enzymes are required for DAF-16-mediated immunity due to generation of reactive oxygen species by *Caenorhabditis elegans*. *Genetics* 176(3). 2007, pp. 1567-1577.

121. **Esposti M D, Hatzinisiriou I, McLennan H, Ralph S.** Bcl-2 and mitochondrial oxygen radicals. New approaches with reactive oxygen species-sensitive probes. *J Biol Chem* 274(42). 1999, pp. 29831-29837.

122. **Scandalios, J G.** Oxidative stress: molecular perception and transduction of signals triggering antioxidant gene defenses. *Braz J Med Biol Res* 38(7). 2005, pp. 995-1014.

123. **Masella R, Di Benedetto R, Vari R, Filesi C, Giovanni C.** Novel mechanisms of natural antioxidant compounds in biological systems: involvement of glutathione and glutathione-related enzymes. *J Nut Biochem* 16. 2005, pp. 577-586.

124. **Blum J, Fridovich I.** Superoxide, hydrogen peroxide, and oxygen toxicity in two free-living nematode species. *Arch Biochem Biophys* 222. 1983, pp. 35-43.

125. **Teufel M, Saudek V, Ledig J P, Bernhardt A, Boularand S, Carreau A, Cairns N J, Carter C, Cowley D J, Duverger D, Ganzhorn A J, Guenet C, Heintzelmann B, Laucher V, Sauvage C, Smirnova T.** Sequence identification and characterization of human carnosinase and a closely related non-specific dipeptidase. *J Biol Chem* 278(8). 2003, pp. 6521-6531.

126. **Davies D R, Mamat B, Magnusson O T, Christensen J, Haraldsson M H, Mishra R, Pease B, Hansen E, Singh J, Zembower D, Kim H, Kiselyov A S, Burgin A B, Gurney M E, Stewart L J.** Discovery of leukotriene A4 hydrolase inhibitors using metabolomics biased fragment crystallography. *J Med Chem* 52(15). 2009, pp. 4694-4715.

127. **Daniel H, Adibi SA.** Functional separation of dipeptide transport and hydrolysis in kidney brush border membrane vesicles. *FASEB J* 8(10). 1994, 753-759.

128. **Dave MH, Schulz N, Zecevic M, Wagner CA, Verrey F.** Expression of heteromeric amino acid transporters along the murine intestine. *J Physiol* 558(Pt 2). 2004, 597-610.
129. **Xie X, Dumas T, Tang L, Brennan T, Reeder T, Thomas W, Klein RD, Flores J, O'Hara BF, Heller HC, Franken P.** Lack of the alanine-serine-cysteine transporter 1 causes tremors, seizures, and early postnatal death in mice. *Brain Res* 1052(2). 2005, 212-221.
130. **Tsumura H, Suzuki N, Saito H, Kawano M, Otake S, Kozuka Y, Komada H, Tsurudome M, Ito Y.** The targeted disruption of the CD98 gene results in embryonic lethality. *Biochem Biophys Res Commun* 308(4). 2003, 847-851.
131. **Hunt-Newbury R, Viveiros R, Johnsen R, Mah A, Anastas D, Fang L, Halfnight E, Lee D, Lin J, Lorch A, McKay S, Okada HM, Pan J, Schulz AK, Tu D, Wong K, Zhao Z, Alexeyenko A, Burglin T, Sonnhammer E, Schnabel R, Jones SJ, Marra MA, Baillie DL, Moerman DG.** High-throughput in vivo analysis of gene expression in *Caenorhabditis elegans*. *PLoS Biol* 5(9). 2007, e 237.
132. **Ishii T, Sugita Y, Bannai S.** Regulation of glutathione levels in mouse spleen lymphocytes by transport of cysteine. *J Cell Physiol* 133(2). 1987, 330-6.
133. **Bannai S, Sato H, Ishii T, Sugita Y.** Induction of cystine transport activity in human fibroblasts by oxygen. *J Biol Chem* 264(31). 1989, 18480-18484.
134. **Sato H, Tamba M, Ishii T, Bannai S.** Cloning and expression of a plasma membrane cystine/glutamate exchange transporter composed of two distinct proteins. *J Biol Chem* 274(17). 1999, 11455-11458.
135. **Boll M, Foltz M, Rubio-Aliaga I, Kottra G, Daniel H.** Functional characterization of two novel mammalian electrogenic proton-dependent amino acid cotransporters. *J Biol Chem* 277(25). 2002, 22966-73.
136. **Rubio-Aliaga I, Boll M, Vogt Weisenhorn DM, Foltz M, Kottra G, Daniel H.** The proton/amino acid cotransporter PAT2 is expressed in neurons with a different subcellular localization than its paralog PAT1. *J Biol Chem* 279(4). 2004, 2754-60.
137. **Forsberg H, Ljungdahl PO.** Sensors of extracellular nutrients in *Saccharomyces cerevisiae*. *Curr Genet* 40(2). 2001, 91-109.
138. **Rubio-Aliaga I, Daniel H.** Peptide transporters and their roles in physiological processes and drug disposition. *Xenobiotica* 38(7-8). 2008, pp. 1022-1042.
139. **Chen M, Singh A, Xiao F, Dringenberg U, Wang J, Engelhardt R, Yeruva S, Rubio-Aliaga I, Nässl AM, Kottra G, Daniel H, Seidler U.** Gene ablation for

PEPT1 in mice abolishes the effects of dipeptides on small intestinal fluid absorption, short-circuit current, and intracellular pH. *Am J Physiol Gastrointest Liver Physiol* 299(1). 2010, G265-74.

140. **Mertl M, Daniel H, Kottra G.** Substrate-induced changes in the density of peptide transporter PEPT1 expressed in *Xenopus* oocytes. *Am J Physiol Cell Physiol* 295(5). 2008, C1332-43.

141. **Ihara T, Tsujikawa T, Fujiyama Y, Bamba T.** Regulation of PepT1 peptide transporter expression in the rat small intestine under malnourished conditions. *Digestion* 61(1). 2000, 59-67.

142. **Shiraga T, Miyamoto K, Tanaka H, Yamamoto H, Taketani Y, Morita K, Tamai I, Tsuji A, Takeda E.** Cellular and molecular mechanisms of dietary regulation on rat intestinal H⁺/Peptide transporter PepT1. *Gastroenterology* 116(2). 1999, 354-62.

143. **Xia Z, Turner GC, Hwang CS, Byrd C, Varshavsky A.** Amino acids induce peptide uptake via accelerated degradation of CUP9, the transcriptional repressor of the PTR2 peptide transporter. *J Biol Chem* 283(43). 2008, 28958-68.

144. **Turner GC, Du F, Varshavsky A.** Peptides accelerate their uptake by activating a ubiquitin-dependent proteolytic pathway. *Nature* 405(6786). 2000, 579-83.

145. **Li Q, Sai Y, Kato Y, Tamai I, Tsuji A.** Influence of drugs and nutrients on transporter gene expression levels in Caco-2 and LS180 intestinal epithelial cell lines. *Pharm Res* 20(8). 2003, 1119-24.

146. **Muller U, Brandsch M, Prasad PD, Fei YJ, Ganapathy V, Leibach FH.** Inhibition of the H⁺/peptide cotransporter in the human intestinal cell line Caco-2 by cyclic AMP. *Biochem Biophys Res Commun* 218(2). 1996, 461-5.

147. **Berlioz F, Julien S, Tsocas A, Chariot J, Carbon C, Farinotti R, Rozé C.** Neural modulation of cephalaxin intestinal absorption through the di- and tripeptide brush border transporter of rat jejunum in vivo. *J Pharmacol Exp Ther* 288(3). 1999, 1037-44.

148. **Wenzel U, Kuntz S, Diestel S, Daniel H.** PEPT1-mediated cefixime uptake into human intestinal epithelial cells is increased by Ca²⁺ channel blockers. *Antimicrob Agents Chemother* 46(5). 2002, 1375-80.

149. **Thamotharan M, Bawani SZ, Zhou X, Adibi SA.** Hormonal regulation of oligopeptide transporter pept-1 in a human intestinal cell line. *Am J Physiol* 276(4 Pt 1). 1999, C821-6.

150. **Buyse M, Berlioz F, Guilmeau S, Tsocas A, Voisin T, Péranzi G, Merlin D, Laburthe M, Lewin MJ, Rozé C, Bado A.** PepT1-mediated epithelial

transport of dipeptides and cephalixin is enhanced by luminal leptin in the small intestine. *J Clin Invest* 108(10). 2001, 1483-94.

151. **Brigelius-Flohé, R.** Glutathione peroxidases and redox-regulated transcription factors. *Biol Chem* 387. 2006, pp. 1329-1335.

152. **Ursini F, Maiorino M, Gregolin C.** The selenoenzyme phospholipid hydroperoxide glutathione peroxidase. *Biochim Biophys Acta* 839. 1985, pp. 62-70.

153. **Nomura K, Imai H, Koumura T, Arai M, Nakagawa Y.** Mitochondrial phospholipid hydroperoxide glutathione peroxidase suppresses apoptosis mediated by a mitochondrial death pathway. *J Biol Chem* 274(41). 1999, pp. 29294-29302.

154. **Maiorino M, Thomas J P, Girotti A, Ursini F.** Reactivity of phospholipid hydroperoxide glutathione peroxidase with membrane and lipoprotein lipid hydroperoxides. *Free Radic Res Commun* 12-13. 1991, pp. 131-135.

155. **Bao Y, Jemth P, Mannervik B, Williamson G.** Reduction of thymine hydroperoxide by phospholipid hydroperoxide glutathione peroxidase and glutathione transferases. *FEBS Lett* 410. 1997, pp. 210-212.

156. **Savaskan N E, Ufer C, Kühn H, Borchert A.** Molecular biology of glutathione peroxidase 4: from genomic structure to developmental expression and neural function. *Biol Chem* 388(10). 2007, pp. 1007-1017.

157. **Aumann K D, Bedorf N, Brigelius-Flohé R, Schomburg D, Flohe L.** Glutathione peroxidase revisited simulation of the catalytic cycle by computer-assisted molecular modelling. *Biomed Environ Sci* 10. 1997, pp. 136-155.

158. **Imai H, Nakagawa Y.** Biological significance of phospholipid hydroperoxide glutathione peroxidase (PHGPx, GPx4) in mammalian cells. *Free Radic Biol Med* 34(2). 2003, pp. 145-169.

159. **Nigam S, Schewe T.** Phospholipase A(2)s and lipid peroxidation. *Biochim Biophys Acta* 1488(1-2). 2000, 167-81.

160. **Schnurr K, Belkner J, Ursini F, Schewe T, Kuhn H.** The selenoenzyme phospholipid hydroperoxide glutathione peroxidase controls the activity of the 15-lipoxygenase with complex substrates and preserves the specificity of the oxygenation products. *J Biol Chem* 271. 1996, pp. 4653-4658.

161. **Chen C J, Huang H S, Chang W C.** Depletion of phospholipid hydroperoxide glutathione peroxidase up-regulates arachidonate metabolism by 12S-lipoxygenase and cyclooxygenase 1 in human epidermoid carcinoma A431 cells. *FASEB J* 17(12). 2003, pp. 1694-1696.

162. **Ran Q, Liang H, Ikeno Y, Qi W, Prolla T A, Roberts L J 2nd, Wolf N, Van Remmen H, Richardson A.** Reduction in glutathione peroxidase 4 increases life span through increased sensitivity to apoptosis. *J Gerontol A Biol Sci Med Sci* 62(9). 2007, pp. 932-942.
163. **Stark, G.** Functional consequences of oxidative membrane damage. *J Membr Biol* 205(1). 2005, pp. 1-16.
164. **Girotti, A W.** Lipid hydroperoxide generation, turnover, and effector action in biological systems. *J Lipid Res* 39(8). 1998, pp. 1529-1542.
165. **Uchida K, Shiraishi M, Naito Y, Torii Y, Nakamura Y, Osawa T.** Activation of stress signaling pathways by the end product of lipid peroxidation. 4-hydroxy-2-nonenal is a potential inducer of intracellular peroxide production. *J Biol Chem* 274(4). 1999, 2234-42.
166. **Shiraga T, Miyamoto K, Tanaka H, Yamamoto H, Taketani Y, Morita K, Tamai I, Tsuji A, Takeda E.** Cellular and molecular mechanisms of dietary regulation on rat intestinal H⁺/Peptide transporter PepT1. *Gastroenterology* 116(2). 1999, 354-62.
167. **Petersen D R, Doorn J A.** Reactions of 4-hydroxynonenal with proteins and cellular targets. *Free Radic Biol Med* 37(7). 2004, pp. 937-945.
168. **Ayyadevara S, Engle M R, Singh S P, Dandapat A, Lichti C F, Benes H, Shmookler Reis R J, Liebau E, Zimniak P.** Lifespan and stress resistance of *Caenorhabditis elegans* are increased by expression of glutathione transferases capable of metabolizing the lipid peroxidation product 4-hydroxynonenal. *Aging Cell* 4(5). 2005, pp. 257-271.
169. **Ayyadevara S, Dandapat A, Singh S P, Siegel E R, Shmookler Reis R J, Zimniak L, Zimniak P.** Life span and stress resistance of *Caenorhabditis elegans* are differentially affected by glutathione transferases metabolizing 4-hydroxynon-2-enal. *Mech Ageing Dev* 128(2). 2007, pp. 196-205.
170. **Bardag-Gorce F, Li J, French B A, French S W.** The effect of ethanol-induced CYP2E1 on proteasome activity: the role of 4-hydroxynonenal. *Exp Mol Pathol* 78(2). 2005, pp. 109-115.
171. **Hill B G, Haberzettl P, Ahmed Y, Srivastava S, Bhatnagar A.** Unsaturated lipid peroxidation-derived aldehydes activate autophagy in vascular smooth-muscle cells. *Biochem J* 410(3). 2008, pp. 525-534.
172. **Zerangue N, Malan M J, Fried S R, Dazin P F, Jan YN, Jan L Y, Schwappach B.** Analysis of endoplasmic reticulum trafficking signals by combinatorial screening in mammalian cells. *Proc Natl Acad Sci U S A* 98(5). 2001, pp. 2431-2436.

173. **Otte S, Belden W J, Heidtman M, Liu J, Jensen O N, Barlowe C.** Erv41p and Erv46p: new components of COPII vesicles involved in transport between the ER and Golgi complex. *J Cell Biol* 152(3). 2001, pp. 503-518.
174. **Belden W J, Barlowe C.** Role of Erv29p in Collecting Soluble Secretory Proteins into ER-Derived Transport Vesicles. *Science* 294. 2001, pp. 1528-1531.
175. **Mitrovic S, Ben-Tekaya H, Koegler E, Gruenberg J, Hauri H P.** The cargo receptors Surf4, endoplasmic reticulum-Golgi intermediate compartment (ERGIC)-53, and p25 are required to maintain the architecture of ERGIC and Golgi. *Mol Bio Cell* 19(5). 2008, pp. 1976-1990.
176. **Armes N, Fried M.** Surfeit Locus Gene Homologs Are Widely Distributed in Invertebrate Genomes. *Mol Cel Biol* 16(10). 1996, pp. 5591-5596.
177. **Haynes C M, Caldwell S, Cooper A A.** An HRD/DER-independent ER quality control mechanism involves Rsp5p-dependent ubiquitination and ER-Golgi transport. *J Cell Biol* 158. 2002, pp. 91-101.
178. **Brock T G, Maydanski E, McNish R W, Peters-Golden M.** Co-localization of leukotriene a4 hydrolase with 5-lipoxygenase in nuclei of alveolar macrophages and rat basophilic leukemia cells but not neutrophils. *J Biol Chem* 276. 2001, pp. 35071-35077.
179. **Baset H A, Ford-Hutchinson A W, O'Neill G P.** Molecular cloning and functional expression of a *Caenorhabditis elegans* aminopeptidase structurally related to mammalian leukotriene A4 hydrolases. *J Biol Chem* 273(43). 1998, pp. 27978-27987.
180. **Hanson H T, Smith E L.** Carnosinase; an enzyme of swine kidney. *J Biol Chem* 179(2). 1949, pp. 789-801.
181. **Lenney J F, Peppers S C, Kucera-Orallo C M, George R P.** Characterization of human tissue carnosinase. *Biochem J* 228. 1985, pp. 653-660.
182. **Unno H, Yamashita T, Ujita S, Okumura N, Otani H, Okumura A, Nagai K, Kusunoki M.** Structural basis for substrate recognition and hydrolysis by mouse carnosinase CN2. *J Biol Chem* 283(40). 2008, pp. 27289-99.
183. **Otani H, Okumura A, Nagai K, Okumura N.** Colocalization of a carnosine-splitting enzyme, tissue carnosinase (CN2)/cytosolic non-specific dipeptidase 2 (CNDP2), with histidine decarboxylase in the tuberomammillary nucleus of the hypothalamus. *Neurosci Lett* 445(2). 2008, pp. 166-169.
184. **Scornik O A, Botbol V.** Bestatin as an experimental tool in mammals. *Curr Drug Metab* 2(1). 2001, pp. 67-85.

185. **Dibble CC, Asara JM, Manning BD.** Characterization of Rictor phosphorylation sites reveals direct regulation of mTOR complex 2 by S6K1. *Mol Cell Biol* 29(21). 2009, 5657-70.
186. **Soukas A A, Kane E A, Carr C E, Melo J A, Ruvkun G.** Rictor/TORC2 regulates fat metabolism, feeding, growth, and life span in *Caenorhabditis elegans*. *Genes Dev* 23(4). 2009, pp. 496-511.
187. **Jones K T, Greer E R, Pearce D, Ashrafi K.** Rictor/TORC2 regulates *Caenorhabditis elegans* fat storage, body size, and development through *sgk-1*. *PLoS Biol* 7(3). 2009, p. e60.
188. **Pan K Z, Palter J E, Rogers A N, Olsen A, Chen D, Lithgow G J, Kapahi P.** Inhibition of mRNA translation extends lifespan in *Caenorhabditis elegans*. *Aging Cell* 6(1). 2007, pp. 111-119.
189. **Long X, Spycher C, Han Z S, Rose A M, Müller F, Avruch J.** TOR deficiency in *C. elegans* causes developmental arrest and intestinal atrophy by inhibition of mRNA translation. *Curr Biol* 12(17). 2002, pp. 1448-1461.
190. **Jia K, Chen D, Riddle D L.** The TOR pathway interacts with the insulin signaling pathway to regulate *C. elegans* larval development, metabolism and life span. *Development* 131(16). 2004, pp. 3897-3906.
191. **H., Daniel.** Molecular and integrative physiology of intestinal peptide transport. *Annu Rev Physiol*. 361-84.
192. **Goberdhan DC, Ogmundsdóttir MH, Kazi S, Reynolds B, Visvalingam SM, Wilson C, Boyd CA.** Amino acid sensing and mTOR regulation: inside or out? *Biochem Soc Trans* 37(Pt 1). 2009, 248-52.
193. **Makky K, Tekiela J, Mayer AN.** Target of rapamycin (TOR) signaling controls epithelial morphogenesis in the vertebrate intestine. *Dev Biol* 303(2). 2007, 501-13.
194. **Rhoads JM, Niu X, Odle J, Graves LM.** Role of mTOR signaling in intestinal cell migration. *Am J Physiol Gastrointest Liver Physiol* 291(3). 2006, G510-7.
195. **Ban H, Shigemitsu K, Yamatsuji T, Haisa M, Nakajo T, Takaoka M, Nobuhisa T, Gunduz M, Tanaka N, Naomoto Y.** Arginine and Leucine regulate p70 S6 kinase and 4E-BP1 in intestinal epithelial cells. *Int J Mol Med* 13(4). 2004, 537-43.
196. **Sakiyama T, Musch MW, Ropeleski MJ, Tsubouchi H, Chang EB.** Glutamine increases autophagy under Basal and stressed conditions in intestinal epithelial cells. *Gastroenterology* 163(3). 2009, 924-32.

197. **Marc Rhoads J, Wu G.** Glutamine, arginine, and leucine signaling in the intestine. *Amino Acids* 37(1). 2009, 111-22.
198. **Kamath R S, Ahringer J.** Genome-wide RNAi screening in *Caenorhabditis elegans*. *Methods* 30. 2003, pp. 313-321.
199. **Ramakers C, Ruijter J M, Deprez R H, Moorman A F.** Assumption-free analysis of quantitative real-time polymerase chain reaction (PCR) data. *Neurosci Lett* 339(1). 2003, pp. 62-66.
200. **Muller P Y, Janovjak H, Miserez A R, Dobbie Z.** Processing of gene expression data generated by quantitative real-time RT-PCR. *Biotechniques* 32(6). 2002 , pp. 1372-1378.
201. **McKay R M, McKay J P, Avery L, Graff J M.** *C. elegans*: a model for exploring the genetics of fat storage. *Dev Cell* 4(1). 2003, pp. 131-142.
202. **Shanker G, Aschner J L, Syversen T, Aschner M.** Free radical formation in cerebral cortical astrocytes in culture induced by methylmercury. *Brain Res Mol Brain Res* 128(1). 2004, pp. 48-57.
203. **Rahman I, Kode A, Biswas S K.** Assay for quantitative determination of glutathione and glutathione disulfide levels using enzymatic recycling method. *Nat Protoc* 1(6). 2006, pp. 3159-3165.
204. **Sijen T, Fleenor J, Simmer F, Thijssen K L, Parrish S, Timmons L, Plasterk R H, Fire A.** On the role of RNA amplification in dsRNA-triggered gene silencing. *Cell* 107(4). 2001, 465-76.
205. **Takiff H E, Chen S-M, Court D L.** Genetic analysis of the *rnc* operon of *E. coli*. *J. Bacteriol.* 171. 1989, pp. 2581-2590.

8. Appendix

8.1. Index of figures

Figure 1: <i>Caenorhabditis elegans</i> hermaphrodite and male	14
Figure 2: Life cycle of a <i>C. elegans</i> hermaphrodite.....	15
Figure 3: Cross-section of <i>C. elegans</i> intestine	16
Figure 4: Mammalian intestinal heteromeric and proton-coupled amino acid and peptide transporters	19
Figure 5: Interaction of different pathways with the TOR pathway	25
Figure 6: Relative amino acid content of <i>pept-1(lg601) C. elegans</i>	29
Figure 7: Brood size of HAT heavy subunit deficient <i>C. elegans</i>	31
Figure 8: Brood size of <i>pept-1(lg601)</i> worms with RNAi double knockdown of HAT subunits.....	32
Figure 9: PEPT-1 protein expression in <i>C. elegans</i> with HSHAT knockout	33
Figure 10: ATGP-1 and ATGP-2 protein expression in <i>C. elegans</i> with HSHAT knockout.....	33
Figure 11: Amino acid content of <i>atgp-1</i> and <i>atgp-2 C. elegans</i> relative to wild type	34
Figure 12: Total GSH and GSSG content of wild type and <i>atgp-2(ok352) C. elegans</i>	35
Figure 13: Functionality of <i>aat-4</i> and <i>aat-9</i> RNAi	36
Figure 14: Brood size of <i>pept-1(lg601) C. elegans</i> with RNAi of LSHAT subunits	37
Figure 15: Brood size of <i>rrf-3(pk1426) C. elegans</i> treated with RNAi of <i>aat-5</i> , <i>aat-6</i> and <i>aat-7</i> LSHAT subunits	38
Figure 16: Brood size of <i>pept-1(lg601) C. elegans</i> treated with RNAi of PAT homologues	39
Figure 17: Brood size of <i>rrf-3(pk1426) C. elegans</i> treated with Y4C6B.2 RNAi ..	39
Figure 18: Functionality of <i>aat-6</i> and Y4C6B.2 RNAi	40
Figure 19: Development of <i>pept-1(lg601)</i> worms on diluted <i>aat-6</i> and Y4C6B.2 RNAi bacteria	42
Figure 20: Brood size of <i>pept-1(lg601)</i> worms treated with diluted <i>aat-6</i> and Y4C6B.2 RNAi	43

Figure 21: Influence of amino acid supplementation on development of <i>pept-1(lg601) C. elegans</i> treated with <i>aat-6</i> and Y4C6B.2 RNAi.....	44
Figure 22: Influence of amino acid supplementation on the number of progeny .	45
Figure 23: PEPT-1 protein level in an <i>aat-6</i> (RNAi) background	46
Figure 24: ATGP-1 and ATGP-2 protein levels in an <i>aat-6</i> (RNAi) background ...	46
Figure 25: β -Ala-Lys-AMCA staining in worms after RNAi silencing of selected genes.....	49
Figure 26: Sudan Black B staining after RNAi silencing of putative regulator genes.....	51
Figure 27: BODIPY-C12 uptake after RNAi silencing of putative PEPT-1 regulator genes.....	52
Figure 28: Development and brood size of worms treated with RNAi of preselected PEPT-1 modulators.....	55
Figure 29: Extended reproduction period in C54H2.5(RNAi) treated <i>C. elegans</i>	56
Figure 30: <i>pept-1</i> promoter activity of worms treated with RNAi of preselected PEPT-1 modulators	57
Figure 31: <i>pept-1</i> mRNA expression of worms treated with RNAi of preselected PEPT-1 modulators	58
Figure 32: PEPT-1 expression is altered by gene silencing of the modulators....	59
Figure 33: ATGP-1 protein expression of worms treated with RNAi of preselected PEPT-1 modulators	60
Figure 34: Mitochondrial ROS load of worms treated with RNAi of preselected PEPT-1 modulators	62
Figure 35: Enzymatic scavenging mechanisms of reactive oxygen species	63
Figure 36: Glutathione homeostasis of worms treated with RNAi of preselected PEPT-1 modulators	64
Figure 37: Stress resistance of worms treated with RNAi of preselected PEPT-1 modulators.....	65
Figure 38: ATGP-2 and PGP-2 protein levels in a C54H2.5(RNAi) background .	66
Figure 39: Effect of amastatin/bestatin on dipeptide uptake and PEPT-1 protein level.....	68
Figure 40: Effect of a free amino acid supplementation on dipeptide uptake and PEPT-1 protein levels.....	69

Figure 41: Impaired TOR signalling alters dipeptide uptake and PEPT-1 protein levels.....	71
Figure 42: Schema for the catalytic cycle of GPx4.....	80
Figure 43: Degradation of misfolded proteins via the HIP pathway.....	84
Figure 44: Postulated interaction of TORC2 and PEPT-1 in <i>C. elegans</i>	88
Figure 45: Postulated mechanisms by which increased levels of 4-HNE may alter PEPT-1 presence in the apical membrane.....	89
Figure 46: Putative role of cellular aminopeptidases on PEPT-1 and TORC2 signalling	90
Figure 48: tGSH standard curve for 5 and 10 minutes.....	104
Figure 49: GSSG standard curve for 5 and 10 minutes	105

8.2. Index of tables

Table 1: Heteromeric amino acid transporters	18
Table 2: Significant results obtained in the β -Ala-Lys-AMCA uptake screen	48
Table 3: List of genes that when silenced altered β -Ala-Lys-AMCA absorption..	50
Table 4: <i>C. elegans</i> strains	106
Table 5: <i>E. coli</i> strains.....	106
Table 6: Used RNAi bacteria for amino acid homeostasis investigations	107
Table 7: Chemicals and reagents	107
Table 8: Kits.....	108
Table 9: Buffers and media for general <i>C. elegans</i> handling	109
Table 10: Buffers and media for molecular biological techniques	110
Table 11: Buffers and media for proteobiochemical methods	111
Table 12: Buffers and media for other experiments	112
Table 13: Oligonucleotides	113
Table 14: Antibodies	114
Table 15: Instruments	114
Table 16: All absolute fluorescence values of the controls used for each β -Ala-Lys-AMCA uptake experiment.....	138
Table 17: Supplementary results of the β -Ala-Lys-AMCA uptake screen	147

8.3. Abbreviations

°C	degree celcius
µg	microgram
µl	microliter
µM	micromolar
A	amperage
<i>aat</i>	amino acid transporter light subunit
<i>atgp</i>	amino acid transporter glycoprotein subunit
BODIPY-C12	4,4-difluoro-5-methyl-4-bora-3a,4a-diaza-3-indacene-dodecanoic acid
bp	base pairs
<i>C. elegans</i>	<i>Caenorhabditis elegans</i>
ccpm	corrected counts per minute
cDNA	complementary DNA
COG	clusters of orthologous groups
<i>D. melanogaster</i>	<i>Drosophila melanogaster</i>
dsRNA	double-stranded RNA
DTNB	2,2'-dinitro-5,5'-dithio-dibenzoic acid
DTT	Dithiothreitol
<i>E. coli</i>	<i>Escherichia coli</i>
e.g.	for example
EDTA	ethylenediaminetetraacetic acid
ER	endoplasmatic reticulum
GFP	green fluorescent protein
GPx	glutathione peroxidase
GTR	glutathione reductase
HAT	heteromeric amino acid transporter
HSAT	HAT heavy subunit
IPTG	Isopropyl-β-D-thiogalactopyranosid
kDa	kilo Dalton
LSAT	HAT light subunit
ml	milliliter
mM	millimolar
mRNA	messenger ribonucleic acid
NGM	nematode growth medium
<i>nhx</i>	sodium-proton exchanger
PAT	proton-assisted amino acid transporter
PCR	polymerase chain reaction
<i>pept</i>	peptide transporter
RNA	ribonucleic acid

RNAi	RNA interference
RNAi	RNA interference
ROS	reactive oxygen species
rpm	rounds per minute
<i>rrf-3</i>	RNA-dependent RNA polymerase family
RT-PCR	reverse transcribed PCR
<i>S. cerevisiae</i>	<i>Saccharomyces cerevisiae</i>
SDS-PAGE	Sodium Dodecyl Sulfate Polyacrylamide Gel Electrophoresis
SDS-PAGE	SDS-polyacrylamide-gel electrophoresis
siRNA	short interfering RNA
SLC	solute carrier
vc	vector control
X-Gal	5-bromo-4-chloro-3-indolyl- β -D-galactoside
β -Ala-Lys-AMCA	β -Ala-Lys-N ϵ -7-amino-4-methylcoumarin-3-acetic acid

8.4. Supplementary data

8.4.1. Absolute fluorescence values of the controls of the β -Ala-Lys-AMCA screen

Table 16: All absolute fluorescence values of the controls used for each β -Ala-Lys-AMCA uptake experiment

Fluorescence	control <i>rff-3;vc</i> (RNAi)				control <i>pept-1;vc</i> (RNAi)				control <i>rff-3;pept-1</i> (RNAi)				control <i>rff-3;vc</i> (RNAi) without β -Ala-Lys-AMCA					
	well 1	well 2	well 3	well 4	well 1	well 2	well 3	well 4	well 1	well 2	well 3	well 4	well 1	well 2	well 1	well 2	well 1	well 2
experiment 1	0,7846	0,8033	1,102	0,8519	0,1517	0,1713	0,16	0,2708	0,1577	0,1874	0,1372	0,1182	0,1028	0,2113				
iteration 1	0,646	0,6942	0,8818	0,7633	0,1361	0,1446	0,17	0,2483	0,11	0,1779	0,1363	0,108	0,103	0,1976				
iteration 2	0,7986	0,6737	0,9417	0,5932	0,1608	0,2195	0,1879	0,2097	0,1308	0,1985	0,1508	0,1298	0,1076	0,2062				
iteration 3	0,6971	0,621	0,9504	0,6429	0,1322	0,1934	0,1575	0,2309	0,0859	0,162	0,1271	0,1195	0,1114	0,1801				
iteration 4	0,6604	0,8584	1,033	0,5901	0,152	0,1458	0,2095	0,2411	0,0986	0,1721	0,1432	0,1371	0,1111	0,1932				
iteration 5	0,8045	0,7722	1,133	0,648	0,1271	0,1911	0,1649	0,1972	0,1206	0,1461	0,1378	0,1188	0,1103	0,1682				
iteration 6	0,758	0,6894	1,198	0,7573	0,1293	0,1552	0,1921	0,2164	0,1371	0,167	0,1509	0,1108	0,1063	0,1816				
iteration 7	0,8133	0,6775	1,234	0,6796	0,1593	0,129	0,2144	0,2266	0,0973	0,1585	0,1138	0,1271	0,1023	0,1694				
iteration 8	0,8743	0,6451	1,109	0,8745	0,1455	0,1455	0,1782	0,2928	0,0918	0,1568	0,1115	0,1221	0,106	0,1897				
iteration 9	0,7063	0,6169	1,173	0,7706	0,1267	0,1241	0,2038	0,1954	0,0926	0,1699	0,1274	0,1182	0,1037	0,1628				
iteration 10																		
experiment 2																		
iteration 1	0,5986	0,5298	0,7566	0,7424	0,2967	0,2279	0,1878	0,1562	0,1422	0,1328	0,1379	0,129	0,1037	0,243				
iteration 2	0,4038	0,5423	0,5893	0,6385	0,2328	0,128	0,1665	0,1203	0,1265	0,1801	0,1397	0,1087	0,1678	0,1993				
iteration 3	0,461	0,4364	0,3785	0,5407	0,2474	0,2323	0,1757	0,1555	0,1017	0,2068	0,1652	0,1291	0,1263	0,2158				
iteration 4	0,4348	0,4202	0,4264	0,444	0,2094	0,1986	0,2025	0,1491	0,1182	0,1772	0,151	0,1307	0,1203	0,2129				
iteration 5	0,3943	0,48	0,3379	0,4554	0,2117	0,1599	0,1599	0,1585	0,0977	0,1696	0,1728	0,1428	0,1039	0,2592				
iteration 6	0,5599	0,3471	0,3382	0,4601	0,1804	0,2575	0,181	0,1282	0,0775	0,1505	0,1539	0,1218	0,1267	0,214				
iteration 7	0,455	0,5377	0,6675	0,6437	0,1921	0,1686	0,1753	0,1455	0,1055	0,165	0,1595	0,1323	0,1153	0,269				
iteration 8	0,4257	0,3332	0,4831	0,6657	0,1817	0,199	0,1941	0,1579	0,1161	0,1722	0,1774	0,1272	0,1256	0,2182				
iteration 9	0,3559	0,4497	0,6662	0,5352	0,153	0,1275	0,2205	0,1658	0,0952	0,1614	0,2017	0,1395	0,1077	0,3053				
iteration 10	0,5059	0,4278	0,6091	0,5418	0,1637	0,1962	0,1824	0,1872	0,0807	0,1571	0,177	0,1699	0,1177	0,2727				

	control <i>rrf-3;vc</i> (RNAi)	control <i>pept-1;vc</i> (RNAi)	control <i>rrf-3;pept-1</i> (RNAi)	control <i>rrf-3;vc</i> (RNAi) without β -Ala-Lys-AMCA									
experiment 3													
iteration 1	1,017	0,9214	0,8546	1,217	0,1648	0,1903	0,2052	0,1294	0,137	0,3641	0,2866	0,1553	0,1719
iteration 2	0,9264	1,095	0,8961	0,9057	0,1306	0,1815	0,208	0,1892	0,1388	0,3816	0,3004	0,2176	0,2506
iteration 3	0,9608	0,6529	0,9557	0,8988	0,1335	0,1763	0,2143	0,1802	0,1362	0,407	0,2924	0,2352	0,2313
iteration 4	1,166	0,6465	1,139	0,8574	0,1853	0,2012	0,1554	0,1657	0,1407	0,3446	0,3648	0,2057	0,1978
iteration 5	1,033	0,7397	1,025	0,9323	0,1757	0,227	0,1953	0,1337	0,1382	0,4666	0,333	0,2487	0,2928
iteration 6	1,006	0,8851	1,264	1,128	0,1655	0,2088	0,1139	0,1607	0,142	0,3582	0,3815	0,268	0,2037
iteration 7	1,034	0,8614	1,384	0,9401	0,1613	0,1868	0,1426	0,1831	0,1422	0,3153	0,3799	0,2317	0,2268
iteration 8	1,094	1,086	1,353	1,221	0,1529	0,1982	0,1817	0,1692	0,1312	0,3468	0,386	0,2458	0,2383
iteration 9	1,145	0,9261	1,291	1,161	0,1554	0,1947	0,1921	0,1419	0,1408	0,3393	0,3394	0,2256	0,2343
iteration 10	0,945	0,7847	0,9798	1,199	0,1857	0,2132	0,1791	0,1553	0,1381	0,3614	0,4586	0,2336	0,2659
experiment 4													
iteration 1	1,127	0,5555	0,8893	0,1918	0,1556	0,1462	0,2014	0,1339	0,1783	0,1466	0,1475	0,0945	0,1054
iteration 2	1,141	0,5416	0,7387	0,1659	0,1887	0,1313	0,2287	0,1552	0,1801	0,1442	0,1156	0,0926	0,0907
iteration 3	0,8957	0,531	0,819	0,1978	0,2116	0,1316	0,2153	0,1513	0,1445	0,1398	0,1312	0,1041	0,1187
iteration 4	0,8602	0,5859	0,8287	0,1735	0,1828	0,1368	0,233	0,1441	0,1589	0,1332	0,1287	0,1023	0,1019
iteration 5	0,9368	0,624	0,9104	0,1646	0,1617	0,1283	0,2412	0,1321	0,1449	0,174	0,1707	0,0979	0,0974
iteration 6	0,9673	0,6497	1,078	0,1702	0,1251	0,1248	0,2343	0,1251	0,1914	0,1116	0,12	0,0976	0,0885
iteration 7	0,8815	0,7371	0,8917	0,159	0,1344	0,1371	0,3076	0,1762	0,1591	0,1414	0,1568	0,0914	0,0958
iteration 8	0,9382	0,6449	0,7446	0,2009	0,1182	0,1514	0,2775	0,1525	0,1713	0,1532	0,1616	0,1038	0,0903
iteration 9	1,013	0,5333	0,9344	0,1912	0,1388	0,1337	0,3431	0,1776	0,1692	0,1466	0,1792	0,1007	0,104
iteration 10	0,8889	0,7371	0,8218	0,1944	0,1276	0,1355	0,2987	0,1751	0,1636	0,1521	0,1443	0,0993	0,0869

Fluorescence	control <i>rff-3;vc</i>(RNAi)		control <i>pept-1;vc</i>(RNAi)		control <i>rff-3;pept-1</i>(RNAi)		control <i>rff-3;vc</i>(RNAi) without β-Ala-Lys-AMCA							
experiment 5														
iteration 1	0,7007	1,337	1,213	0,956	0,294	0,3035	0,276	0,4299	0,2005	0,1834	0,2246	0,2169	0,0666	0,0317
iteration 2	0,7283	1,504	1,054	1,217	0,3183	0,2716	0,2744	0,4274	0,1801	0,2069	0,2247	0,2212	0,0687	0,0305
iteration 3	0,8568	1,173	1,106	1,21	0,2938	0,3293	0,2431	0,4651	0,1871	0,2287	0,1915	0,1798	0,0703	0,0289
iteration 4	0,9127	1,609	1,068	0,7001	0,3125	0,3021	0,2754	0,4212	0,2221	0,2684	0,1857	0,2094	0,0695	0,0321
iteration 5	0,9808	0,8597	0,8812	0,853	0,3209	0,2816	0,262	0,4593	0,1959	0,2061	0,1927	0,2669	0,072	0,0323
iteration 6	0,8889	0,9914	0,7582	0,9792	0,3368	0,2668	0,2588	0,5098	0,1884	0,213	0,1622	0,2241	0,0698	0,0289
iteration 7	0,8044	1,13	1,382	1,022	0,3383	0,2862	0,2524	0,4841	0,2082	0,1987	0,1798	0,2245	0,0707	0,0304
iteration 8	0,5904	0,9188	1,216	0,7197	0,37	0,2842	0,26	0,4658	0,1837	0,2046	0,185	0,2084	0,0723	0,0305
iteration 9	0,7038	1,213	1,041	0,7754	0,3448	0,3186	0,2525	0,4691	0,2003	0,1811	0,1882	0,2452	0,0708	0,032
iteration 10	0,6593	1,268	0,9652	0,8836	0,354	0,3254	0,2587	0,4321	0,1926	0,2135	0,2205	0,3824	0,0706	0,0336
experiment 6														
iteration 1	0,6548	0,5153	0,9162	0,5778	0,3004	0,2273	0,2309	0,2245	0,2395	0,1686	0,196	0,1819	0,2814	
iteration 2	0,781	0,5488	0,773	0,6394	0,253	0,2676	0,2526	0,178	0,2401	0,1695	0,1848	0,1868	0,2573	
iteration 3	0,823	0,5153	0,8647	0,4429	0,2511	0,2072	0,2943	0,1938	0,2324	0,1625	0,1755	0,1686	0,2626	
iteration 4	0,6178	0,5036	0,6581	0,4155	0,2856	0,2504	0,2533	0,263	0,2374	0,1513	0,2033	0,1549	0,2206	
iteration 5	0,6464	0,3712	0,7539	0,4754	0,2375	0,2542	0,2805	0,2672	0,2358	0,16	0,2151	0,1554	0,2348	
iteration 6	0,5056	0,4829	0,896	0,5071	0,2357	0,205	0,3223	0,3128	0,2545	0,1792	0,1923	0,1673	0,264	
iteration 7	0,6203	0,5383	0,9223	0,5224	0,2792	0,2341	0,2711	0,2655	0,2368	0,1962	0,2094	0,1705	0,2215	
iteration 8	0,7831	0,5219	0,603	0,4522	0,2643	0,1974	0,235	0,2933	0,2185	0,1752	0,1871	0,1838	0,2688	
iteration 9	0,5392	0,4628	0,5939	0,5821	0,2325	0,2106	0,3005	0,2707	0,2288	0,1943	0,1979	0,1924	0,2783	
iteration 10	0,7575	0,4431	0,7289	0,6658	0,26	0,2513	0,3309	0,2452	0,2206	0,191	0,2025	0,1875	0,2744	

Fluorescence	control <i>rff-3;vc</i>(RNAi)	control <i>pept-1;vc</i>(RNAi)	control <i>rff-3;pept-1</i>(RNAi)	control <i>rff-3;vc</i>(RNAi) without β-Ala-Lys-AMCA										
experiment 7														
iteration 1	0,499	0,5465	0,5098	0,7578	0,2026	0,263	0,371	0,1632	0,265	0,2466	0,492	0,5103	0,3188	0,226
iteration 2	0,5708	0,5735	0,4243	0,6963	0,1918	0,278	0,33	0,2022	0,2513	0,2783	0,5648	0,6593	0,3883	0,1931
iteration 3	0,6563	0,5415	0,4833	0,6698	0,169	0,2334	0,328	0,1861	0,2489	0,3033	0,5183	0,5003	0,2613	0,2214
iteration 4	0,5208	0,6155	0,4078	0,6428	0,2318	0,2134	0,3255	0,193	0,332	0,246	0,5295	0,3768	0,2688	0,2258
iteration 5	0,5385	0,5785	0,4578	0,7203	0,192	0,2241	0,301	0,1917	0,3015	0,3043	0,5605	0,5498	0,3458	0,2214
iteration 6	0,5585	0,5893	0,5775	0,673	0,1724	0,213	0,3845	0,191	0,29	0,264	0,4933	0,4665	0,2878	0,2605
iteration 7	0,7163	0,4488	0,5208	0,6145	0,2061	0,1905	0,3555	0,219	0,3228	0,2259	0,5593	0,4638	0,3443	0,2445
iteration 8	0,5355	0,5808	0,4315	0,6425	0,254	0,2289	0,3628	0,1718	0,2495	0,2913	0,542	0,467	0,3185	0,2475
iteration 9	0,4895	0,5283	0,4308	0,7005	0,2508	0,2477	0,3353	0,2312	0,2918	0,3195	0,5858	0,524	0,2813	0,2261
iteration 10	0,4458	0,6468	0,4958	0,6218	0,2663	0,2323	0,3153	0,2528	0,2723	0,237	0,5478	0,5248	0,3055	0,2387
experiment 8														
iteration 1	0,6192	0,7096	1,0256	0,6788	0,1425	0,1074	0,1105	0,3928	0,2176	0,3406	0,327	0,177	0,0519	0,091
iteration 2	0,6258	0,7152	0,9912	1,05	0,1345	0,1137	0,1061	0,3778	0,2088	0,2296	0,349	0,202	0,0516	0,0983
iteration 3	0,3736	0,9392	0,9656	0,9486	0,1475	0,0956	0,1124	0,395	0,2378	0,2234	0,2466	0,1997	0,0467	0,095
iteration 4	0,596	0,6572	0,8678	0,9166	0,1701	0,0891	0,1101	0,3914	0,2258	0,2348	0,2756	0,1515	0,0524	0,0976
iteration 5	0,4796	0,751	0,8662	0,9886	0,1812	0,1179	0,1027	0,3986	0,236	0,2502	0,4374	0,148	0,0543	0,0997
iteration 6	0,5222	0,8114	0,6156	0,9568	0,1455	0,098	0,13	0,396	0,2388	0,2064	0,3662	0,1509	0,0538	0,1024
iteration 7	0,513	0,5054	0,7642	0,994	0,1473	0,1196	0,1072	0,4048	0,2238	0,2376	0,2646	0,2784	0,051	0,0972
iteration 8	0,6886	0,692	0,6862	0,8322	0,1786	0,1108	0,1236	0,4056	0,1938	0,2806	0,305	0,3152	0,0526	0,1004
iteration 9	0,7434	0,6674	0,8168	0,8834	0,1775	0,0957	0,1228	0,3898	0,2098	0,2364	0,294	0,2322	0,0464	0,0955
iteration 10	0,6306	0,5372	0,6344	0,9002	0,1568	0,0963	0,0824	0,3878	0,1801	0,2596	0,3236	0,2014	0,0474	0,0985

Fluorescence	control <i>rff-3;vc</i>(RNAi)	control <i>pept-1;vc</i>(RNAi)	control <i>rff-3;pept-1</i>(RNAi)	control <i>rff-3;vc</i>(RNAi) without β-Ala-Lys-AMCA										
experiment 9														
iteration 1	0,6728	0,8352	1,3756	0,8976	0,0984	0,1459	0,1273	0,1225	0,4528	0,5766	0,5474	0,2562	0,203	
iteration 2	0,5588	0,652	1,1104	0,965	0,0968	0,196	0,1035	0,0994	0,4458	0,5954	0,5352	0,2764	0,202	
iteration 3	0,5808	0,8958	1,1564	0,9208	0,1084	0,1765	0,141	0,0964	0,503	0,5432	0,557	0,2772	0,2112	
iteration 4	0,6068	0,7634	1,0696	0,6494	0,1165	0,1485	0,0914	0,0916	0,473	0,5442	0,5244	0,2886	0,2048	
iteration 5	0,6238	0,712	0,848	0,9822	0,1365	0,2632	0,1593	0,1159	0,5124	0,5334	0,5498	0,272	0,2088	
iteration 6	0,463	0,563	1,2932	0,9562	0,113	0,212	0,1146	0,0946	0,4746	0,5474	0,5528	0,2762	0,2042	
iteration 7	0,4986	0,677	0,885	1,0192	0,1387	0,1884	0,1077	0,1104	0,4516	0,5482	0,5548	0,2786	0,2114	
iteration 8	0,7684	0,6708	0,9502	0,9724	0,1093	0,19	0,1131	0,1116	0,4578	0,5418	0,5686	0,2726	0,2	
iteration 9	0,5778	0,816	0,966	1,043	0,1156	0,267	0,1301	0,104	0,4618	0,5464	0,517	0,2782	0,2084	
iteration 10	0,5616	0,7304	0,8632	0,8548	0,1073	0,1364	0,15	0,0869	0,4716	0,556	0,5552	0,2724	0,206	
experiment 10														
iteration 1	0,5046	0,6264	1,0317	0,6732	0,0738	0,1094	0,0955	0,0918	0,3396	0,4325	0,4106	0,1922	0,1523	
iteration 2	0,4191	0,489	0,8328	0,7238	0,0726	0,147	0,0776	0,0745	0,3344	0,4466	0,4014	0,2073	0,1515	
iteration 3	0,4356	0,6719	0,8673	0,6906	0,0813	0,1323	0,1058	0,0723	0,3773	0,4074	0,4178	0,2079	0,1584	
iteration 4	0,4551	0,5726	0,8022	0,4871	0,0873	0,1114	0,0686	0,0687	0,3548	0,4082	0,3933	0,2165	0,1536	
iteration 5	0,4679	0,534	0,636	0,7367	0,1024	0,1974	0,1195	0,0869	0,3843	0,4001	0,4124	0,204	0,1566	
iteration 6	0,3473	0,4223	0,9699	0,7172	0,0848	0,159	0,0859	0,0709	0,356	0,4106	0,4146	0,2072	0,1532	
iteration 7	0,374	0,5078	0,6638	0,7644	0,104	0,1413	0,0807	0,0828	0,3387	0,4112	0,4161	0,209	0,1586	
iteration 8	0,5763	0,5031	0,7127	0,7293	0,082	0,1425	0,0848	0,0837	0,3434	0,4064	0,4265	0,2045	0,15	
iteration 9	0,4334	0,612	0,7245	0,7823	0,0867	0,2003	0,0976	0,078	0,3464	0,4098	0,3878	0,2087	0,1563	
iteration 10	0,4212	0,5478	0,6474	0,6411	0,0805	0,1023	0,1125	0,0652	0,0352	0,3537	0,417	0,4164	0,2043	0,1545

Fluorescence	control <i>rff-3;vc</i>(RNAi)	control <i>pept-1;vc</i>(RNAi)	control <i>rff-3;pept-1</i>(RNAi)	control <i>rff-3;vc</i>(RNAi) without β-Ala-Lys-AMCA									
experiment 11													
iteration 1	1,017	0,8579	0,9682	0,8852	0,2263	0,2868	0,1311	0,2985	0,2904	0,21	0,3515	0,2089	0,2708
iteration 2	0,89	0,7642	0,7456	0,9098	0,2208	0,2776	0,1193	0,2991	0,2614	0,2332	0,349	0,1962	0,2813
iteration 3	1,401	0,8033	0,5512	0,8024	0,2195	0,2671	0,1102	0,2766	0,2719	0,2179	0,3789	0,2188	0,2559
iteration 4	1,703	0,7834	0,7525	0,7829	0,2139	0,2818	0,1385	0,2376	0,2684	0,2578	0,3878	0,1772	0,2336
iteration 5	1,5	0,8581	0,7264	0,8168	0,2001	0,279	0,1352	0,2239	0,256	0,2956	0,3629	0,1869	0,2306
iteration 6	1,914	0,7434	0,7667	0,7206	0,174	0,2692	0,1127	0,2123	0,2526	0,2727	0,3488	0,229	0,209
iteration 7	1,409	0,7421	0,8153	0,6601	0,1534	0,2592	0,0849	0,2131	0,2869	0,3003	0,3144	0,2149	0,2265
iteration 8	1,2	0,8136	0,8467	0,6553	0,1425	0,2486	0,0871	0,2087	0,2164	0,3267	0,3209	0,2061	0,2224
iteration 9	1,354	0,8376	0,9031	0,6454	0,1423	0,2428	0,0951	0,215	0,2263	0,3008	0,3277	0,2021	0,2183
iteration 10	1,246	0,8227	1,061	0,6926	0,1471	0,2444	0,0943	0,2223	0,2478	0,2988	0,3104	0,2244	0,2226
experiment 12													
iteration 1	0,68	0,617	0,4261	0,591	0,135	0,0754	0,0972	0,2002	0,1115	0,0948	0,1204	0,0995	0,0271
iteration 2	0,5824	0,5935	0,5712	0,735	0,1216	0,0751	0,098	0,1995	0,1241	0,0999	0,1012	0,1322	0,0285
iteration 3	0,6776	0,5872	0,4217	0,6265	0,1285	0,0789	0,097	0,1934	0,1104	0,0975	0,1151	0,1012	0,0269
iteration 4	0,5858	0,5481	0,3929	0,637	0,118	0,0736	0,1065	0,1929	0,1159	0,0967	0,105	0,1104	0,029
iteration 5	0,6213	0,5705	0,5134	0,5618	0,1484	0,0691	0,0967	0,1918	0,1048	0,1182	0,0992	0,1291	0,0253
iteration 6	0,6907	0,8242	0,5786	0,4712	0,1459	0,0718	0,0945	0,1931	0,1197	0,1015	0,1075	0,1114	0,0436
iteration 7	0,6971	0,5426	0,5016	0,473	0,2014	0,0814	0,1048	0,201	0,1076	0,1421	0,1169	0,1138	0,0449
iteration 8	0,7346	0,4835	0,5869	0,5059	0,1836	0,0726	0,0952	0,1925	0,1302	0,1027	0,0953	0,113	0,0459
iteration 9	0,813	0,5394	0,4913	0,5087	0,1774	0,0675	0,0899	0,2047	0,1161	0,1033	0,1097	0,1063	0,0482
iteration 10	0,7955	0,5135	0,4823	0,4843	0,2081	0,0743	0,0924	0,1959	0,1197	0,1328	0,1075	0,116	0,0439

Fluorescence		control <i>rff-3;vc</i> (RNAi)	control <i>pept-1;vc</i> (RNAi)	control <i>rff-3;pept-1</i> (RNAi)	control <i>rff-3;vc</i> (RNAi) without β -Ala-Lys-AMCA									
experiment 13														
iteration 1	0,5311	0,4707	0,6253	0,4803	0,0674	0,0646	0,0758	0,0725	0,1058	0,1049	0,1767	0,0924	0,0249	0,0264
iteration 2	0,5071	0,5234	0,5423	0,5033	0,0728	0,0696	0,0729	0,0794	0,0979	0,1037	0,1813	0,092	0,0257	0,0251
iteration 3	0,638	0,4948	0,5624	0,5548	0,0843	0,0641	0,0727	0,0856	0,0868	0,1142	0,2015	0,0979	0,0242	0,0265
iteration 4	0,5574	0,5647	0,5568	0,5829	0,1	0,0619	0,0843	0,0976	0,088	0,1087	0,1848	0,0862	0,0248	0,026
iteration 5	0,5897	0,5	0,5771	0,5947	0,0969	0,0666	0,0677	0,0718	0,0987	0,1003	0,1841	0,0958	0,023	0,027
iteration 6	0,5339	0,5045	0,5483	0,6342	0,0635	0,0741	0,0704	0,0829	0,1047	0,1178	0,178	0,0965	0,0241	0,0266
iteration 7	0,6565	0,5268	0,5618	0,4549	0,0704	0,0741	0,085	0,0918	0,0882	0,0983	0,1781	0,0941	0,0277	0,0283
iteration 8	0,4869	0,5625	0,6555	0,5173	0,0818	0,0665	0,0774	0,0863	0,1015	0,1085	0,1826	0,0886	0,0254	0,0267
iteration 9	0,517	0,632	0,5678	0,5619	0,0774	0,068	0,0776	0,0741	0,1076	0,1058	0,1795	0,0916	0,0238	0,0268
iteration 10	0,535	0,5531	0,528	0,6201	0,0791	0,0716	0,0681	0,072	0,1049	0,1014	0,1957	0,097	0,1419	0,1094
experiment 14														
iteration 1	0,798	0,6556	0,5688	0,8846	0,1913	0,1566	0,2776	0,251	0,2286	0,3734	0,1868	0,5468	0,1161	0,2685
iteration 2	0,8706	0,6838	0,6014	1,035	0,1594	0,2218	0,2306	0,2054	0,225	0,311	0,1917	0,4774	0,1088	0,2257
iteration 3	0,776	0,4548	0,6966	0,7722	0,1409	0,1302	0,2422	0,2168	0,247	0,2644	0,1985	0,4918	0,1069	0,1412
iteration 4	0,7594	0,5594	0,5606	0,802	0,1546	0,1596	0,2248	0,2076	0,1838	0,3138	0,2068	0,4658	0,1099	0,1113
iteration 5	0,7012	0,4152	0,519	0,8872	0,1312	0,1272	0,2244	0,1933	0,2058	0,269	0,1901	0,6638	0,0957	0,0975
iteration 6	0,5742	0,4348	0,4556	0,889	0,1453	0,1354	0,1995	0,2716	0,1893	0,2874	0,2152	0,2754	0,1007	0,09
iteration 7	0,6788	0,6966	0,4198	0,8836	0,1163	0,15	0,2388	0,2118	0,225	0,2724	0,1994	0,4174	0,0978	0,0938
iteration 8	0,666	0,6318	0,4634	0,7764	0,1315	0,1749	0,2088	0,1952	0,2174	0,3344	0,1675	0,529	0,0933	0,0956
iteration 9	0,6146	0,5796	0,576	0,8184	0,1572	0,147	0,1929	0,2162	0,1955	0,2708	0,2006	0,5376	0,0992	0,0833
iteration 10	0,5782	0,6682	0,54	0,8	0,1608	0,1524	0,2374	0,1886	0,1803	0,3082	0,2164	0,674	0,1014	0,1621

8.4.2. Calculation of the relative β -Ala-Lys-AMCA uptake of *C. elegans* with individual RNAi gene silencing compared to control

For each control and each RNAi construct (treatment) four biological replicates (4x 20 worms per well 1 - 4) were measured at the VarioSkan ten times (ten technical replicates per well, iteration 1-10) with shaking in between.

The used controls are: *rrf-3;vc*(RNAi) worms with a normal (= 100 %) β -Ala-Lys-AMCA uptake in intestinal cells and *pept-1;vc*(RNAi) knockout worms with abolished (= 0 %) dipeptide uptake. Additionally *rrf-3;vc*(RNAi) worms were treated the same way, but without β -Ala-Lys-AMCA supplementation (auto-fluorescence). Reduced dipeptide uptake in *rrf-3;pept-1*(RNAi) worms was a control for an efficient RNAi knockdown.

In the following all calculation steps are described which were used to get a relative β -Ala-Lys-AMCA uptake of *rrf-3;pept-1*(RNAi) worms (as an example for RNAi treatment) to *rrf-3;vc*(RNAi) control.

1. Step:

For each well the mean of the 10 technical replicates (10 iterations) was calculated.

1. Step

	control <i>rrf-3;vc</i> (RNAi)				control <i>pept-1;vc</i> (RNAi)				<i>rrf-3;vc</i> (RNAi) without β -Ala- Lys-AMCA		<i>rrf-3;pept-1</i> (RNAi)			
	well 1	well 2	well 3	well 4	well 1	well 2	well 3	well 4	well 1	well 2	well 1	well 2	well 3	well 4
iteration 1	0,8846	0,5688	0,6556	0,798	0,251	0,2776	0,15656	0,19132	0,2685	0,1161	0,5468	0,18678	0,3734	0,2286
iteration 2	1,035	0,6014	0,6838	0,8706	0,2054	0,2306	0,2218	0,15944	0,2257	0,1088	0,4774	0,19168	0,311	0,225
iteration 3	0,7722	0,6966	0,4548	0,776	0,2168	0,2422	0,13024	0,14094	0,1412	0,1069	0,4918	0,19854	0,2644	0,247
iteration 4	0,802	0,5606	0,5594	0,7594	0,2076	0,2248	0,15964	0,15458	0,1113	0,1099	0,4658	0,2068	0,3138	0,18382
iteration 5	0,8872	0,519	0,4152	0,7012	0,19332	0,2244	0,12724	0,13122	0,09746	0,09569	0,6638	0,19006	0,269	0,2058
iteration 6	0,889	0,4556	0,4348	0,5742	0,2716	0,19954	0,1354	0,14534	0,08999	0,1007	0,2754	0,2152	0,2874	0,18928
iteration 7	0,8836	0,4198	0,6966	0,6788	0,2118	0,2388	0,15002	0,11628	0,09383	0,09777	0,4174	0,1994	0,2724	0,225
iteration 8	0,7764	0,4634	0,6318	0,666	0,19522	0,2088	0,17486	0,13148	0,0956	0,09328	0,529	0,16752	0,3344	0,2174
iteration 9	0,8184	0,576	0,5796	0,6146	0,2162	0,19294	0,14702	0,15722	0,08327	0,09915	0,5376	0,2006	0,2708	0,19552
iteration 10	0,8	0,54	0,6682	0,5782	0,18864	0,2374	0,15244	0,16076	0,1621	0,1014	0,674	0,2164	0,3082	0,18028
Mean	0,85484	0,54012	0,57798	0,7017	0,21576	0,22771	0,15552	0,14886	0,1369	0,10297	0,5079	0,1973	0,30048	0,20977

2. Step: Auto-fluorescence (mean of well 1 and well 2 of *rrf-3;vc*(RNAi) without β -Ala-Lys-AMCA) is subtracted from all other means.

2. Step

	control <i>rrf-3;vc</i> (RNAi)				control <i>pept-1;vc</i> (RNAi)				<i>rrf-3;vc</i> (RNAi) without β -Ala- Lys-AMCA		<i>rrf-3;pept-1</i> (RNAi)			
	well 1	well 2	well 3	well 4	well 1	well 2	well 3	well 4	well 1	well 2	well 1	well 2	well 3	well 4
Mean	0,85484	0,54012	0,57798	0,7017	0,21576	0,22771	0,15552	0,14886	0,1369	0,10297	0,5079	0,1973	0,30048	0,20977
Mean - autofluorescence	0,73491	0,42019	0,45805	0,58177	0,09583	0,10778	0,03559	0,02893	0,11993		0,38797	0,07737	0,18055	0,08984

3. Step:

We found that some RNAi treatments influenced body length of the *C. elegans*. To eliminate the impact of this factor on the fluorescence signal intensity, for each control/treatment body length of two worms per experiment was measured. The body length was related to *rrf-3;vc*(RNAi) control length and the calculated values were included.

3. Step	control <i>rrf-3;vc</i> (RNAi)				control <i>pept-1;vc</i> (RNAi)				<i>rrf-3;pept-1</i> (RNAi)			
	well 1	well 2	well 3	well 4	well 1	well 2	well 3	well 4	well 1	well 2	well 3	well 4
Mean - autofluorescence	0,73491	0,42019	0,45805	0,58177	0,09583	0,10778	0,03559	0,02893	0,38797	0,07737	0,18055	0,08984
body length [μm]	worm 1 942,6	worm 2 990,7			worm 1 699,7	worm 2 707,6			worm 1 761,4	worm 2 776,4		
mean body length	966,7				703,7				768,9			
relative body length	1				1,37				1,26			
(Mean - autofluorescence)* relative body length	0,73491	0,42019	0,45805	0,58177	0,13164	0,14806	0,04889	0,03974	0,48775	0,09726	0,22698	0,11294

4. Step:

For wells 1-4 of *pept-1;vc*(RNAi) the mean value was calculated and subtracted from each well of *rrf-3;vc*(RNAi) and the example *rrf-3;pept-1*(RNAi). The fluorescence measured for *pept-1;vc*(RNAi) displayed the remaining β -Ala-Lys-AMCA located in the gut lumen. Hence, it is possible that values might be negative after subtraction. These values were set to zero in those cases.

4. Step	control <i>rrf-3;vc</i> (RNAi)				control <i>pept-1;vc</i> (RNAi)				<i>rrf-3;pept-1</i> (RNAi)			
	well 1	well 2	well 3	well 4	well 1	well 2	well 3	well 4	well 1	well 2	well 3	well 4
(Mean - autofluorescence)* relative body length	0,73491	0,42019	0,45805	0,58177	0,13164	0,14806	0,04889	0,03974	0,48775	0,09726	0,22698	0,11294
[(Mean - autofluorescence)* relative body length] - mean <i>pept-1</i>	0,64283	0,32811	0,36597	0,48969	Mean	0,09208			0,39566	0,00518	0,1349	0,02086

5. Step:

Statistical analysis was performed using a Student's *t*-Test, because each single independent treatment (here *rrf-3;pept-1*(RNAi)) was compared with the control (*rrf-3;vc*(RNAi)).

5. Step	control <i>rrf-3;vc</i> (RNAi)				<i>rrf-3;pept-1</i> (RNAi)			
	well 1	well 2	well 3	well 4	well 1	well 2	well 3	well 4
[(Mean - autofluorescence)* relative body length] - mean <i>pept-1</i>	0,64283	0,32811	0,36597	0,48969	0,39566	0,00518	0,1349	0,02086
Student's <i>t</i> -Test					0,03265			

6. Step:

In the last step the mean of the control *rrf-3;vc(RNAi)* was calculated and each well (control and treatment) was set relative to this value. Hence, in the end we got the relative β -Ala-Lys-AMCA uptake of the RNAi treatment (here *rrf-3;pept-1(RNAi)*) \pm standard deviation compared with control *rrf-3;vc(RNAi)*.

6. Step	control <i>rrf-3;vc(RNAi)</i>				<i>rrf-3;pept-1(RNAi)</i>			
	well 1	well 2	well 3	well 4	well 1	well 2	well 3	well 4
[(Mean - autofluorescence)* relative body length] - mean <i>pept-1</i>	0,64283	0,32811	0,36597	0,48969	0,39566	0,00518	0,1349	0,02086
Mean	0,45665							
Relative to control	1,40771	0,71851	0,80142	1,07235	0,86646	0,01134	0,29541	0,04568
Mean	1				0,30473			
SD	0,31098				0,39531			

8.4.3. Entire relative results of the β -Ala-Lys-AMCA uptake screenTable 17: Supplementary results of the β -Ala-Lys-AMCA uptake screen

Cosmid number	Gene	Chromosome	Relative β -Ala-Lys-AMCA uptake	Significance
K04E7.7	<i>pept-1</i>	X	0.13 \pm 0.04	p<0.001
B0495.4	<i>nhx-2</i>	II	0.45 \pm 0.08	p<0.001
C32E8.9		I	1.25 \pm 0.32	
C34G6.4	<i>pgp-2</i>	I	1.18 \pm 0.28	
M01A10.3		I	1.12 \pm 0.28	
B0041.5		I	0.37 \pm 0.08	p<0.001
F55A12.7	<i>apm-1</i>	I	0.52 \pm 0.15	p<0.01
C24A11.8	<i>frm-4</i>	I	1.23 \pm 0.37	
T08B2.10	<i>rps-17</i>	I	0.11 \pm 0.08	p<0.001
F27D4.1		I		
K02F2.2		I	0.80 \pm 0.07	
K06A5.6		I	0.34 \pm 0.08	p<0.001
F13G3.9	<i>mif-3</i>	I	0.41 \pm 0.03	p<0.001
R11A5.4		I	0.34 \pm 0.06	p<0.001
T10B11.2		I	1.05 \pm 0.05	
W01A8.2		I	1.06 \pm 0.18	
F43G9.1		I	0.76 \pm 0.10	
F43G9.3		I	1.01 \pm 0.16	
C17E4.5	<i>papb-2</i>	I	0.66 \pm 0.11	p<0.01
F26E4.12		I	2.95 \pm 0.43	p<0.001
F46A9.5	<i>skr-1</i>	I	1.19 \pm 0.47	
F25H2.5		I	0.80 \pm 0.16	

K11D2.2	<i>asah-1</i>	I	1.07 ± 0.18	
Y25C1A.13		II	1.26 ± 0.43	
ZK430.2	<i>tag-231</i>	II	1.06 ± 0.46	
T05A7.4	<i>hmg-11</i>	II	0.78 ± 0.21	
C27D6.4		II	1.27 ± 0.19	
F28B12.2	<i>egl-44</i>	II	0.94 ± 0.29	
C17G10.5	<i>lys-8</i>	II	0.98 ± 0.15	
C18A3.6	<i>rab-3</i>	II	1.33 ± 0.25	
C32D5.2	<i>sma-6</i>	II	1.11 ± 0.30	
C32D5.9	<i>lgg-1</i>	II	1.51 ± 0.35	
T28D9.2	<i>rsp-5</i>	II	1.00 ± 0.37	
B0228.7		II	1.13 ± 0.13	
T05A6.1	<i>cki-1</i>	II	1.74 ± 0.35	
F43E2.8	<i>hsp-4</i>	II	1.20 ± 0.22	
C56C10.8	<i>icd-1</i>	II	1.23 ± 0.29	
T02G5.8	<i>kat-1</i>	II	1.71 ± 0.41	
C27H5.3		II	1.51 ± 0.35	
F54C9.7		II	0.47 ± 0.06	p<0.001
K01C8.10	<i>cct-4</i>	II	1.62 ± 0.48	
K08F8.1		II	1.76 ± 0.38	
F49E12.9		II	1.13 ± 0.17	
D2013.10	<i>tag-175</i>	II	1.45 ± 0.33	
R03D7.1		II	1.65 ± 0.30	
B0334.4		II	1.88 ± 0.34	
F52H3.3	<i>bath-38</i>	II	1.61 ± 0.28	
F35C5.6	<i>cllec-63</i>	II	0.84 ± 0.11	
F35C5.8	<i>cllec-65</i>	II	1.27 ± 0.22	
F58G1.4	<i>dct-18</i>	II	1.64 ± 0.36	
F26H11.5	<i>exl-1</i>	II	1.36 ± 0.30	
H10E21.3	<i>nhr-80</i>	III	0.88 ± 0.03	
F42G9.2	<i>cyn-6</i>	III	1.03 ± 0.15	
F23H11.5		III	0.88 ± 0.01	
C09F5.2	<i>orai-1</i>	III	0.81 ± 0.10	
C36A4.9		III	0.88 ± 0.43	
C35D10.2		III	0.86 ± 0.27	
ZC395.2	<i>clk-1</i>	III	0.75 ± 0.19	
C35D10.14	<i>cllec-5</i>	III	0.86 ± 0.21	
F26F4.6		III	0.74 ± 0.16	
B0285.3		III	1.01 ± 0.32	
F54D8.3	<i>alh-1</i>	III	0.88 ± 0.05	
R07E5.7		III	0.92 ± 0.06	
B0336.2	<i>arf-1.2</i>	III	1.25 ± 0.02	
B0336.7		III	1.14 ± 0.24	
B0280.3		III	0.89 ± 0.03	
F37C12.9	<i>rps-14</i>	III	0.39 ± 0.04	p<0.001
F01F1.2		III	0.99 ± 0.14	
F47D12.4	<i>hmg-1.2</i>	III	0.85 ± 0.06	
C16A3.10		III	0.81 ± 0.11	
C05D11.5		III	0.76 ± 0.17	

C05D11.10		III	1.44 ± 0.49	
F56C9.7		III	0.03 ± 0.02	p<0.001
K12H4.5		III	1.26 ± 0.14	
R13A5.8	<i>rpl-9</i>	III	0.37 ± 0.15	p<0.001
C30C11.2	<i>rpn-3</i>	III	0.73 ± 0.11	
ZK112.1	<i>pcp-1</i>	III	0.97 ± 0.15	
ZK652.2	<i>tomm-7</i>	III	0.90 ± 0.49	
ZK1098.10	<i>unc-16</i>	III	0.68 ± 0.21	
Y47D3B.2	<i>nlp-21</i>	III	0.85 ± 0.06	
Y76A2B.5		III	1.17 ± 0.05	
F53A2.4	<i>nud-1</i>	III	0.94 ± 0.24	
Y56A3A.18		III	0.77 ± 0.17	
Y56A3A.19		III	1.25 ± 0.13	
Y75B8A.4		III	0.76 ± 0.39	
K02D7.4	<i>dsc-4</i>	III	0.35 ± 0.08	p<0.001
Y66H1B.4	<i>spl-1</i>	IV	0.54 ± 0.09	p<0.001
ZC416.6		IV	0.58 ± 0.04	p<0.001
F49E8.4	<i>cdd-2</i>	IV	1.06 ± 0.02	
F49E8.5	<i>dif-1</i>	IV	0.67 ± 0.03	p<0.001
F33D4.1	<i>nhr-8</i>	IV	0.93 ± 0.03	
F59B8.2		IV	0.88 ± 0.12	
B0218.8	<i>clcc-52</i>	IV	1.07 ± 0.15	
C49C8.5		IV	0.83 ± 0.10	
T04B2.5		IV	0.82 ± 0.09	
W08D2.4	<i>fat-3</i>	IV	0.88 ± 0.28	
K08F4.7	<i>gst-4</i>	IV	0.89 ± 0.07	
M7.1	<i>let-70</i>	IV	1.20 ± 0.26	
K08C7.2	<i>fmo-1</i>	IV	0.85 ± 0.08	
F01G10.1		IV	0.83 ± 0.18	
F01G4.1	<i>psa-4</i>	IV	1.16 ± 0.19	
F01G4.6		IV	0.88 ± 0.06	
F28D1.7	<i>rps-23</i>	IV	0.45 ± 0.10	p<0.001
K08E4.1	<i>spt-5</i>	IV	0.78 ± 0.14	
K08E7.1		IV	0.23 ± 0.07	p<0.001
C49C3.5		IV	0.30 ± 0.05	p<0.001
F11E6.5	<i>elo-2</i>	IV	0.30 ± 0.09	p<0.001
F26D10.4	<i>gem-4</i>	IV	0.70 ± 0.21	
F56E10.4	<i>rps-27</i>	V	1.06 ± 0.37	
ZK6.7		V	0.73 ± 0.07	p<0.01
C39F7.4	<i>rab-1</i>	V	0.19 ± 0.03	p<0.001
F39G3.1	<i>ugt-61</i>	V	0.37 ± 0.04	p<0.001
C18G1.5	<i>hil-4</i>	V	0.79 ± 0.11	
C02A12.4	<i>lys-7</i>	V	0.61 ± 0.05	p<0.001
CD4.2	<i>crn-2</i>	V	1.10 ± 0.17	
F46E10.9	<i>dpy-11</i>	V	0.99 ± 0.16	
K11G9.6	<i>mtl-1</i>	V	0.98 ± 0.20	
F52E1.13		V	0.98 ± 0.22	
T27E4.8	<i>hsp-16.1</i>	V	1.32 ± 0.24	
Y22F5A.4	<i>lys-1</i>	V	0.10 ± 0.03	p<0.001

T19B10.11	<i>mxl-1</i>	V	0.56 ± 0.47	
R13H4.5		V	0.65 ± 0.38	
R11D1.11	<i>dhs-21</i>	V	0.85 ± 0.27	
C52E4.1	<i>cpr-1</i>	V	0.71 ± 0.22	
C13C4.5		V	0.37 ± 0.11	p<0.001
F58E10.4	<i>aip-1</i>	V	0.44 ± 0.09	p<0.001
T08G5.10	<i>mtl-2</i>	V	0.52 ± 0.11	p<0.001
H39E23.1	<i>par-1</i>	V	1.12 ± 0.16	
C53A5.3	<i>hda-1</i>	V	0.18 ± 0.04	p<0.001
R11H6.1	<i>pes-9</i>	V	0.06 ± 0.02	p<0.001
F44G3.6	<i>skr-3</i>	V	0.19 ± 0.02	p<0.001
T03E6.7	<i>cpl-1</i>	V	1.41 ± 0.42	
F38A6.3	<i>hif-1</i>	V	0.75 ± 0.22	
R04A9.4	<i>ife-2</i>	X	1.10 ± 0.14	
M6.1	<i>ifc-2</i>	X	1.25 ± 0.15	
C44C1.2		X	0.73 ± 0.15	
C04F6.1	<i>vit-5</i>	X	0.73 ± 0.27	
C46C11.2		X	0.81 ± 0.56	
K10B3.8	<i>gpd-2</i>	X	1.48 ± 0.53	
K05B2.5	<i>pes-22</i>	X	1.17 ± 0.27	
M03F4.7	<i>calu-1</i>	X	0.79 ± 0.77	
F35C8.6	<i>pfn-2</i>	X	1.02 ± 0.11	
H22K11.1	<i>asp-3</i>	X	0.66 ± 0.08	p<0.01
C03B1.12	<i>lmp-1</i>	X	0.59 ± 0.02	p<0.001
C54H2.5	<i>sft-4</i>	X	0.41 ± 0.03	p<0.001
C07B5.2		X	1.23 ± 0.67	
F41D9.3	<i>wrk-1</i>	X	1.14 ± 0.11	
F15G9.1		X	1.13 ± 0.09	
R07B1.10	<i>lec-8</i>	X	1.20 ± 0.21	
F21G4.2	<i>mrp-4</i>	X	1.37 ± 0.23	
F22F1.1	<i>hil-3</i>	X	0.35 ± 0.04	p<0.001
F53A9.10	<i>tnt-2</i>	X	0.86 ± 0.09	
B0272.3		X	0.75 ± 0.09	
C33D3.1	<i>elt-2</i>	X	0.43 ± 0.03	p<0.001
C26F1.10	<i>flp-21</i>	X	0.86 ± 0.05	
M163.3	<i>his-24</i>	X	0.88 ± 0.09	
T22H6.2		X	0.87 ± 0.08	
C29F7.3		X	0.79 ± 0.12	
K02A4.1	<i>bcat-1</i>	X	0.61 ± 0.23	
C37E2.5	<i>ceh-37</i>	X	0.40 ± 0.13	
F48C11.3	<i>nlp-3</i>	X	0.20 ± 0.03	p<0.001
K05G3.3	<i>cah-3</i>	X	0.54 ± 0.15	p<0.01
C06G1.4	<i>ain-1</i>	X	0.86	0.29

8.5. Danksagung

Vielen Dank, Frau Prof. Daniel, dass Sie es mir ermöglicht haben, die Doktorarbeit bei Ihnen am Lehrstuhl zu machen. Die fachlichen Diskussionen mit Ihnen haben mich soweit reifen lassen, dass ich meine Hypothese bis zuletzt verteidigen konnte. Herzlichen Dank auch an Herrn Prof. Haller und Herrn Prof. Schemann für die Anregungen und die Beurteilung meiner Arbeit.

Britta, vielen lieben Dank für Deine engagierte Betreuung und Deine tatkräftige Unterstützung in allen Bereichen. Ohne Dich hätte ich den Wurm niemals so lieben gelernt. Du bist einfach eine gute Wurm-Mama.

Anne, wir als alte Ökos haben die ganze Zeit zusammengehalten und sind gemeinsam durch gute und durch schlechte (Labor-)Zeiten gegangen. Dafür möchte ich Dir wirklich von ganzem Herzen danken.

Gregor, vielen Dank für Deine stets aufmunternden Worte und Deine Jacke nach unserer Ankunft aus Sevilla.

Katrin, Dich kenn ich seit meinem ersten Tag im Labor und ich konnte mich immer auf Dich verlassen. Wir haben gemeinsam gerechnet, Platten gegossen, Zeitpläne erstellt und pep-2 Würmer gedealt. Die Zeit mit Dir war einfach toll.

Kerstin, die fachlichen Diskussionen, methodischen Anregungen und Deine persönliche Unterstützung haben mir, vor allem in der Endphase, wirklich sehr, sehr geholfen. Meine Arbeit und ich wären nicht das was wir jetzt sind, ohne Dich.

Meine Zeit am Institut werde ich immer in guter Erinnerung behalten. Dafür möchte ich mich bei allen Mitgliedern der Arbeitsgruppe bedanken, besonders bei Manu S., Caro und allen ehemaligen Mitgliedern der Wurmgruppe. Danke Clare, Lisa, Julia und Jan für Eure Arbeit.

Ganz herzlichen Dank an meine Eltern, die mich bei all meinen Entscheidungen unterstützen und auf die ich immer zählen kann.

Stefan, was würde ich nur ohne Dich machen? Danke!

8.6. List of scientific publications

Selected poster contributions

- 2006 Wallwitz J, Spanier B, Daniel H
Iron deficiency and metallomics in *Caenorhabditis elegans*
2nd NuGO Introduction course, Hohenkammer, Germany
- 2006 Wallwitz J, Spanier B, Daniel H
Effects of iron deficiency on reproduction and life span of *Caenorhabditis elegans*
NuGO week 2006, 3rd European Nutrigenomics Conference, Oxford, UK
- 2007 Wallwitz J, Spanier B, Daniel H
The role of intestinal amino acid and peptide transporters and modulator proteins in *Caenorhabditis elegans* assessed via RNA-interference
NuGO week 2007, 4th European Nutrigenomics Conference, Oslo, Norway
- 2008 Benner J, Lasch K, Naumann K, Spanier B, Daniel H
The role of intestinal amino acid and peptide transporters in amino acid homeostasis in *Caenorhabditis elegans*
European C. elegans Meeting, Carmona (Seville), Spain
- 2008 Benner J, Lasch K, Eckl J, Spanier B, Daniel H
The role of intestinal amino acid transporters in *Caenorhabditis elegans* lacking the intestinal peptide transporter
Transporters 2008, Murten, Switzerland

Peer reviewed original papers

- 2009 Spanier B, Lasch K, Marsch S, Benner J, Liao W, Hu H, Kienberger H, Eisenreich W, Daniel H: How the intestinal peptide transporter PEPT-1 contributes to an obesity phenotype in *Caenorhabditis elegans*, PLoS One 4(7):e6279
- 2011 Benner J, Daniel H, Spanier B: A glutathione peroxidase, intracellular peptidases and the TOR complexes regulate peptide transporter PEPT-1 in *C. elegans*, PLoS One 6(9):e25624

8.7. Curriculum Vitae

Name	Benner
Vorname	Jacqueline
Geburtsdatum	30.10.1980
Geburtsort	München

Promotion und Studium

10/2005 – 10/2011	Promotion an der TU München-Weihenstephan, Lehrstuhl für Ernährungsphysiologie
09/2005	Studienabschluss als Diplom Ökotrophologin
10/2000 – 09/2005	Studium der Ökotrophologie an der TU München
05/2000	Abitur am Gymnasium Ottobrunn

Berufliche Erfahrungen

06/2010 – 02/2011	Universitätsassistentin, Universität Wien
06/2004 – 08/2004	Praktikum beim Cateringunternehmen Lohmeier & Deimel, Bonn
07/2003 – 10/2003	Praktikum bei der IKK Nordrhein, Bergisch Gladbach
02/2001 – 04/2001	Praktikum bei D.I.B. Gesellschaft für Standortbetriebsdienste, München

8.8. Erklärung

Hiermit versichere ich, dass ich die vorliegende Arbeit

Amino acid homeostasis in *Caenorhabditis elegans* lacking the intestinal peptide transporter PEPT-1 and identification of PEPT-1 modulator proteins

selbständig verfasst und keine anderen als die angegebenen Quellen und Hilfsmittel verwendet habe. Die den benutzten Quellen wörtlich oder inhaltlich übernommenen Stellen sind als solche kenntlich gemacht.

Die Arbeit hat in gleicher oder ähnlicher Form noch keiner anderen Prüfungsbehörde vorgelegen.

Freising, den

Jacqueline Benner